

FILE COPY

2

DC-TR-90-320
House Report
October 1990

AD-A229 276



CLOSED LOOP DIGITAL AND COMPUTER CONTROL OF AN ULTRAGRAVIMETRIC MICROBALANCE

Joseph V. Beasock

DTIC
ELECTE
NOV 26 1990
S D CS D

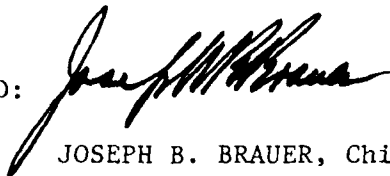
APPROVED FOR PUBLIC RELEASE; DISTRIBUTION UNLIMITED

Rome Air Development Center
Air Force Systems Command
Griffiss Air Force Base, NY 13441-5700

This report has been reviewed by the RADC Public Affairs Division (PA) and is releasable to the National Technical Information Services (NTIS) At NTIS it will be releasable to the general public, including foreign nations.

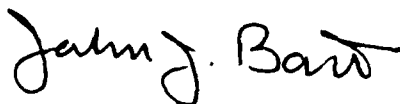
RADC-TR-90-320 has been reviewed and is approved for publication.

APPROVED:



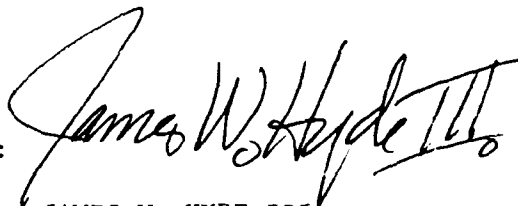
JOSEPH B. BRAUER, Chief
Microelectronics Reliability Division
Directorate of Reliability & Compatibility

APPROVED:



JOHN J. BART
Technical Director
Directorate of Reliability & Compatibility

FOR THE COMMANDER:



JAMES W. HYDE III
Directorate of Plans & Programs

If your address has changed or if you wish to be removed from the RADC mailing list, or if the addressee is no longer employed by your organization, please notify RADC (RBRE) Griffiss AFB NY 13441-5700. This will assist us in maintaining a current mailing list.

Do not return copies of this report unless contractual obligations or notices on a specific document require that it be returned.

REPORT DOCUMENTATION PAGE

Form Approved
OMB No. 0704-0188

Public reporting burden for this collection of information is estimated to average 1 hour per response, including the time for reviewing instructions, searching existing data sources, gathering and maintaining the data needed, and completing and reviewing the collection of information. Send comments regarding this burden estimate or any other aspect of this collection of information, including suggestions for reducing this burden, to Washington Headquarters Services, Directorate for Information Operations and Reports, 1215 Jefferson Davis Highway, Suite 1204, Arlington, VA 22202-4302, and to the Office of Management and Budget, Paperwork Reduction Project (0704-0188), Washington, DC 20503.

1. AGENCY USE ONLY (Leave Blank)		2. REPORT DATE October 1990		3. REPORT TYPE AND DATES COVERED In-House Oct 86 - Apr 90	
4. TITLE AND SUBTITLE CLOSED LOOP DIGITAL AND COMPUTER CONTROL OF AN ULTRAGRAVIMETRIC MICROBALANCE				5. FUNDING NUMBERS PE - 62702F PR - 2338 TA - 01 WU - 4V	
6. AUTHOR(S) Joseph V. Beasock					
7. PERFORMING ORGANIZATION NAME(S) AND ADDRESS(ES) Rome Air Development Center (RBRE) Griffiss AFB NY 13441-5700				8. PERFORMING ORGANIZATION REPORT NUMBER	
9. SPONSORING/MONITORING AGENCY NAME(S) AND ADDRESS(ES) Rome Air Development Center (RBRE) Griffiss AFB NY 13441-5700				10. SPONSORING/MONITORING AGENCY REPORT NUMBER RADC-TR-90-320	
11. SUPPLEMENTARY NOTES RADC Project Engineer: Joseph V. Beasock/RBRE/(315) 330-4055					
12a. DISTRIBUTION/AVAILABILITY STATEMENT Approved for public release; distribution unlimited.				12b. DISTRIBUTION CODE	
13. ABSTRACT (Maximum 200 words) This report summarizes the development of a control system for an ultragravimetric microbalance. Included are the different control methodologies investigated and the characteristics of each. These methodologies are based on two types of control systems: one is a digital control system implemented totally in hardware and the other a computer controlled system. The intent of the project was to replace the existing analog controller with a system that was more stable, had better response to transient conditions, was less temperature sensitive and could be operated unattended for long periods of time. Much of the work to date, on the computer controlled system, has concentrated on bringing the balance to equilibrium quickly and reliably, maintaining equilibrium once achieved and reliably tracking mass change. Data analysis and reduction techniques are still being developed and evaluated. As yet, there is no indication of the ultimate sensitivity obtainable with a computer controlled system, but a sensitivity of 0.2 microgram, with a sample mass of 5 grams, should be routinely obtainable. In addition to the electrical/electronic characteristics, there is some discussion of the mechanical characteristics that affect the performance of the balance. But because of time constraints, the mechanical aspects are not discussed in detail. (Continued)					
14. SUBJECT TERMS Microbalance, Computer Control, Digital Control, Calibration of Microbalance, Quartz Beam Microbalance				15. NUMBER OF PAGES 140	
				16. PRICE CODE	
17. SECURITY CLASSIFICATION OF REPORT UNCLASSIFIED	18. SECURITY CLASSIFICATION OF THIS PAGE UNCLASSIFIED	19. SECURITY CLASSIFICATION OF ABSTRACT UNCLASSIFIED	20. LIMITATION OF ABSTRACT UL		

Block 13 (Continued)

An adsorption/desorption experiment, on a devitrifying, microcircuit package, sealing glass (type 75-83), is presented to demonstrate the use of the system and illustrate the mass tracking behavior. Mention is also made of a number of analysis that have been completed or are in progress.

FOREWORD

This in-house report documents the development and utilization of the RADC/RBRE ultragravimetric microbalance system. This report was prepared by Rome Air Development Center at Griffiss Air Force Base, New York. Manpower for this in-house effort was charged to RADC's JON 2338014V.

The ultragravimetric microbalance was developed for RADC at Clarkson University, by Dr. A.W. Czanderna, during the late 70's. Numerous studies on materials used for microelectronic components have been carried out and reported in various periodicals, technical reports and technical journals.

The RADC microbalance is a unique analytical system capable of measuring submicrogram mass changes in samples of up to 10 grams. The most recent work has been involved in upgrading the electronics and automation of the system. Due to changes in personnel and work directives the project was delayed several times.

The author gratefully acknowledges the help, support, and contributions of the following individuals:

Dr. R.W. Thomas, RADC/RBE-1.
A. Andrews, RADC/RBRE (co-op).
L. Bushunow, RADC/RBRE (co-op).
E. Doyle, RADC/RBRE.
Dr. W.H. Debany, RADC/RBRA.



Accession For	
NTIS CRA&I	<input checked="" type="checkbox"/>
DTIC TAB	<input type="checkbox"/>
Unannounced	<input type="checkbox"/>
Justification	
By	
Distribution /	
Availability Codes	
Dist	Avail and/or Special
A-1	

D. Fayette, RADC/RBRA.

Dr. P. Kornreich, Syracuse University.

J. McCarthy, Rome Research Corporation.

P. Spiecher, RADC/RBRE.

Dr. L. Walsh, RADC/RBRE.

TABLE OF CONTENTS

Section	Page
I. INTRODUCTION	1
II. BALANCE DESCRIPTION	5
III. THEORY OF OPERATION AND CONTROL	8
IV. DIGITAL CIRCUIT DESCRIPTION	13
V. COMPUTER CONTROL DESIGN	
A. STATIC CONTROL	29
B. DYNAMIC CONTROL	41
C. MODIFIED DYNAMIC CONTROL	55
VI. CALIBRATION	60
VII. EXPERIMENTAL	70
VIII. SUMMARY	76
BIBLIOGRAPHY	83
APPENDIX A	
IBM DATA ACQUISITION AND CONTROL ADAPTER	85
ANALOG INPUTS	85
ANALOG OUTPUTS	87
APPENDIX B	
SYSTEM FLOW CHARTS	90
APPENDIX C	
SOURCE CODE FOR SOFTWARE CONTROL	103
APPENDIX D	
ULTRAGRAVIMETRIC MICROBALANCE CONTROL AND DATA ACQUISITION SOFTWARE DOCUMENTATION	113
APPENDIX E	
VARIABLE LIST	120
APPENDIX F	
PUBLICATIONS	125

LIST OF ILLUSTRATIONS.

Figure		Page
1.	Ultramicrogravimetric balance and residual gas analysis system.	4
2.	Construction of microbalance quartz beam.	5
3.	Diagram of a symmetric microbalance beam.	9
4.	Rodder control circuit.	10
5.	Drawing illustrating the modular approach to construction of the digital control system.	13
6.	Simple digital control system.	15
7.	Increase in oscillation amplitude as a result of an increase in the clock rate.	17
8a.	Ideal transfer curve.	21
8b.	Zero offset error.	21
8c.	Gain error.	21
8d.	Linearity error.	21
8e.	Differential linearity error.	21
9.	Transients in control voltage, caused by improper timing of counter circuits.	23
10.	Two phase clock and timing diagram.	23
11.	Schematic of clock frequency selection by multiplexing.	26
12.	Schematic of timing circuit for disabling the DAC counter while the beam equilibrium position is at the null position.	28
13.	Block diagram of digital control system for a microbalance, using magnetic coupling for controlling the beam position.	28
14.	Plot of detector signal under "static" conditions.	31

LIST OF ILLUSTRATIONS.
(continued)

Figure		Page
15.	Illustration of the damped oscillation that occurs when the DAC code is incremented or decremented. .	32
16.	Plot of average readings of the detector codes over a period of several hours.	34
17.	Plot of ADC code average values during monotonic mass change.	35
18.	Illustration of discontinuities in mass data represented by combining DAC and ADC codes.	38
19a.	Illustration of the effect of a change in the equilibrium position on the detector signal.	40
19b.	Translation of the position change in the equilibrium into a phase change.	40
20.	Illustration of the forced oscillation resulting from application of a periodic, intermittent force of constant magnitude to the tare side of the balance.	41
21a.	Illustration of natural damping of the detector output signal.	43
21b.	Scale expansion illustrating the decay of the oscillation below the noise level.	43
22a.	Illustration of the relationship between the ideal position, velocity, and acceleration parameters of the oscillating beam.	45
22b.	Illustration of the DC position (horizontal line at 2 on the vertical scale) of the beam, found by summing the ideal acceleration and position values at any point in time.	45
23a.	Dynamic control waveform simulation for an amplitude of 200.	49
23b.	Dynamic control waveform simulation for an amplitude of 2000.	49
24a.	Illustration of dynamic behavior for oscillation	

LIST OF ILLUSTRATIONS.
(continued)

Figure		Page
	amplitude of 100.	50
24b.	Illustration of dynamic behavior for an oscillation amplitude of 500.	50
24c.	Illustration of dynamic behavior for an oscillation amplitude of 1000.	51
24d.	Illustration of dynamic behavior for an oscillation amplitude of 2000.	51
25a.	Illustration of the detector signal nonlinearity. .	51
25b.	Slope of the detector linearity curve.	51
26a.	Illustration of mass dependency on temperature. . .	58
26b.	Illustration of pressure dependency on temper- ature.	58
26c.	Illustration of amplitude dependency on temper- ature.	58
26d.	Illustration of period dependency on temperature. .	58
27.	Illustration of the mass parameter temperature dependency.	59
28a.	Sample buoyancy plot for gold metal in dry nitrogen.	67
28b.	Sample buoyancy plot for gas density bulb in dry nitrogen.	68
29.	Sample calibration calculation.. . . .	69
30.	Adsorption of water vapor on sample of processed sealing glass.	72
31.	Adsorption of water vapor on unprocessed sealing glass powder at 210 °C.	73
32.	Differential scanning calorimeter (DSC) spectra showing irreversible change in sealing glass at processing temperatures.	75

LIST OF TABLES

TABLE I.	Dependence of sensitivity on DAC resolution. .	18
TABLE II.	Calibration data.	66

I. INTRODUCTION

New and better materials are continuously being developed to handle the increasing complexity of microcircuits and microcircuit packaging techniques. Along with the development of these materials is the need to characterize their chemical and physical properties which are important to the long term reliability of a finished device. Designing and packaging a device that is impervious to its environment does not insure long term reliability unless the ambient sealed into the device package is free of harmful contaminants and moisture. The presence of even small amounts of water vapor in the enclosed volume of a semiconductor package can lead to serious degradation of semiconductor device performance by various mechanisms^{1,2} with possible catastrophic results. As little as 1000 ppmv water has led to device failure.³

Even a hermetic seal cannot protect a device from moisture trapped inside the package during processing. Typically an SSI circuit package contains an enclosed volume of 40 mm³ and requires less than one microgram of water vapor to saturate (100% relative humidity >25,000ppm) the enclosed ambient at 22°C. By contrast the glass used to seal the package may release several micrograms⁴ of adsorbed water vapor. Glassivation, surface passivation, epoxy die attach and other materials inside the package may also trap and release significant amounts of water. It was for the purpose of studying the moisture adsorption/desorption processes of electronic materials that a unique

analytical system was proposed and developed. The system was designed by Vasofsky and Czanderna.⁴ It is capable of ultramicrogravimetric study of materials loaded from a controlled uncontaminated environment. This system has been used to study vapor sorption properties of materials used in integrated circuit and microcircuit package manufacture. This system is illustrated in Figure 1 and consists of:

1. An ultramicrobalance, in a vacuum housing, for measuring mass change and the rate of mass change of a sample in a controlled environment.
2. A UTI-100C quadrapole mass analyzer for determining the molecular species present in the system during the desorption process.
3. A vacuum oven, dry box combination on the sample introduction side of the system for baking and loading samples from a controlled atmosphere.
4. Lindbergh Hevi-Duty tube furnaces, model 55070-S for heating the sample and compensation hangdown tubes.
5. A gas handling system for controlling the atmosphere in the system.

6. Ultrahigh vacuum pumping station consisting of a TRIBODYNE roughing and molecular drag pump combined with a BALZER's turbomolecular pump for an ultimate pressure capability in the 10^{-9} torr range.

Epoxies, polyimides, sealing glasses, gold plated kovar lids, and ceramic substrates are examples of materials that have been evaluated, using this system.

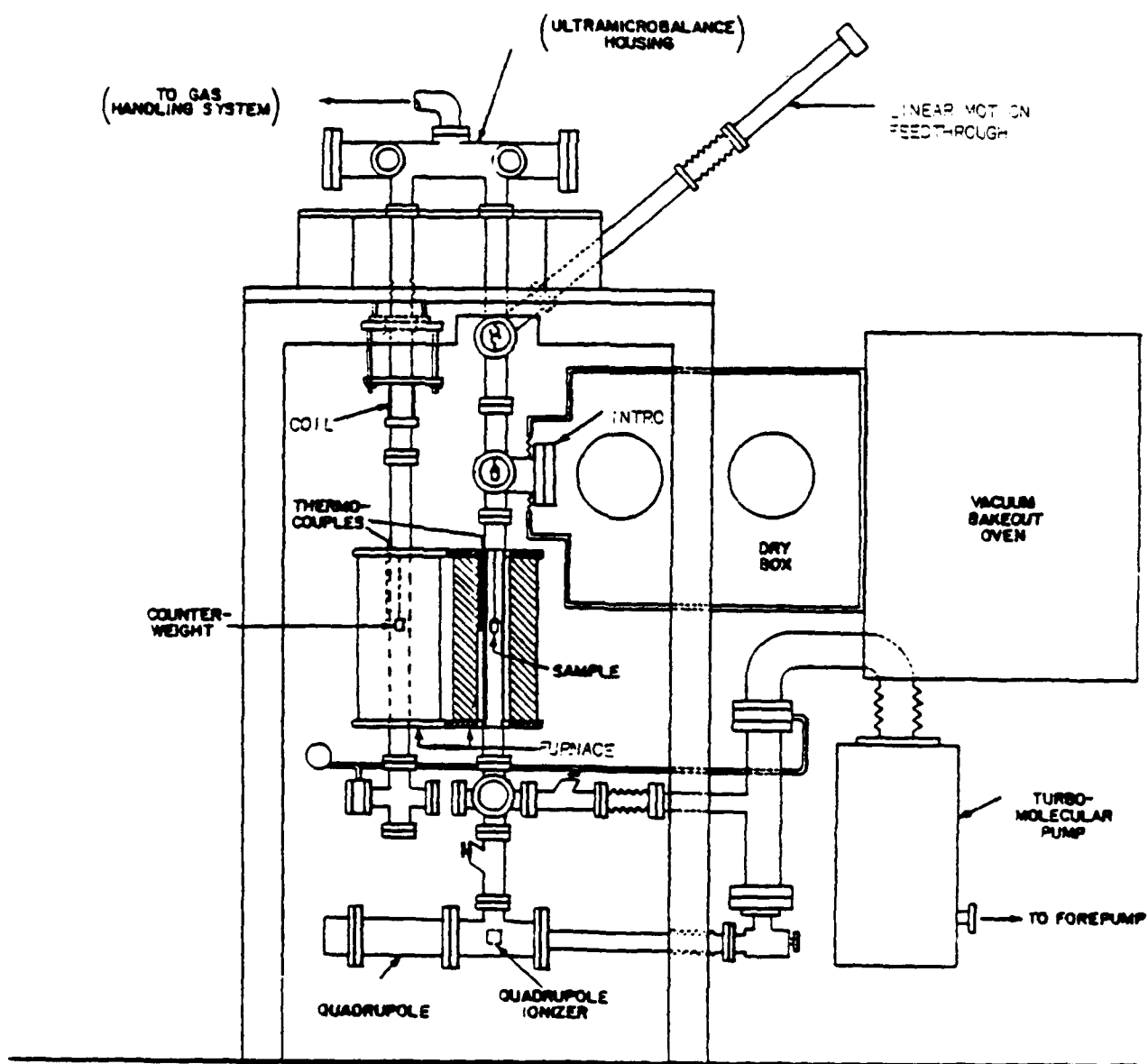


Figure 1. Ultramicrogravimetric balance and residual gas analysis system.

II. BALANCE DESCRIPTION

The ultramicrobalance beam (see Figure 2) is a bakeable, pivotal, trussed quartz-beam developed by Czanderna and described by him in detail.⁵ The beam has the following characteristics: a length of 180mm, a maximum capacity of 20 grams, a load to precision ratio of $1-2 \times 10^8$, a sensitivity of < 0.1 microgram with 4-10 gram loads, and a null reading stability of greater than six months⁴. The quartz beam has a mass of approximately 2 grams. It is mounted in a stainless steel housing and can be pumped to pressures in the ultra high vacuum

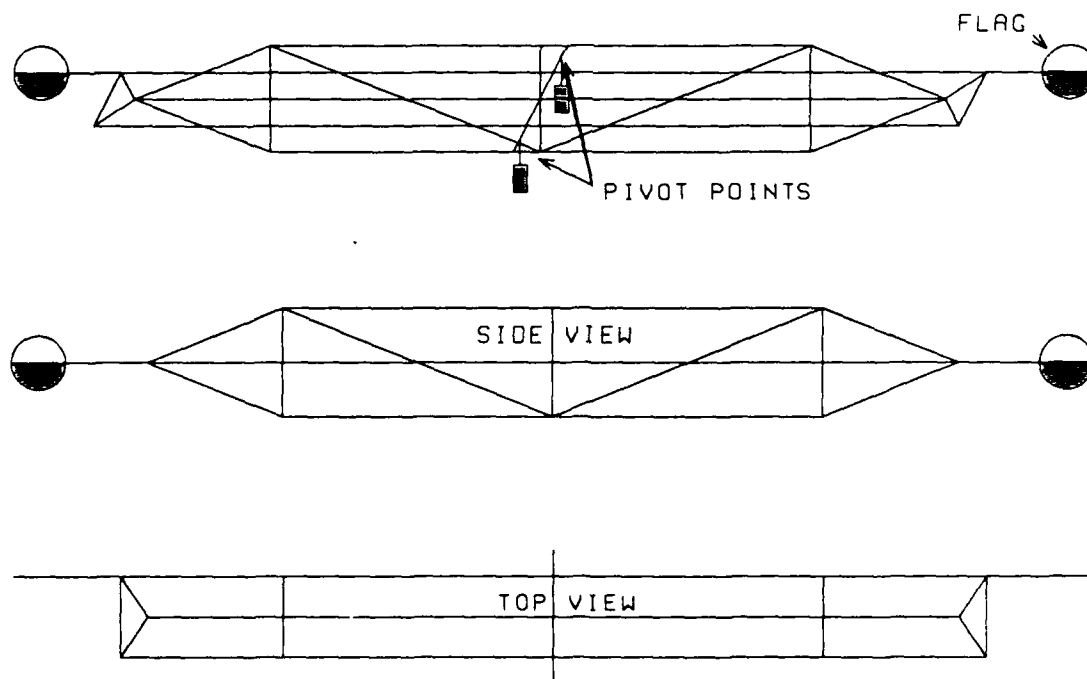


Figure 2. Construction of microbalance quartz beam.

region (10^{-9} torr).

The balance beam has vertically mounted quartz flags at each end. The lower half of each flag is coated with 600 angstroms of gold metal. Beam deflection is detected optically through the use of infrared emitting diode sources and photodiode detectors. The optical path between the source and detector is intercepted by the quartz flag. The gold coating is semiopaque to the infrared energy. As the beam moves more or less energy is blocked by the gold coating. The photodetector output then is a measure of the beam position.

Other methods of detecting mass change through beam deflection include the use of differential transformers and differential capacitance bridges. However, these methods are more difficult to use because of extreme temperature sensitivity, adverse effects on beam deflection sensitivity, reactivity to gases being studied, pressure dependency, and difficulty of installing in a high vacuum enclosure. The photoelectric technique provides high sensitivity to beam deflection, is readily adaptable to high vacuum enclosures and can be made temperature and pressure insensitive.¹¹

The beam is supported on tungsten needle points (this limits the load to about 20 grams maximum before plastic deformation of the tungsten degrades performance), to minimize friction. The tungsten needle points are, in turn, mounted with the beam on a stainless steel platform, and this assembly sets inside a stainless steel vacuum housing. Other materials (e.g. sapphire) could be used for the fulcrum support, to increase the load capability, but much of our work

has been done on samples of less than 5 grams total mass.

At each end of the beam there is a long quartz fiber, 125 micrometers in diameter, for suspending the sample and the tare masses. (The tare mass counterbalances the sample mass). The suspension fibers are actually short lengths of optical fiber with the protective coating removed. The use of optical grade quartz fiber has eliminated the need to draw fibers from quartz rod, which was a tedious and often frustrating process. The use of optical fiber has not noticeably affected the performance of the balance.

On the tare side of the balance there is a quartz encapsulated permanent magnet. Its magnetic field interacts with the magnetic field of a coil outside the vacuum enclosure. By controlling the current which flows through the coil windings, it is possible to compensate for mass changes in the sample during an analysis and maintain the beam at the null position.

III. THEORY OF OPERATION AND CONTROL

Ideally, for a small difference in mass, the equilibrium condition of the balance (see figure 3) is given by:

$$W_1[L_1 \cos \Theta - d \sin \Theta] - Mx \sin \Theta = W_2[L_2 \cos \Theta + d \sin \Theta] \quad (1)$$

from this equation for small deflection angles the angular deflection of the balance beam Θ is approximated by:

$$\Theta \sim \frac{W_1 L_1 - W_2 L_2}{(W_1 + W_2)d + Mx} \quad (2)$$

From equation (2) it is deduced that the center of mass must be close to the point of support to maximize the sensitivity and the deflection angle for a given mass difference between the two sides. Also, the center of mass of the beam when loaded must be below the suspension point for stability.

A general scheme for automation of the microbalance would include the following sequence of events. (It is general practice to operate the balance in reference to its null position.) A position sensor provides an error signal determined by the mechanical movement of the beam away from the null position. This error signal is then converted to a voltage and applied to a servo feedback circuit. The feedback circuit generates a force on the beam that minimizes the error voltage. Electrical changes relating to the force in the compensating

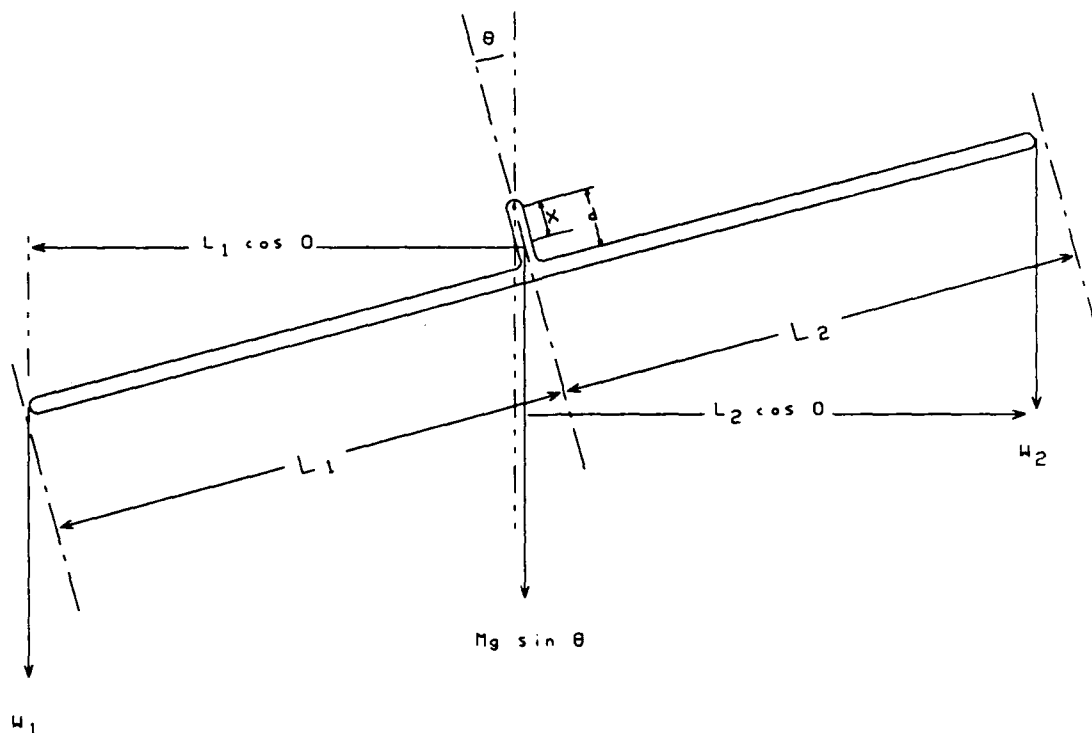


Figure 3. Diagram of a symmetric microbalance beam.

circuit are then calibrated to provide mass change information.

The original control system developed by Rodder⁶ (see figure 4) was a photoelectric, null-sensing, high-gain electronic circuit. The design was totally analog and highly sensitive. High gain op amps with ultralow offset, ultralow temperature drift and ultralow aging drift were required for long term stability. However, the operating characteristics of the circuit had several drawbacks. First, the system would not automatically seek the null state on start up but had to be initialized through a rather complex and time consuming startup procedure. The startup procedure involved adjusting the electronics

to bring the system under control followed by additional adjustments to maximize the stability. Improper adjustment during the startup procedure often resulted in the loss of many hours of analytical time. The circuit would drift excessively or eventually become unstable and lose control. Second, the control system could not respond to mass changes that passed through the electronic zero. As a result, an initial difference of several milligrams between the sample and tare masses was required to insure that the coil current did not try to pass through zero during an analysis. Miscalculation of this required mass difference often resulted in the loss of valuable analytical time through premature termination of an analysis and the making of adjustments to and/or changing of the sample mass. (Sample changing is a tedious process at best. It can take several hours and there is always the danger of breaking the suspension fiber which can take a day or more to replace). Third, the analyst had to be present continuously making minor adjustments and collecting data.

As a result, it was decided to develop a circuit that would be inherently stable, would not require adjustments to prevent instability and drift, did not require the constant presence of an "operator" and could also be easily integrated into an automated instrumentation system. Initially an analog design was considered. However, a digital design with an analog driver stage to interface various signals with the compensation coil was selected to reduce the number of temperature sensitive components in the system. Ultimately, a computer control system that would be capable of total automation

of all processes except sample loading was to be constructed.

IV. DIGITAL CIRCUIT DESCRIPTION

It was decided that the best approach to the digital system would be modular (see figure 5), with each module being a plug in card performing a specific function. This would allow increasing the complexity and functional capability of the design as needed, and the instrument would be operational while the controller was in a primitive stage of development. In addition, poorly functioning modules could be redesigned and replaced without major rework or

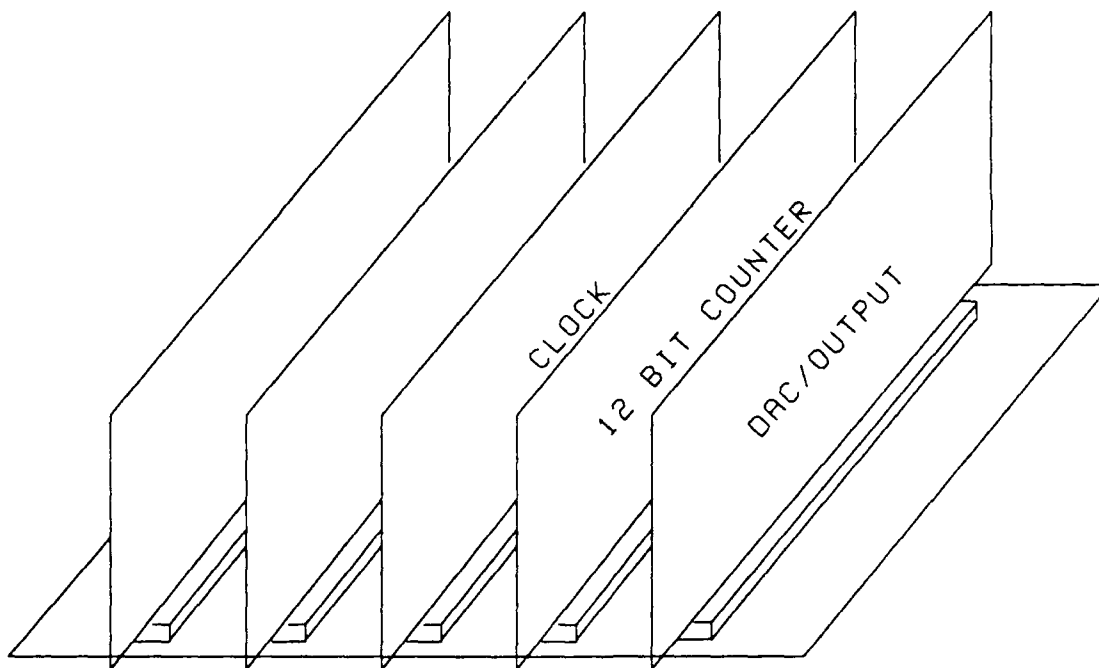


Figure 5. Drawing illustrating the modular approach to construction of the digital control system.

needless instrument downtime.

The simplest fully functional digital control circuit (see figure 6) consists of the following:

1. A clock to maintain the proper timing of state changes in the control logic and counter circuits.
2. A position sensitive detector circuit that generates a digital output.
3. A binary up/down counter of n bits.
4. An n bit digital to analog converter (DAC).
5. A voltage to current transducer to drive the coil. (A current source is used to generate the magnetic field rather than a voltage source because the coil resistance is temperature dependent and this is "transparent" to a current source).

During operation the relative position of the beam is sensed by the photocurrent generated in a silicon photodiode. Any change in the position of the beam produces a corresponding change in the generated photocurrent. This electrical current is then amplified, converted to a voltage, filtered to reduce noise, and fed to a comparator circuit for conversion to a logic level error signal. This digital error signal determines the position of the balance in reference to the null position and selects the direction of count of

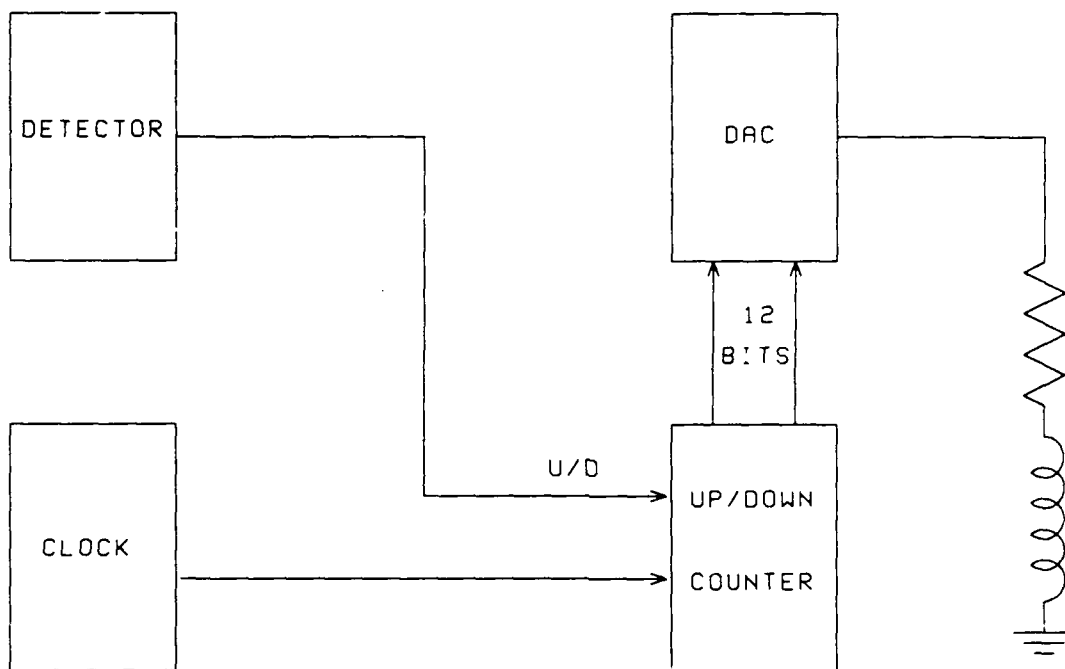


Figure 6. Simple digital control system.

the up/down counters. The counters generate the code necessary to control the DAC output which controls the intensity of the magnetic field. Changes in the counter code cause a corresponding change in the magnetic field intensity. The error signal is applied such that the force applied to the beam causes the beam to move in the direction of the null position. When the beam crosses the null position the error output will switch to its alternate state indicating the beam has moved to the other side of the null position and the controlling force will increase or decrease accordingly. Thus the beam is constantly being driven toward equilibrium. As a result the output

voltage of the DAC and the motion of the beam will oscillate about the null position. The magnitude of the oscillation will be determined by the clock rate, the sensitivity of the balance to an LSB (least significant bit) change in DAC code, the period of the balance, the type of gas in the system and the pressure of the gas in the system. The change in mass of the sample can be related to the change in the DAC output.

As the clock frequency increases the magnitude of the force driving the beam toward the null position increases proportionally. Because of the inertia of the system this becomes a positive feedback loop and results in an increase in the amplitude of the oscillation. Increasing the clock rate provides a method of operating the system in a controlled, sustained oscillation mode. Figure 7 illustrates the response of the system to an increase in clock rate. As the clock rate continues to increase, the amplitude of the oscillation will increase until it is sufficient to cause the beam to hit the stops. This is analogous to what occurs in an underdamped analog control circuit. It may be desirable to operate in an underdamped mode to obtain an oscillation of constant amplitude, because more information is available concerning equilibrium conditions. (Underdamped operation will be discussed further under computer control.)

The control coil is driven by a current source which is driven by the output voltage from the DAC. This voltage to current converter must be designed around a temperature stable op amp with low offset voltage similar to the OP-07. Low temperature coefficient resistors

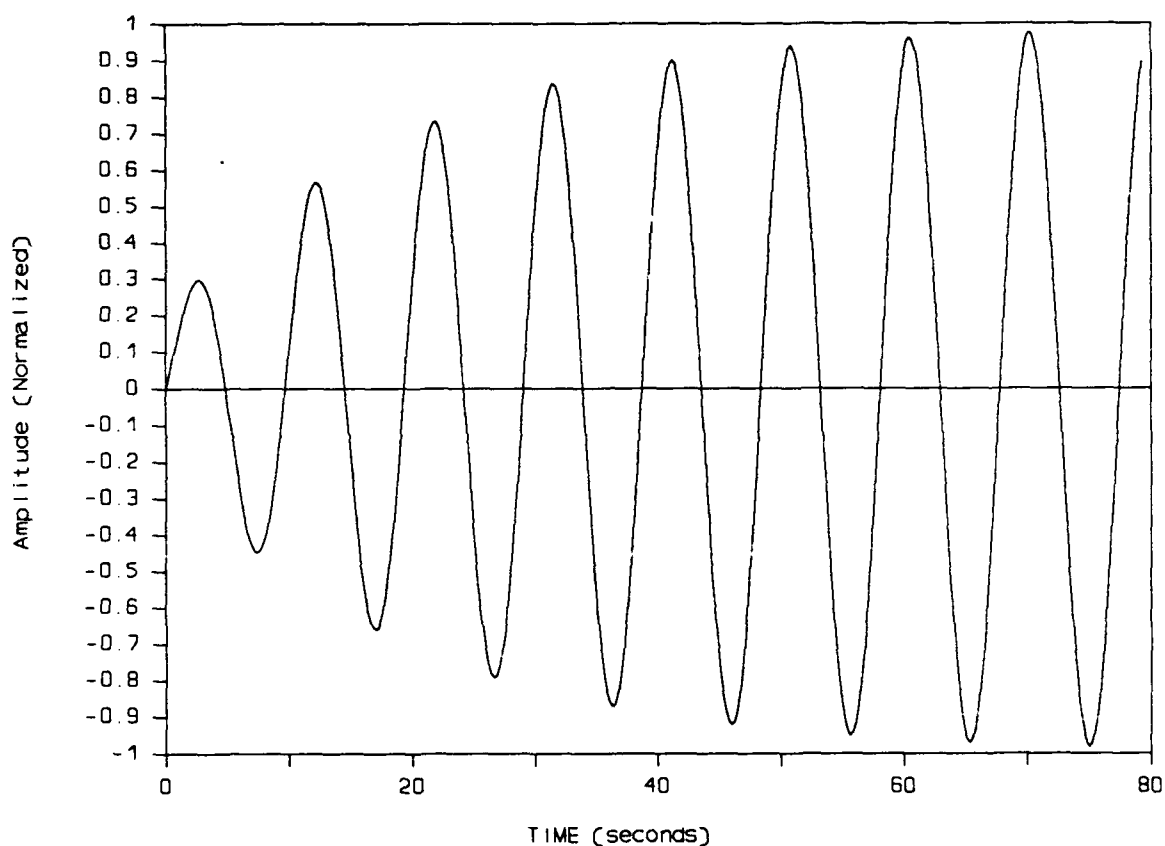


Figure 7. Increase in oscillation amplitude as a result of an increase in the clock rate.

such as metal film resistors should also be used. A DAC with a current output could have been used to drive the coil directly, however the available current is generally on the order of 1 to 2 milliamperes. The coil on the system requires approximately 2.5 ma of current per milligram of mass change. Thus a DAC with a current output would be too restrictive to provide adequate headroom to allow for buoyancy effects and weighing errors when matching the sample mass to the tare mass. The use of the voltage to current converter also provides for ease of adding other control signals, such as tare adjust

and damping, to the system.

The DAC resolution directly controls the range to sensitivity ratio of the control system. This is illustrated in Table I, which compares the mass sensitivity vs DAC resolution for mass ranges of

TABLE I

Dependence of sensitivity on DAC resolution.

DAC Resolution (bits)	SENSITIVITY (10 mg/100 mg)
12	2.441/24.41 ugr/LSB
14	0.6104/6.104
16	0.1562/1.526

10 and 100 milligram respectively.

Given the desired sensitivity, the mass range for a particular DAC resolution can be determined from the simple relationship:

$$\text{RANGE} = \text{sensitivity} \times 2^n$$

where n = the resolution in bits

As an example, we can illustrate for the case where a sensitivity of 0.1 $\mu\text{gr/LSB}$ is desired and the available DAC has a resolution of 12 bits. Using the formula with $n = 12$, this gives a mass range of:

$$4096 \times 0.1 = 409.6 \text{ micrograms}$$

This mass range of 409.6 micrograms is the maximum dynamic range but not necessarily the useful range. The DAC code required to bring the balance to the null position can be 1000 LSB's off from the desired code due to weighing inaccuracies in matching the sample and tare masses. In addition, small differences in the total volumes on the tare and sample sides will cause a change in the required DAC code when the pressure is changed, due to buoyancy effects. Some samples may require a much greater range than is available. This problem can be resolved in one of several ways: the sensitivity of the instrument could be made variable to allow for greater but less sensitive ranges, a higher resolution DAC could be used, or a tare voltage could be connected to the voltage to current converter. A calibrated voltage source was used to provide a tare voltage on the RADC instrument.

Basically there are four types of error associated with the DAC (see figure 8):

1. Zero offset. The error when the input code calls for 0 output. This value is an additive constant that shifts the transfer curve up or down.
2. Gain error. This shows as an error in the slope of the transfer curve and affects all codes by the same percentage.

3. Linearity error. This is caused by a deviation of the transfer curve from a straight line.
4. Differential linearity. This is a measure of the difference in the actual output of the DAC for adjacent changes in codes and the theoretical difference for adjacent changes.

Fortunately, these errors do not affect the operation or accuracy of the mass data generated by the system. All measurements with the controller are relative to an initial output voltage measured externally, as opposed to an absolute measurement. Due to the relative nature of the measurement, the offset voltage has no affect on the accuracy of the data. Because the output of the DAC is read directly, gain and linearity errors also do not affect the accuracy of the readings or the corresponding mass conversions.

Upon initial installation, and prior to operation of the control system, the detector circuit must be adjusted to give an output of zero volts for a predetermined beam position, preferably near a deflection angle (θ) of zero. This is the equilibrium or null position of the balance and corresponds to a particular photodetector current. The comparator is adjusted to change output state when the input passes through this predefined zero, and the coil is connected so that adjustments to the DAC voltage drives the balance beam in the

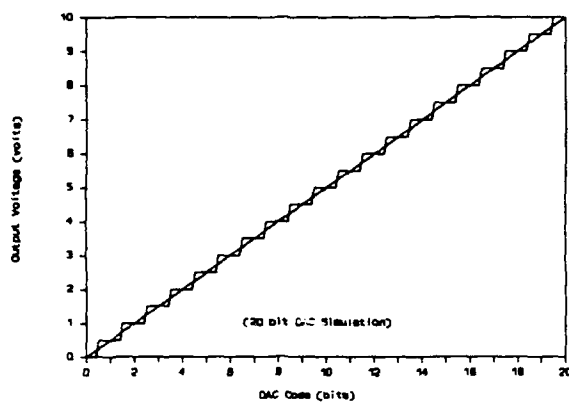


Figure 8a. Ideal transfer.

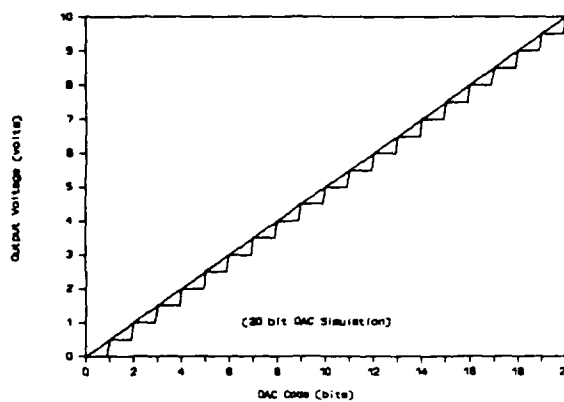


Figure 8b. Zero offset error.

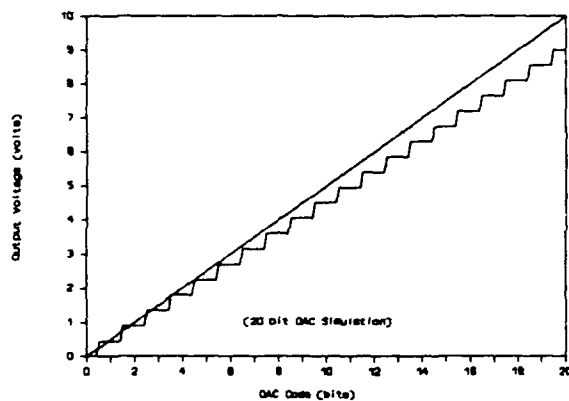


Figure 8c. Gain error.

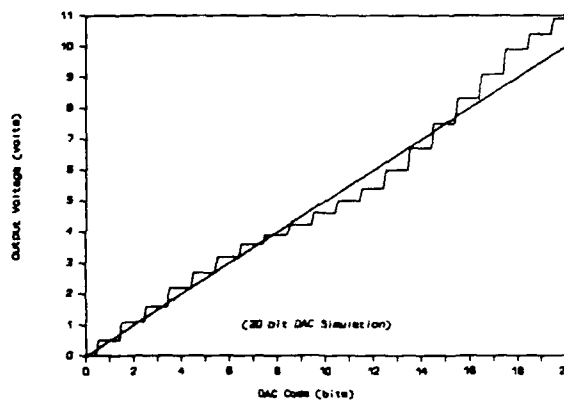


Figure 8d. Linearity error.

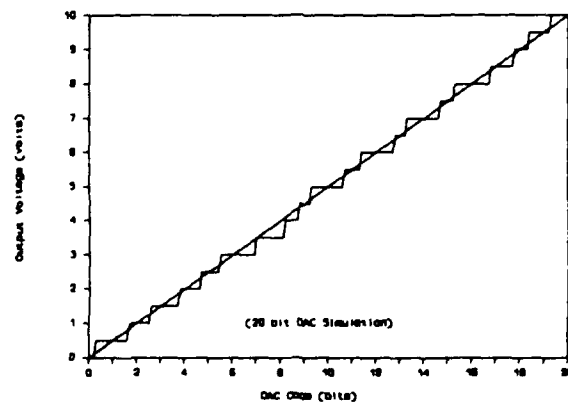


Figure 8e. Differential linearity error.

direction of the null position. No other adjustments are required. Operation of the controller is automatic, the only manual control being the on/off switch. The system has run on a continuous basis for periods of several months with no signs of instability.

The circuit was implemented using standard TTL logic gates, because they were readily available. This use of standard TTL gates imposes a penalty on the power requirements and a hefty 5 volt supply was required. (The power requirements could be reduced significantly by replacing the standard TTL logic devices with their low power Schottky (LS) counterparts or, for even greater power savings, CMOS devices. However, use of CMOS counters would require a major redesign of the printed circuit boards since there are no CMOS counters that are pin compatible with the TTL counters used.)

The timing characteristics of the up/down counters presented an additional and somewhat more serious problem. The simple clock circuit proposed above gave unexpected random state changes as illustrated in Figure 9. A close look at the counter specification sheet showed the presence of a transition problem in the control circuits. To eliminate this problem a timing circuit using a two phase clock was developed (see figure 10) and added to the system. No further occurrence of random state changes have been observed.

This completes the description of the basic control system. It is inherently stable, totally automatic, and will track any mass change in the range of the controller. However, the circuit is far from ideal. It suffers from several deficiencies which are identified

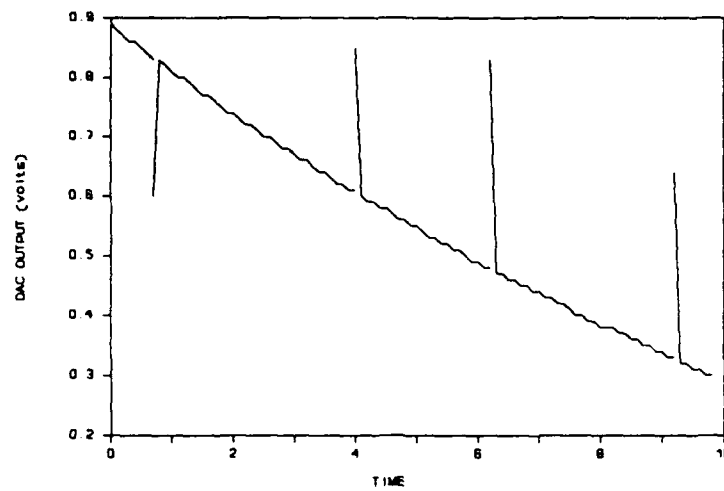


Figure 9. Transients in control voltage, caused by improper timing of counter circuits.

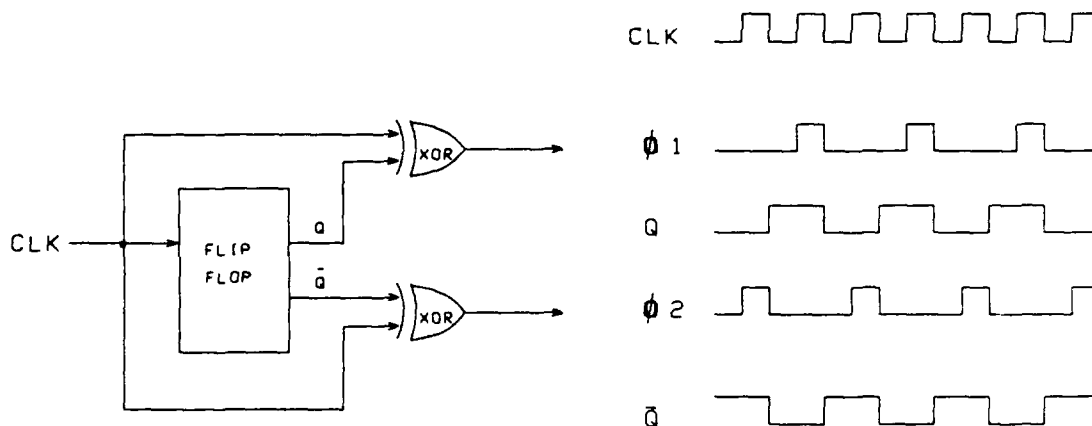


Figure 10. Two phase clock and timing diagram.

and listed below.

1. The mass range for which control can be maintained is limited.

2. To maintain a constant equilibrium position, around which the mass related parameter does not have a significant amplitude of oscillation, requires a slow clock frequency.
3. A slow clock means that on start up there is a long time lapse before equilibrium is reached and, also, the response of the system to mass changes will often be unacceptably slow.

The limited range is easily corrected by using a DAC with higher resolution, by addition of selectable gain in the voltage to current converter circuit with a corresponding decrease in sensitivity, or by operating the controller in harmonic oscillation with reduced sensitivity and collecting and reducing the data by statistical methods using a computer. Several techniques may be used to decrease the system response time:

1. The clock frequency can be made variable, and a faster clock frequency used when the balance is far from equilibrium or a rapid mass change occurs. This technique is most useful if data is being collected and analyzed by a computer since averaging will remove undesired oscillations and the faster clock speed greatly improves

the response. However, it should be remembered that if the clock rate becomes too large the beam will oscillate with an excessive amplitude, which will cause problems with stability of the equilibrium position.

2. The counter increment can be made variable so that a larger increment is used when the beam position is far from the equilibrium position. One way to implement this would be to use a counter that acts as a timing circuit which selects a higher clock rate, using simple logic, to increment the DAC counters. The time out period would have to be greater than $1/2$ of a period to prevent activation while the balance was at the equilibrium position.
3. The clock could be disabled while the balance beam is at or near the equilibrium position. This would allow using a faster clock frequency to increment the counter with some improvement in response. The limitations of (1) apply, and as with (1), the most benefit is derived when a computer is used to collect and analyze the data.

Of the techniques listed (1) and (3) were found to give the best response. Implementation of a selectable clock frequency was accomplished using a multiplexer, an eight bit counter, and three switches

to build a circuit (see figure 11) that allows the manual selection of one of 8 frequencies. The system clock is divided by the counter to give eight outputs of decreasing frequencies. These outputs go to the multiplexer and one is selected by applying the proper binary input code to the multiplexer through the three switches. The selected frequency is determined from the equation

$$f = \frac{f_o}{2^n}$$

Where f_o is the system clock frequency and n is the bit weight of the selected counter output. Using this method results in a compromise of automatic operation for an improvement in the response time. However, the improvement in response time more than offsets the occasional need to manually set the clock frequency. An automatic method of frequency selection could have been implemented at this time

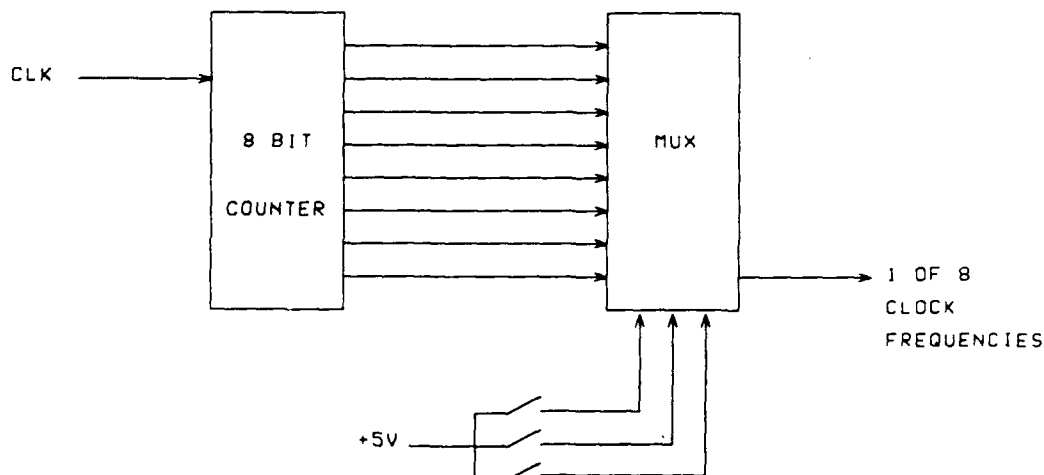


Figure 11. Schematic of clock frequency selection by multiplexing.

but this alone would not have given an added increase in speed of response over manual frequency selection. The use of a digital error signal for detecting equilibrium of the beam is itself a limiting factor to the speed of response, and a human operator can select appropriate frequencies much faster.

Disabling the counter while the balance is at equilibrium was a little more difficult to implement. The only indication that equilibrium had been reached was the length of time the beam spent on each side of the equilibrium position. Therefore a counter circuit (see figure 12), which acts as a timer, was added that disabled the clock signal to the DAC counter for a length of time slightly longer than one half the beam (loaded) period each time the balance crosses the null position.

These last two control circuit modifications made it possible to obtain reasonable start up and response times. Figure 13 illustrates the enhanced version of the design.

V. COMPUTER CONTROL DESIGN

All of the advantages of the digital control circuit described above can be realized with a computer controlled system. In addition, automatic control of the gas handling system, and collection and subsequent analysis of mass, pressure and mass spec data can be accomplished with the same system through software modification. The complete computer control system consists of a personal computer, data acquisition and control adapter, distribution adapter, voltage to current converter, detector circuitry and data acquisition/control software.

Several control software design options were investigated and considered to have merit. These include the following:

1. Static control.
2. Dynamic control.
3. Modified dynamic control.

Each of these options will be discussed at length.

A. STATIC CONTROL

This method was the simplest to implement and the most successful of the initial development efforts. The method involves reading the

error signal provided by the photo circuits and using the resulting error code to determine the position of the balance beam with respect to the null position code. If the error code is outside a predefined range of the null position, the DAC output is adjusted until the error code is forced within the desired range. The following assumptions must be true for good response and accuracy:

1. The balance beam is at rest.
2. The response of the system to changes in the DAC voltage are instantaneous.
3. Changes in DAC voltage do not cause oscillation of the beam.
4. The detector readings are stable and free of interfering noise.
5. The system is insensitive to temperature changes.

The microbalance is at ground level and bolted directly to the floor without provision for eliminating or damping vibration entering through the floor. Inspection of the photodetector amplifier output, using an oscilloscope, shows the presence of mechanical vibration, continuous small amplitude oscillations of low frequency and random

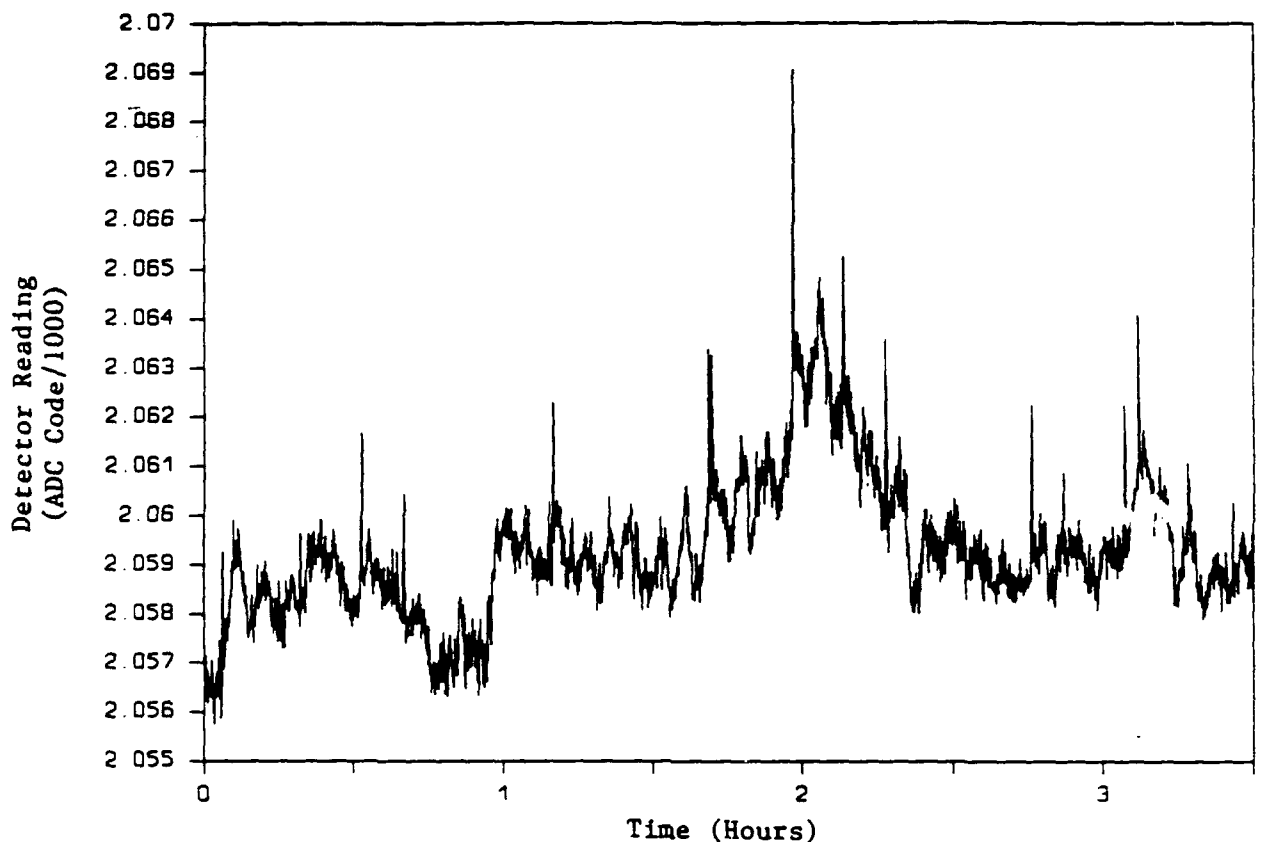


Figure 14. Plot of detector signal under "static" conditions.

transients. In addition, there is a high frequency (greater than 1 MHz) signal superimposed on the signal. Thus the detector signal is inherently noisy (see figure 14) and unsuitable for direct interpretation of the beam position. Much of the noise is removed by passive filtering but the improvement is not sufficient for direct interpretation.

Any change in the DAC output generates an uncompensated force on the tare side of the balance. This results in movement of the beam in the direction that will equilibrate the imbalance of forces. However, the total mass of the beam and weights is on the order of

12 grams. The force generated per LSB change in DAC code is equivalent to a few tenths to a few micrograms of mass. This is a ratio on the order of 1 part per million. Because of inertia the system does not react instantaneously to these small changes and it does not come to rest immediately when the equilibrium position is reached. Thus the time response of the system is limited. The only damping forces present are a small mechanical force generated by friction at the supports and a much larger force due to viscous flow created by the movement of gas over the surfaces. As a result damped

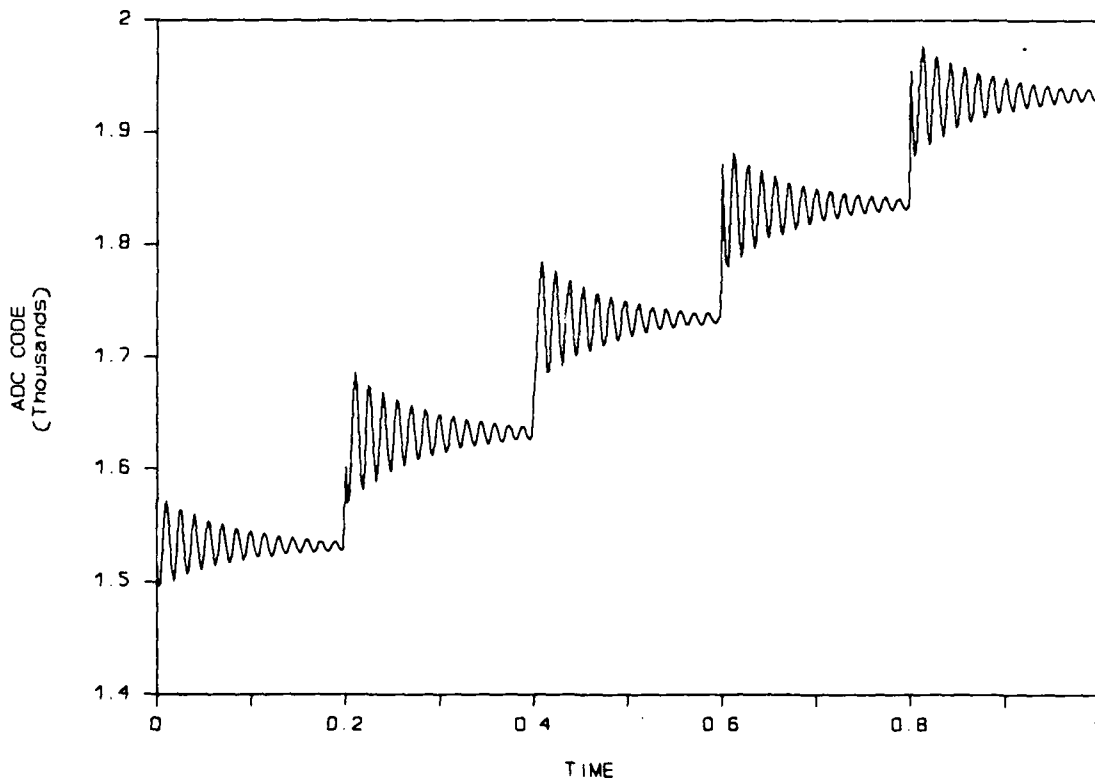


Figure 15. Illustration of the damped oscillation that occurs when the DAC code is incremented or decremented.

oscillation (see figure 15) of the beam about the null position occurs each time the control code is changed. Therefore, readings of the detector signal, after a change in control code, will be subject to larger errors if incorrectly interpolated than similar data after the beam has settled. In addition to the above characteristics the physical and electrical properties of the system are not stable to temperature changes.

To deal with these limitations a number of modifications had to be made to the control software. Under normal conditions the amplitude of oscillation is small and mass changes can be controlled to prevent wildly oscillating conditions and/or rapid changes. The small changes in the beam position are ignored as long as the error code is within a predefined range. When the error exceeds this range the control code will be adjusted to bring the error code back within the null position range. As long as the amplitude of oscillation does not become large the correction to the ADC code can be relatively quick. By making changes to the control code in small increments at appropriately spaced intervals, the amplitude of the resulting oscillation can be controlled and maintained at an acceptable level. However, to make the appropriate adjustment to the control code requires a knowledge of what change in code is needed to return the beam to the null position. This information is provided by the creation of a "look up" table that correlates the error code with the appropriate change in control code. When the beam position is outside the acceptable limits of the null position, the error code is found

in the table, the required change in control code is retrieved, and the DAC is adjusted incrementally until the desired change has been made. This process is repeated whenever necessary for as long as the controller is on.

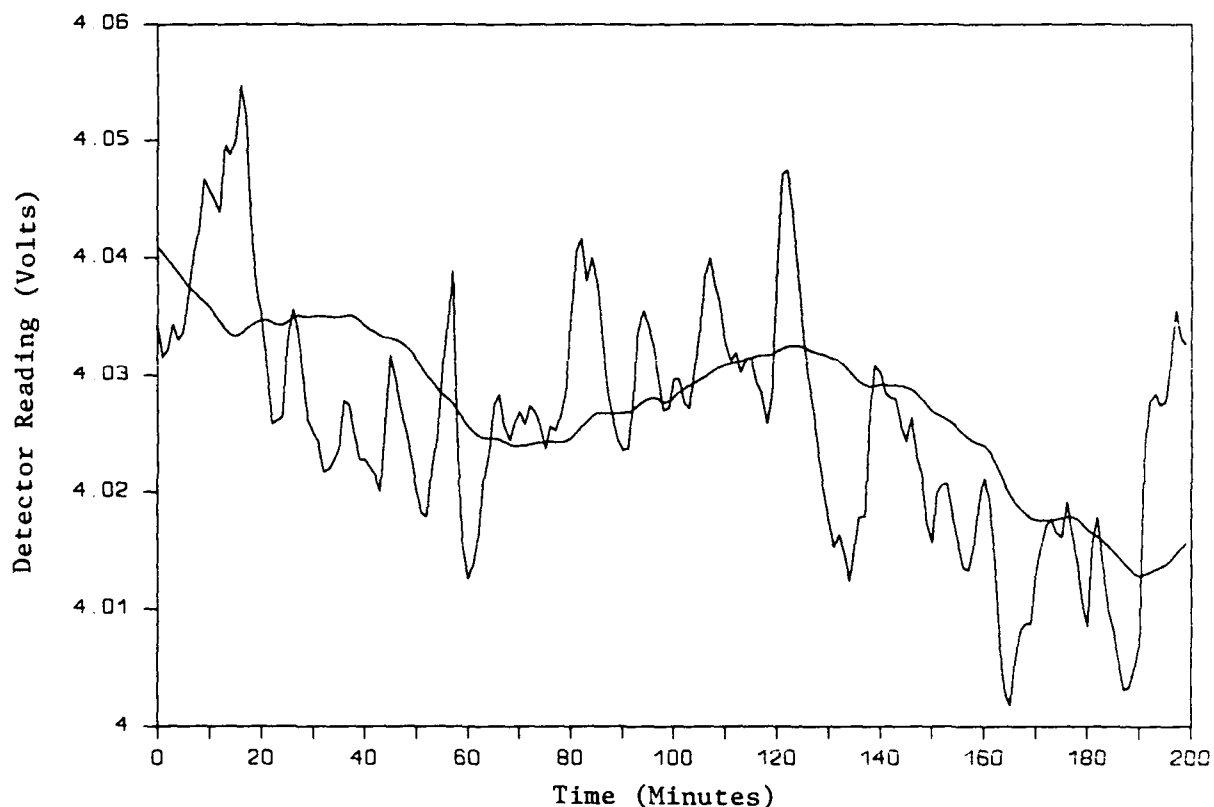


Figure 16. Plot of average readings of the detector codes over a period of several hours. The smoother curve illustrates the effect of increasing the number of points averaged.

To obtain an accurate indication of mass change occurring at the sample, the error codes are sampled for an appropriate period of time and an average value is calculated and stored. Figure 16 shows a plot of average values for a period of several hours. Longer sampling

periods generally give a smoother curve. In general a sampling period that is a multiple of the period of oscillation is best. However, the length of the sampling period is limited by the required response time of the system to normal mass changes in the sample as well as unanticipated rapid changes in mass.

Figure 17 shows how the error code tracks continuous monotonic mass change. The collected data has the form of a sawtooth due to the incrementing of the DAC. Several methods of tracking mass changes

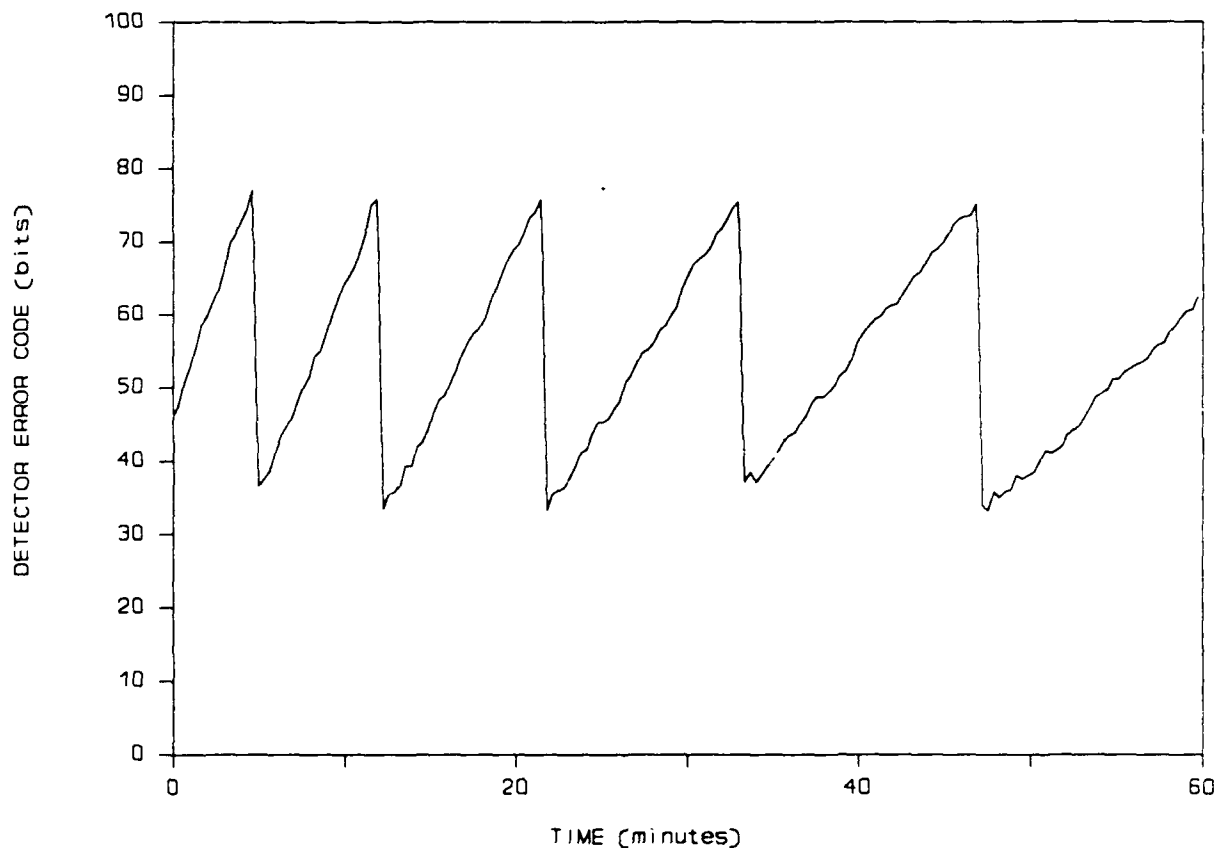


Figure 17. Plot of ADC code average values during monotonic mass change. The sawtooth pattern is the result of incrementing of the DAC code when the ADC code exceeds the defined range.

greater than the null position range are possible. These methods include:

1. Summation of incremental changes in the control code with time.
2. Summation of incremental changes in the error code with time.
3. A combination of (1) and (2).
4. Summation of incremental changes in the phase angle with time. (Dynamic system only.)

It was desired to maintain the capability of tracking large mass changes without sacrificing sensitivity. This eliminates the use of method 1 for less than 16 bit DAC resolution. With 12 bit resolution a large range requires that the change in the control force be relatively large (equivalent to a 1 microgram mass change or larger) for an LSB change in the control code. This of course decreases the ability to relate small changes in mass to changes in the control code. Summing the incremental changes in time of the control code correlates to the incremental mass change with respect to time. Using statistical techniques the mass versus time plot can be smoothed to increase the resolution. This, however, is not accurate in many

applications, particularly when small changes occur. The linearity errors of the DAC compound the problem, making this method unreliable in most applications.

The error codes are more than an order of magnitude more sensitive to mass change than the control codes, and are not subject to the linearity errors of the DAC. Therefore, summing the incremental changes in time of the error codes provides a more accurate method of monitoring mass information. The magnitude of the linearity errors of the ADC is lost in the noise of the detector signal and therefore does not significantly contribute to the inaccuracy of the mass data. An alternate and perhaps more appealing method is to use the error codes to calculate fractional mass information and add this to the control codes. Subtracting the $t = 0$ control code value from the data would then give a representative plot of the mass change vs time that has occurred. This, however, does not give entirely satisfactory results. A typical plot (figure 18) of the resulting data shows discontinuities in the mass data. It is not clear at this time whether this information is relevant or not. Similar discontinuities have been observed in the past and were found to be related to magnetic fields generated by relays in nearby instrumentation.

The mass change can also be tracked by a parameter that is almost totally independent of ADC and/or DAC errors, namely the phase of the beam oscillation referenced to equilibrium (phase = 0). This method depends on a single ADC code that is defined through software. Since the error in reading this code is noise dependent the digital

converter errors would not be reflected in the data. The important parameters for phase measurement are time and the ADC equilibrium code. As the mass of the sample changes, the position of the beam equilibrium will change with respect to the null position. This can be translated into a shift in the starting position of the oscillation as shown in Figure 19. When a predefined phase angle magnitude is reached the DAC is adjusted accordingly and the process is repeated. The accuracy of this method is determined by the accuracy of the phase difference, which is limited by the stability of the ADC code, and the

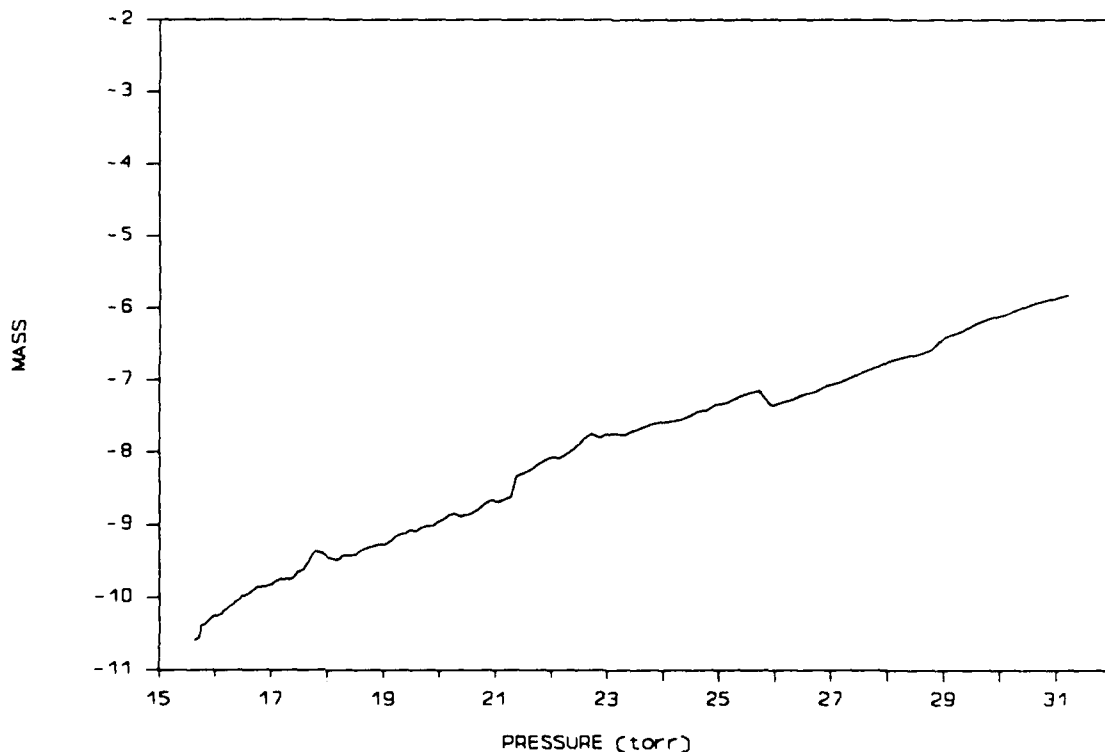


Figure 18. Illustration of discontinuities in mass data represented by combining DAC and ADC codes.

accuracy of the method of timing. However, it is not possible to obtain phase information with the static method of control, because a beam oscillation of significant amplitude is required. Thus control by phase angle relations is restricted to dynamic operation of the control system.

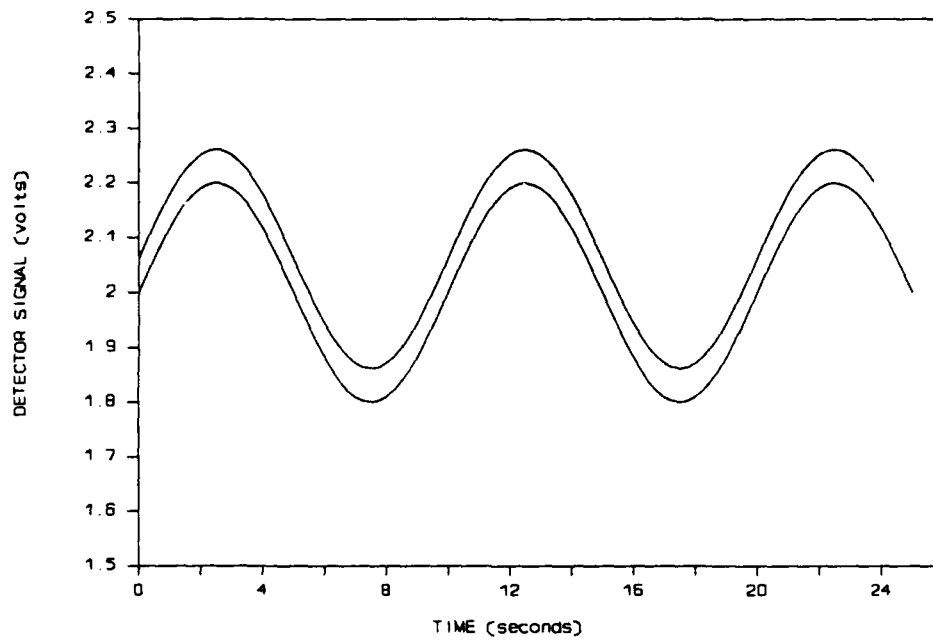


Figure 19a. Illustration of the effect of a change in the equilibrium position on the detector signal.

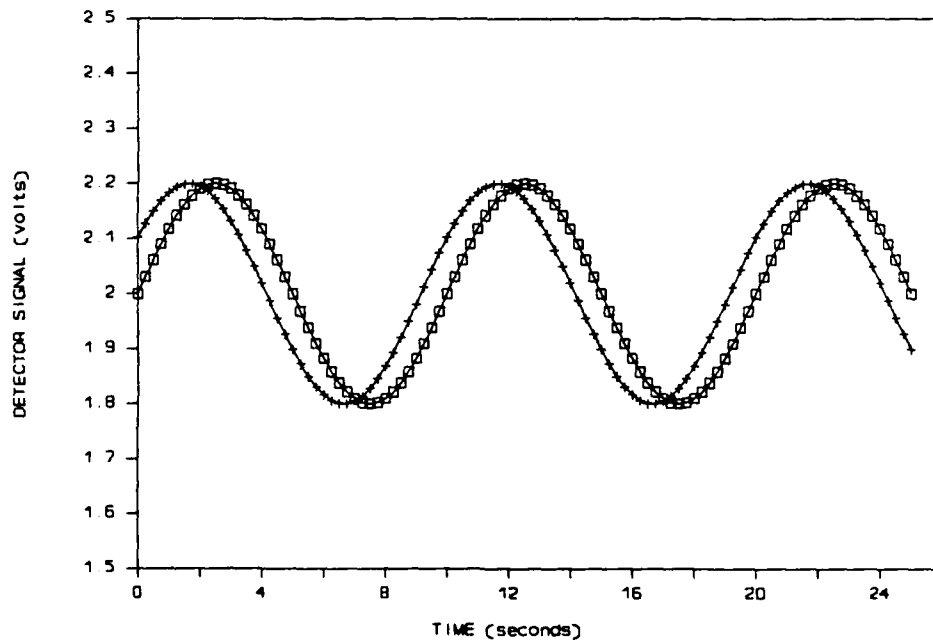


Figure 19b. Translation of the position change in the equilibrium into a phase change.

B. DYNAMIC CONTROL

"Dynamic" control is based on use of a controlled sustained beam oscillation of constant amplitude. When an intermittent force of constant magnitude is periodically applied to the tare side of the balance inphase with the natural oscillation of the beam, a forced oscillation ensues (see figure 20) which has a reasonably constant amplitude and period of oscillation at constant temperature and

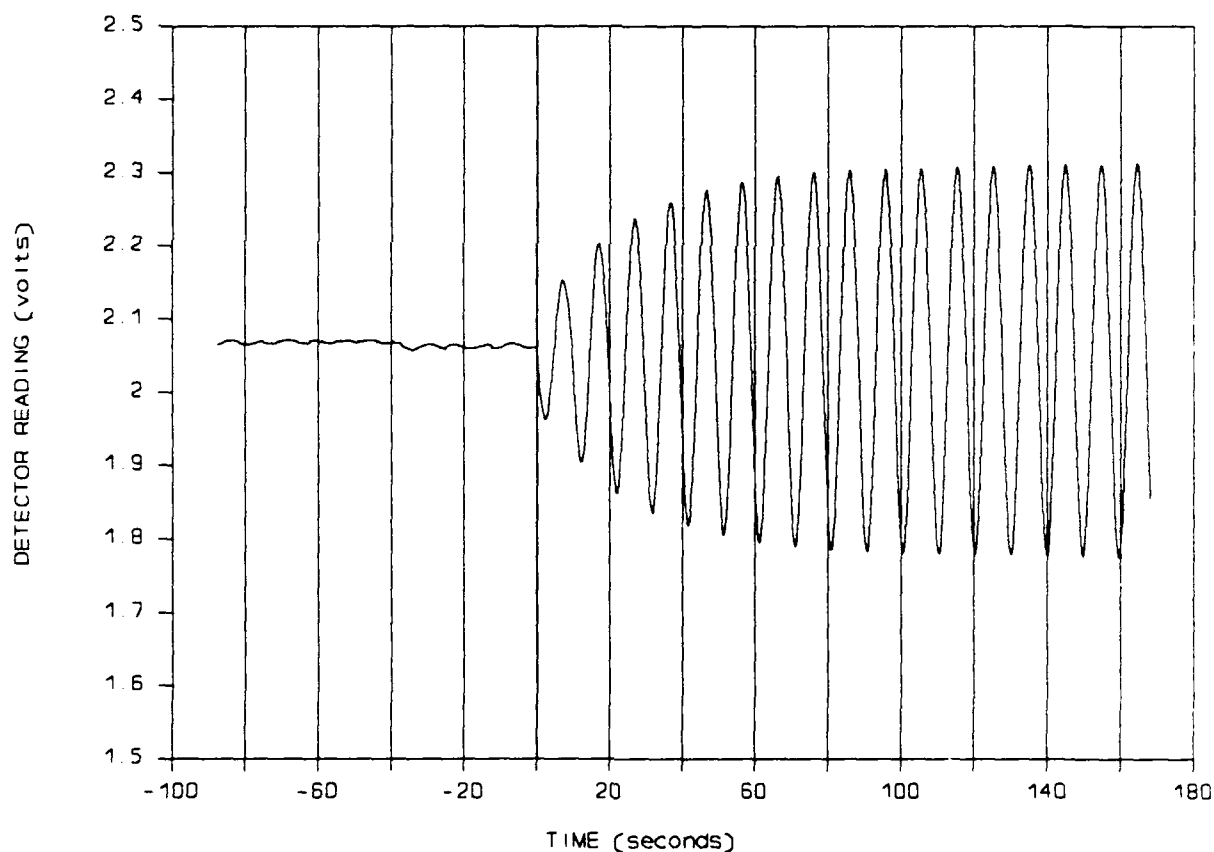


Figure 20. Illustration of the forced oscillation resulting from application of a periodic, intermittent force of constant magnitude to the tare side of the balance.

pressure. The error signal ADC code can then be determined from the dynamic behavior of the moving beam with the added benefit of having several new control parameters available for use. These parameters include the period of oscillation, the phase angle of the waveform with respect to the null position (user defined), the angular velocity of the beam, and the angular acceleration of the beam. Theoretically this method can provide instantaneous response to equilibrium condition changes. Practically the response time will be much faster than static control but it is limited by a number of factors which include ADC resolution, the magnitude of the control force that can be utilized, the magnitude of the oscillation that can be tolerated, delays introduced by signal conditioning, the inertia of the system, and the speed limitations imposed by software overhead and the computer itself. Assuming that these inherent problems are resolvable, a number of benefits derived from the physical characteristics of the controlled oscillating beam make this an attractive method of control. These include temperature drift compensation, fast response times and the possibility of increased sensitivity.

The output signal from the IR detector circuitry while the beam is oscillating is a damped sine wave (see figure 21). Although the actual signal is a complex function of the various modes of oscillation combined with electronic, magnetic and optical noise, for demonstration purposes, it can be assumed that the oscillation is a pure sinusoidal waveform with a constant amplitude and period. The

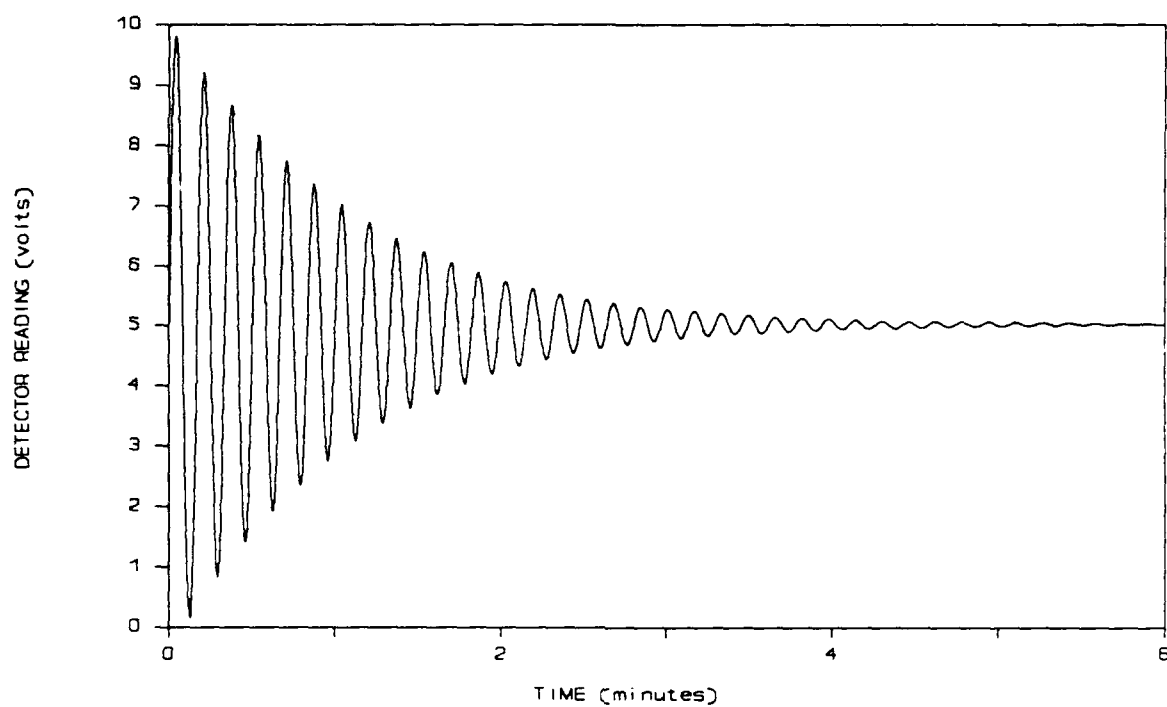


Figure 21a. Illustration of natural damping of the detector output signal.

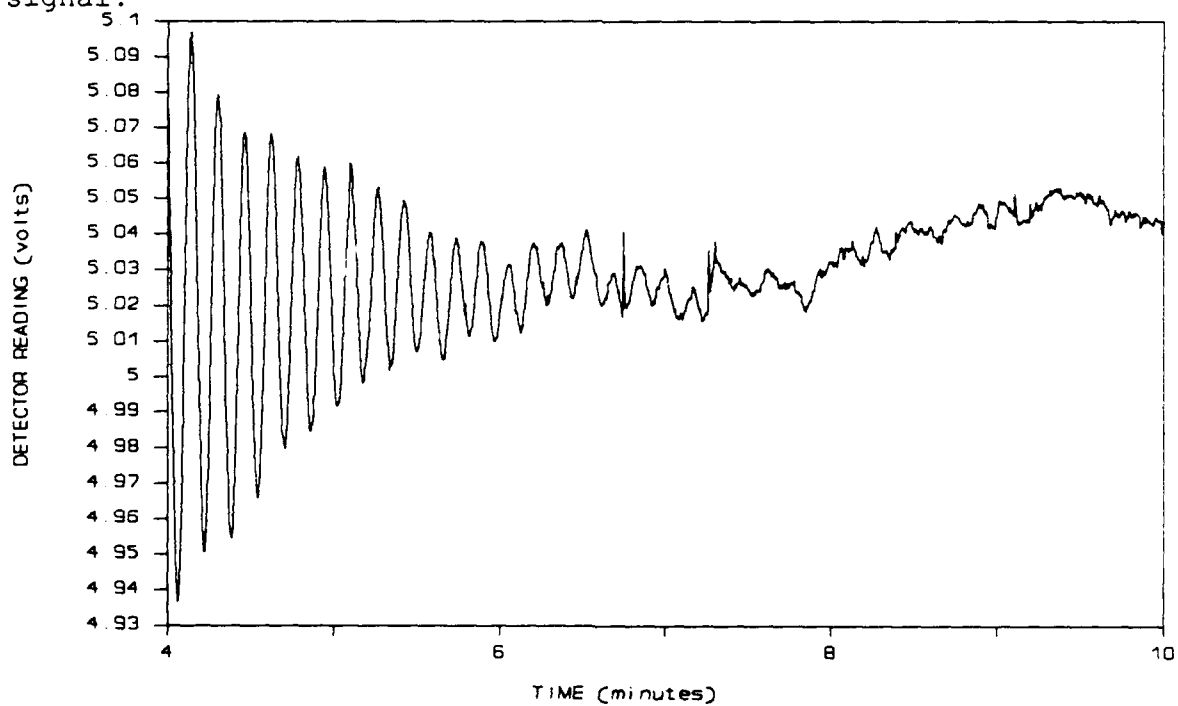


Figure 21b. Scale expansion illustrating the decay of the oscillation below the noise level.

(ideal -- 0th order approximation):

$$y = A \sin \omega t + B \quad (1)$$

$$y' = A \cos \omega t \quad (2)$$

$$y'' = -A \sin \omega t \quad (3)$$

where

y = position vector in terms of detector ADC code

y' = velocity vector from position delta

y'' = acceleration vector from velocity delta

A = the amplitude of oscillation

B = the null position on the sine curve

$\omega = 2 * \text{Pi} * 1/T$

T = period

t = time

Figure 22a illustrates the relation that these three parameters have to each other. Basically, other than the shift in the "dc" value, the velocity and acceleration waveforms are shifted in phase by 90° and 180° respectively relative to the position waveform. Summing the position and the acceleration waveforms (Figure 22b) gives a straight line which, from the following differential equation (equation 4), is seen to be the "dc" value of the error code (the equilibrium position of the beam).

$$y + y'' = B \quad (4)$$

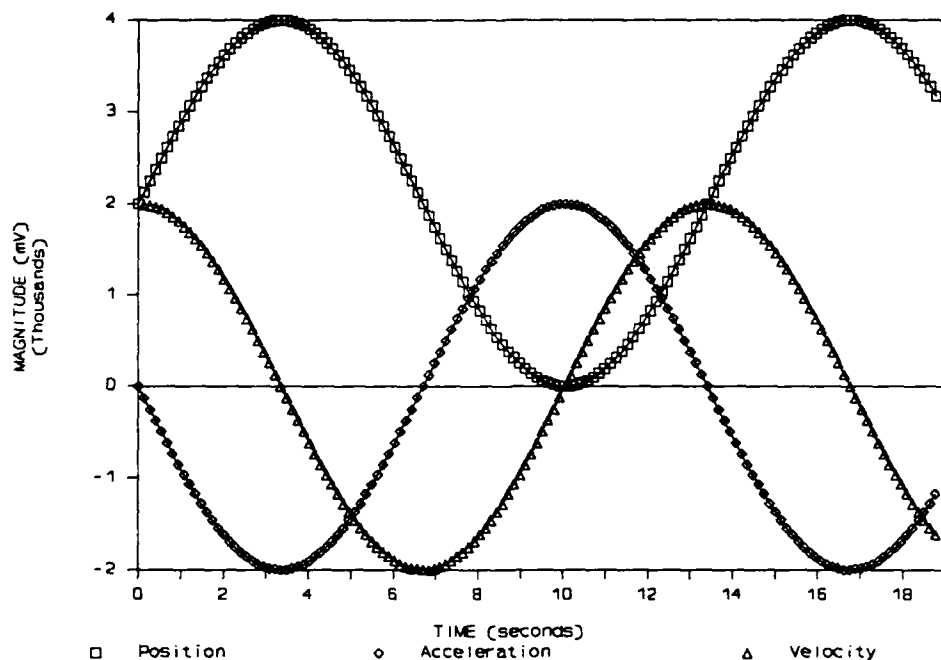


Figure 22a. Illustration of the relationship between the ideal position, velocity, and acceleration parameters of the oscillating beam.

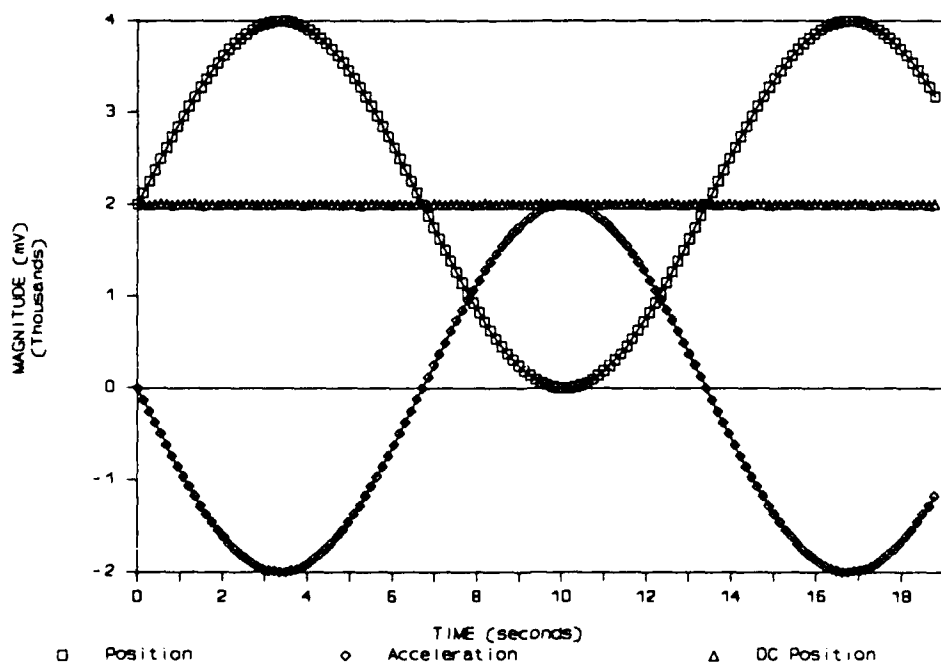


Figure 22b. Illustration of the DC position (horizontal line at 2 on the vertical scale) of the beam, found by summing the ideal acceleration and position values at any point in time.

The difference between the dc value of the error code and the null code gives the mass difference between the sample and tare masses when multiplied by the appropriate conversion factor. Thus the change in mass can be calculated at any point in time quickly and accurately if the acceleration data is sufficiently accurate.

During operation the control software essentially causes the following series of events to occur.

1. The detector is sampled for a short period of time. Ideally three consecutive, equally spaced detector readings are sufficient.
2. The position, velocity and acceleration of the beam motion are calculated.
3. The acceleration is added to the appropriate value for the position code. (This determines the "dc" or equilibrium ADC code. The "dc" value of the error code corresponds to the static position of the beam.)
4. The "dc" code is compared with the acceptable maximum and minimum values allowed for equilibrium. (A look up table similar to the table used with the "static" method is queried to determine the required change in the control code to position the beam within the acceptable

null range.)

5. If the "dc" value is not within this range the appropriate change is made to the control code and the above process repeated.

Assuming that the DAC has been properly calibrated with respect to the detector, the DAC output will be periodically adjusted to restore and maintain equilibrium indefinitely. For normal changes in mass the control code can be corrected relatively quickly and the effect of changes to the control code will be evident almost immediately as a change in the acceleration. Thus, in theory at least, a faster response time is possible than when using static control. Practically, the response is limited to the speed at which the acceleration can be determined and the degree of accuracy of the acquired value. These factors are controlled by the resolution of the DAC, the amplitude of oscillation, the magnitude of the noise present on the error signal, and the time required to process the data to obtain the correction factor. For the ideal case the process is trivial, but in reality there are many problems and limitations.

To get an idea of the feasibility and complexity of implementing this method of control and data collection, a simulation was done using digitized ideal waveforms. The position, velocity and acceleration of the beam oscillation at constant amplitude and under ideal conditions has already been discussed and illustrated (see

figure 22). These waveforms were obtained from continuous functions without the noise or extraneous modes of oscillation and vibration that normally accompany and distort the actual physical data. What was needed for the simulation was a model more representative of the effects of digitization on the experimental data.

As a first approximation the ideal data was rounded to the nearest whole number to represent the effect of digitization. (Truncating was also tried but this resulted in a shift in the phase of the velocity waveform). Rounding results in an ideal digitized representation of the waveform without the nonlinearity and other forms of error normally associated with digital converters. Figure 23 illustrates the effect of this ideal digitization on the waveforms. Initially, the simulation was done for two amplitudes and two sampling rates. Velocity calculations were made by using the difference between successive position data points and acceleration calculations were made using the difference of successive velocity data points. In general, plots of the acceleration calculations do not give a recognizable function. Only the larger oscillation amplitude with the longer sampling rate shows a reasonable approximation to a sine function. However, even after repeated smoothing of the curve, the resulting data was not acceptable for accurately tracking mass changes. Therefore, an additional simulation was performed using an effective sampling rate of 25 points per period at an amplitude of 2000. This resulted in data that approximated the beam position to within 2 LSB's of the correct control code (equivalent to an error of

several micrograms). Although this is not acceptable for tracking mass change, it is adequate for tracking abnormally large changes in mass and improving the start up time. On the other hand, the response

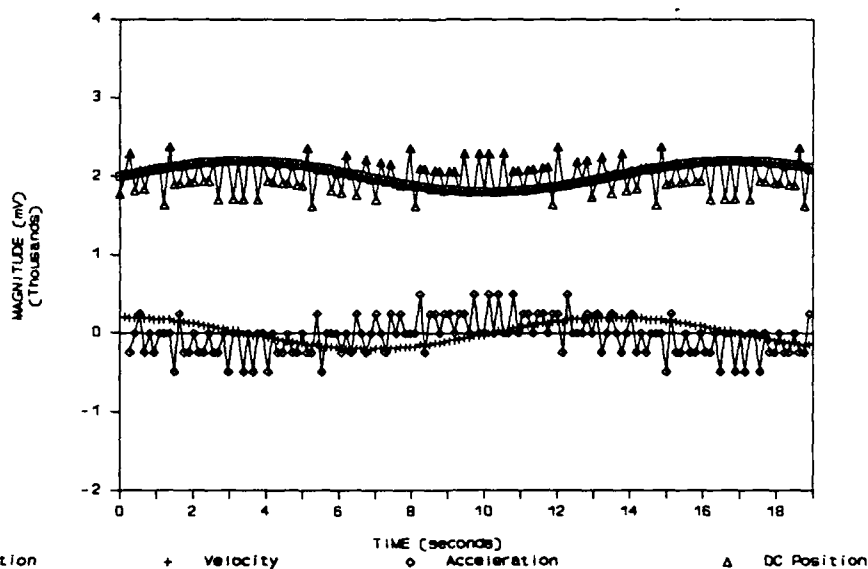


Figure 23a. Dynamic control waveform simulation for an amplitude of 200.

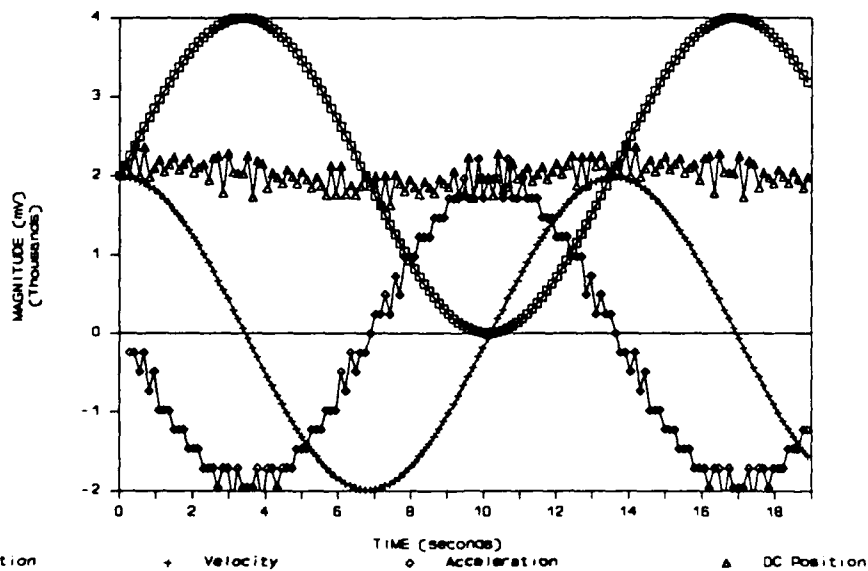


Figure 23b. Dynamic control waveform simulation for an amplitude of 2000.

time is degraded to something on the order of 1 second.⁹ However, considering the performance presently being obtained (20 seconds = average response time) this is a tremendous improvement if it can in fact be realized using experimental data.

Experimental data has an overabundance of nonlinearity and noise problems that need to be resolved (see figure 24). In addition to the digital conversion induced nonlinearity, there is a detector induced nonlinearity problem (figure 24d) which has not been discussed. The larger amplitude represents a significant range of beam motion and the detector output is extremely nonlinear (see figure 25). Worse yet, the balance is subject to shifting of the equilibrium position during large excursions, particularly if the beam should strike one of the stops. Thus, in order to realize reliable performance of the system the range of beam motion must be limited and care

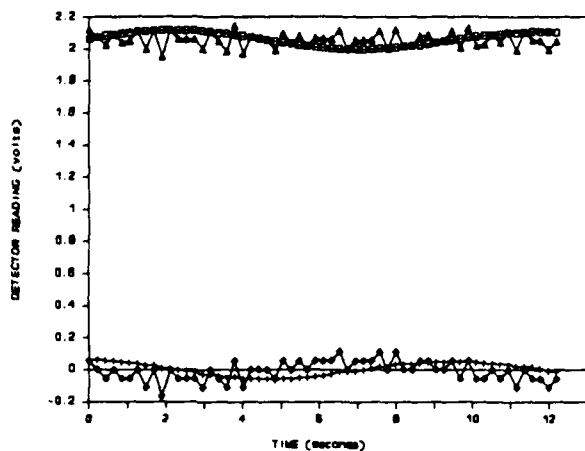


Figure 24a. Illustration of dynamic behavior for oscillation amplitude of 100.

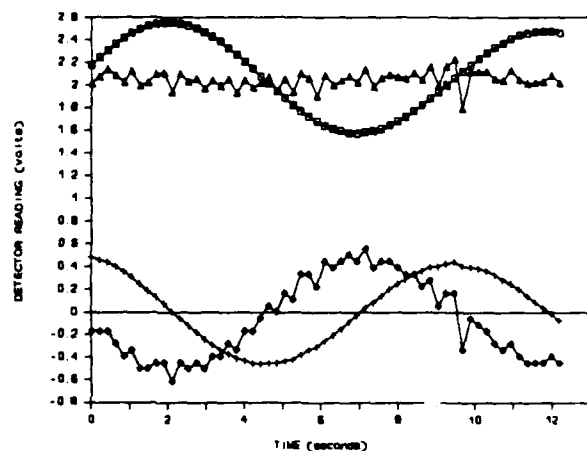


Figure 24b. Illustration of dynamic behavior for an oscillation amplitude of 500.

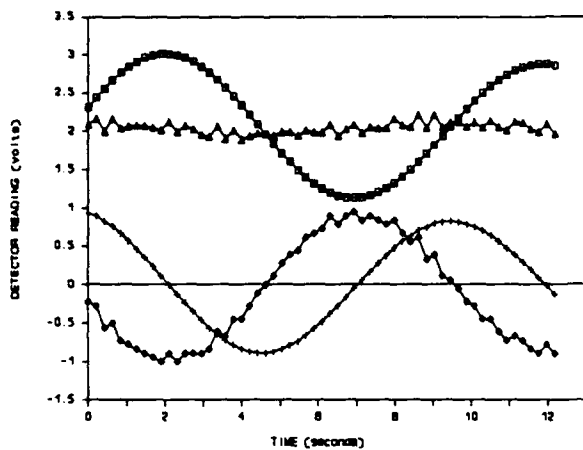


Figure 24c. Illustration of dynamic behavior for an oscillation amplitude of 1000.

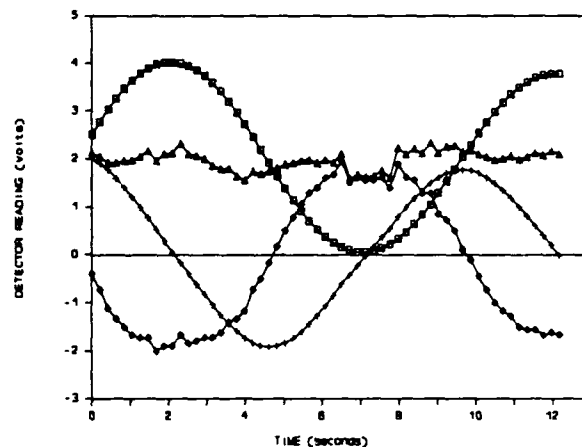


Figure 24d. Illustration of dynamic behavior for an oscillation amplitude of 2000.

must be exercised to ensure that linearity of the detector output is preserved.

Ideally the goal of computer control is to provide rapid response

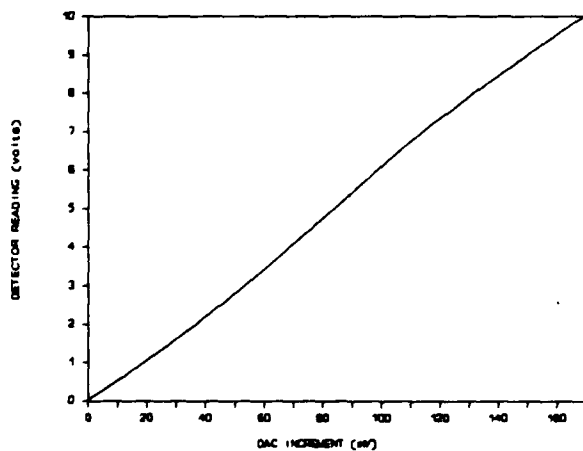


Figure 25a. Illustration of the detector signal nonlinearity.

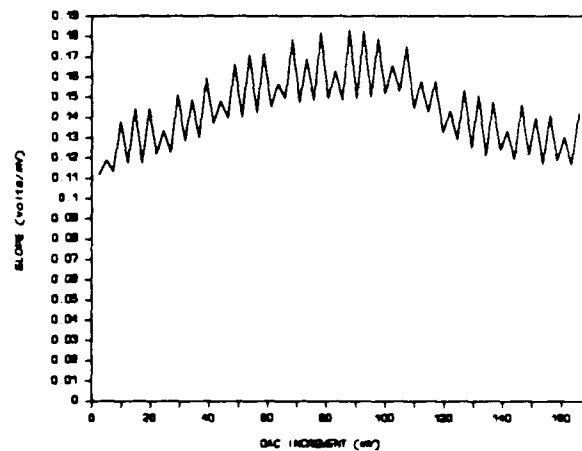


Figure 25b. Slope of the detector linearity curve.

to potentially catastrophic changes in the equilibrium conditions. To this end, several alternate methods of determining acceleration are being considered to obtain a more accurate determination of the acceleration. These methods include:

1. A phase shift of the velocity vector by 90 deg. This gives an equivalent acceleration that is considerably more accurate. After a single pass 3 point moving average the error in the "dc" value was ± 3 LSB's. This is based on a sample rate of 100 points per period and an oscillation amplitude of 2000 LSB's. There is no evidence that the delay can be accurately positioned with experimental data or that the signal noise can be satisfactorily filtered.
2. The use of the velocity to calculate ωt for the acceleration calculation. The angle can be calculated from equation (5) below

$$\omega t = \arccos (y'/A) \quad (5)$$

Here as in (1) the higher accuracy of the velocity provides a more accurate value of the acceleration and therefore a more accurate indication of the mass change with time. The simulation does in fact show a tremen-

dous improvement in the accuracy of the acceleration data and the "dc" error as well for a large range of the period.

3. The use of the time rate of change of the ADC code to determine acceleration values. This appears to be the most promising alternative, but timing problems are impeding progress on this method.

From the simulations it is obvious that the digitized waveforms for the velocity and particularly the acceleration are not well defined. In fact, they are grossly inaccurate for tracking mass changes. Even with large amplitudes, low sampling rates (slow response) and smoothing of the data, acceptable accuracy for tracking mass is not obtainable. However, with an effective sampling rate of 50 points per second the acceleration data is sufficient for tracking mass changes on the order of 1 microgram which is acceptable for maintaining control provided that experimental data can be processed to provide comparable results. This would reduce the response time to about 1 second. It is apparent that high sensitivity and fast response are not feasible with this method of dynamic control. However, during transient conditions which could be deleterious to the continuity of experimental data, there is not a real need for high sensitivity. The important task is preventing the beam from developing excessive oscillation amplitude and correcting for short term

effects that temporarily upset the equilibrium and could be catastrophic to the continuity and integrity of analytical data.

C. MODIFIED DYNAMIC CONTROL

During the development of the dynamic control software several promising characteristics of the detector signal, during forced oscillation of the beam, were observed which had not previously been encountered. These characteristics include the following:

1. Temperature dependency of the oscillation amplitude.
2. Pressure dependency of the oscillation amplitude.
3. Amplitude dependency of the oscillation period.
4. Temperature dependency of the oscillation period.

At the time these characteristics were observed, there was no method of control capable of characterizing this behavior or its temperature relationship. The static control algorithm was not capable of recording dynamic information because there was no characteristic oscillation to record it from. The dynamic control algorithm was capable of collecting the amplitude and period information, but it had not progressed to the state of development which would allow maintaining equilibrium and collecting and/or determining mass data. Interest in being able to collect period and amplitude information during the data collection process stems from the need to filter temperature drift

from the mass data. The capability of temperature compensation from an existing easily filterable parameter would be a significant advance in the development of the control software, giving analytical capability for measuring submicrogram quantities over extended periods of time with a high degree of confidence, and without the use of accurate, but costly temperature control.

Therefore, to evaluate the potential value of the temperature related characteristics, the dynamic control algorithm was modified to average the detector readings over a full period of the forced oscillation. The control process is essentially very similar to the dynamic control method except that on alternate cycles, the beginning of a cycle signals the start of the data sampling process and the end of the cycle signals the end of the sampling process. The data points collected for that 1 cycle are then averaged to give a single data point representing the equilibrium position for the beam during the sampling cycle. The sampling routine was designed to sample on alternate cycles so that the effect of the control force on beam motion would have time to stabilize. At the same time, the idle cycle could be put to good use processing the data, moving data to disk, taking pressure readings, etc. The utilization of the idle cycle for "house-keeping" tasks, also makes possible data collection without upsetting the continuity of the critical data collection process. This results in an increase in the number of samples obtained during the cycle and an improvement in the stability and accuracy of the period and amplitude measurements. It was suspected that the controlled oscillation

would improve the sensitivity. However, this possibility has not been investigated.

There were problems in the initial sampling procedures due to noise in the detector signal. Much of the problem was due to false indications of crossings of the null position. This was corrected by adjusting the number of samples averaged per data point, but it could also have been done by increasing the amplitude of the oscillation. The objective is to detect the null point crossing as accurately and reliably as possible. This is critical to obtaining accuracy and consistency in the data.

Many of the observations in this characterization study are directly applicable to the dynamic control system. Thus far, the results have been promising, but inconclusive. Figure 26 shows the relation of the amplitude, period, pressure and mass parameter drift to each other. Figure 27 shows an earlier illustration of the mass and temperature dependency. The figures illustrate the similarities of the parameter drift characteristics with temperature changes. Several attempts at correcting the mass drift, at constant pressure, by adding the appropriately scaled period drift data to the mass parameter have given promising results. Under conditions of slowly changing pressure, this method of compensation does not give reproducible results. The temperature dependency of the oscillation amplitude has not been characterized, as yet. Assuming that the temperature drift is predominantly dependent on the temperature drift of the photodetector circuitry, amplitude is most likely to be the

appropriate temperature sensitive parameter. However, amplitude is also sensitive to pressure changes in the system particularly at low pressures (below 10 torr). This behavior has not been well characterized and its affect at higher pressure is not known at this time. Further investigation is in progress.

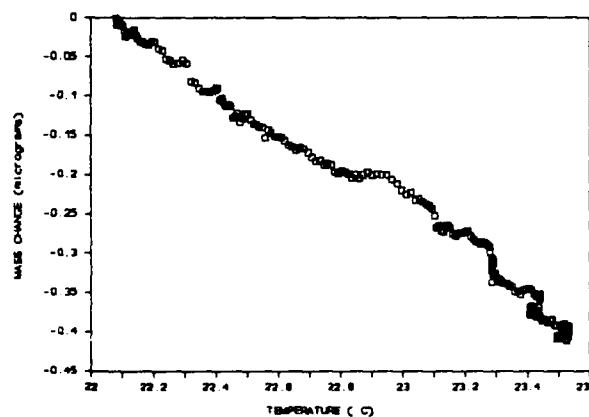


Figure 26a. Illustration of mass dependency on temperature.

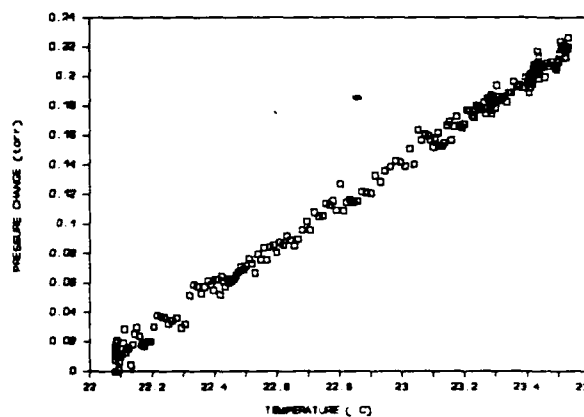


Figure 26b. Illustration of pressure dependency on temperature.

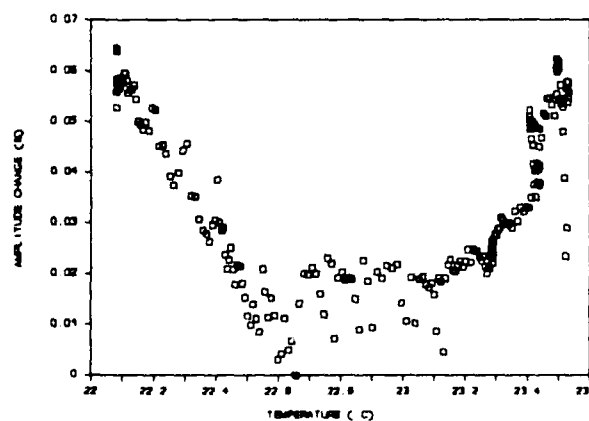


Figure 26c. Illustration of amplitude dependency on temperature.

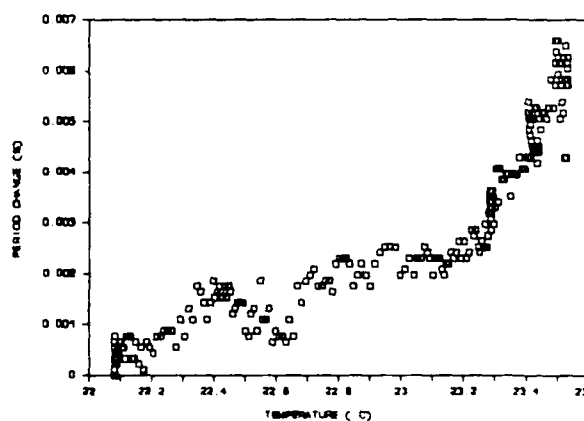


Figure 26d. Illustration of period dependency on temperature.

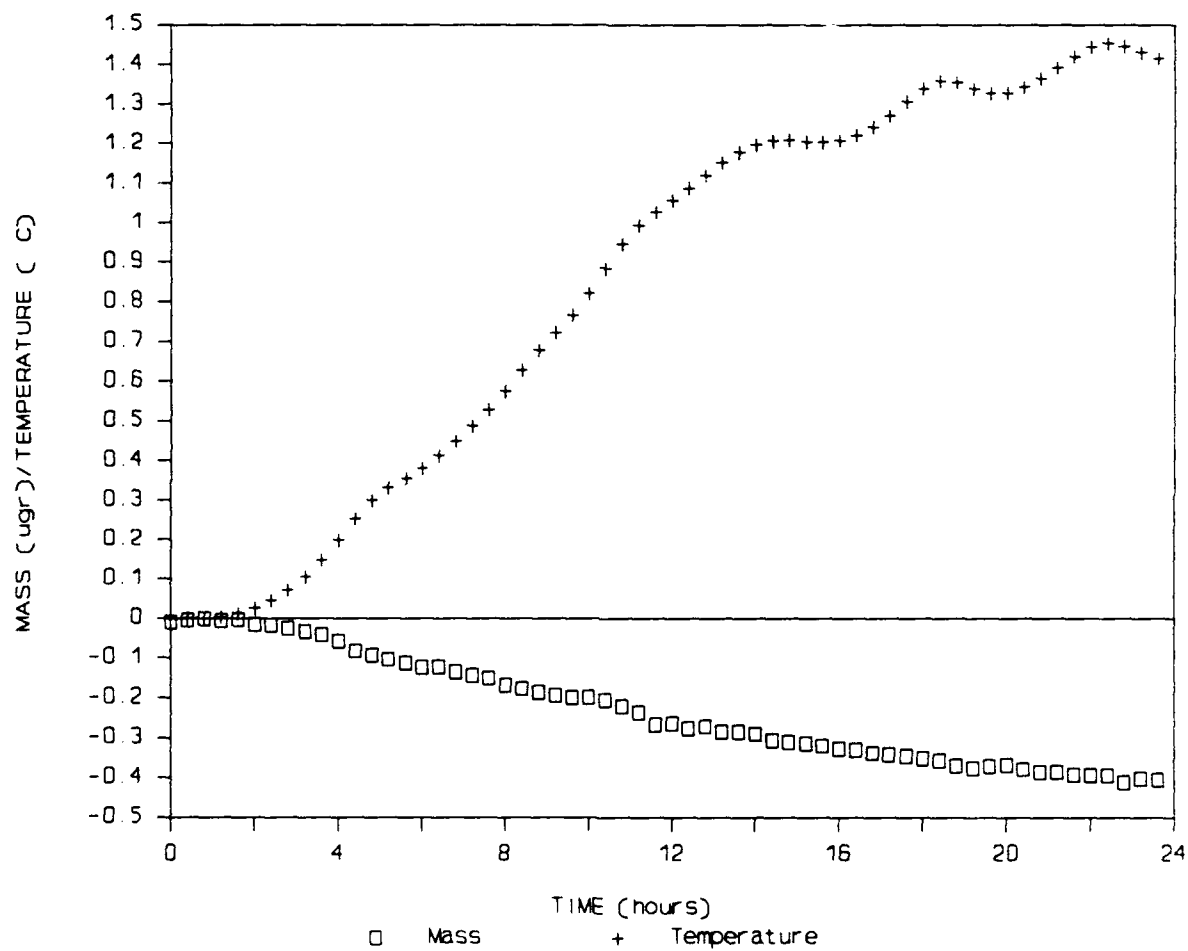


Figure 27. Illustration of the mass parameter temperature dependency.

VI. CALIBRATION •

Some method of accurate calibration of the instrument and its control system is necessary if accurate measurements of mass change are required. The most widely used technique for calibration is probably the direct method. This procedure involves adding known amounts of mass to the sample side of the balance and recording the change in the mass related parameter (in this case the output voltage of the DAC or the DAC/ADC code) required to return the balance to equilibrium. However, this method of calibration is inappropriate for some balance designs. The RADC balance for example, because the tare and sample masses are suspended from quartz fibers which are not rigidly attached to the beam, is subject to shifting of the equilibrium position. This occurs because of slight changes in the position of the fibers where they hook over the beam. The result is a slight imbalance in the equilibrium conditions requiring a corresponding change in the coil current required to maintain equilibrium which corresponds to an equivalent mass change that can range from several tenths to several micrograms. Therefore, to minimize such errors, a different method of calibration is needed for this instrument. The principle of Archimedes provides an accurate method not only of calibrating the balance but for determining sensitivity and reproducibility as well.

The ideal force equation for the balance in equilibrium can be written as:

$$F_c = F_2 + F_{b1} - F_1 + F_{bt} \quad (3)$$

where F_2 and F_1 are forces associated with the two weights W_2 and W_1 , F_c is the compensation force generated by the coil, and F_{b1} and F_{bt} are forces resulting from buoyancy effects acting on the sample and tare weights respectively. It is assumed the two weights W_2 and W_1 have equal masses ($m_2 = m_1 = m$), the balance beam arm lengths are equal, and for simplicity, first and higher order error terms due to asymmetry in the balance and friction (mechanical and gas related) are considered negligible. Therefore, in this ideal case, the required force F_c is due only to the difference in volumes of the gas displaced by the two weights. This is known as the "buoyancy" effect. Since $F_2 = F_1$ and $F = m \times a$, the force equation can be rewritten as

$$\frac{F_{c1}}{a} = m_{b1} - m_{bt} \quad (4)$$

and F_{c1}/a can be represented as an equivalent mass m_c^* . This results in an equation that expresses the equivalent compensation mass (m_c^*) in terms of the two masses of gas displaced by the sample (m_{b1}) and the tare (m_{bt}) weights:

$$m_c^* = m_{b1} - m_{bt} \quad (5)$$

Using the ideal gas law ($PV = nRT$) the mass difference of this displaced gas can be written as:

$$m_x = PV \times \frac{MW}{62.364 \times T} \quad (6)$$

where

P = the pressure in atmospheres corrected to 0°C (273.13°K)

V = the volume of gas displaced, by the mass m_x , in liters
(or $\text{cm}^3 \times 10^{-3}$)

MW = the molecular weight of the gas displaced.

62.364 is the molar gas constant (R) of an ideal gas in $\text{cm}^3 \text{ torr/mole } ^\circ\text{K}$, and T is the temperature of the displaced gas in $^\circ\text{K}$. Combining equations (5) and (6) gives:

$$m_c^* = P(V_{b1} - V_{bt}) \times \frac{MW}{62.364 \times T} \quad (7)$$

In arriving at equation (7), it was assumed that symmetrical or negligible volume effects were contributed by the balance beam, suspension fibers, and the magnet. Since this is not the case and because their contributions are unknown, equation (7) cannot be used directly. However, the unknown contributions can be lumped into a single term (V_x). Then using two samples with equal masses but different volumes, and taking the difference between their equivalent compensation masses under identical conditions of pressure and temperature gives:

$$m_{c2} - m_{c1} = P[(V_{b2} - V_{bt} - V_x) - (V_{b1} - V_{bt} - V_x)] \times \frac{MW}{62.364 \times T} \quad (8)$$

Finally, differentiating equation 8 with respect to pressure, gives the following useful result:

$$\frac{d(m_{c2})}{dP} - \frac{d(m_{c1})}{dP} = (V_{b2} - V_{b1}) \times \frac{MW}{62.364 \times T} \quad (9)$$

Notice that equation (9) does not contain the unknown quantities.

Referring again to figure 11 and the control circuit description we see that F_c , and thus m_c^* , is related to the output voltage of the DAC. Therefore, we can define m_c^* and its derivative in terms of the DAC output voltage¹ E_c . Thus,

$$m_c^* = S \times E_c \quad (10)$$

and

$$\frac{d(m_c^*)}{dP} = S \times \frac{d(E_c)}{dP} \quad (11)$$

where S is the voltage to mass conversion factor (e.g. micrograms per millivolt) and $d(E_c)/dP$ is the slope (s_{b1}) of the voltage versus pressure curve for the calibration sample. From equations 9,10 and

¹. The use of digital to analog converters reduces the desirability of voltage to mass correlation. The voltage output of the DAC can not be determined directly. ADC or DAC codes must be converted to voltage. Such conversions unnecessarily complicate the mass conversion calculation and introduce additional, undesirable errors. Since the mass is being tracked through changes in the digital converter codes, it follows that mass changes are more appropriately calculated directly from the converter codes.

11 we arrive at the following ideal equation for calibrating the balance using two weights of equal mass and different but known volumes:

$$S = \frac{(V_{b2} - V_{b1})}{(S_{b2} - S_{b1})} \frac{(MW)}{62.364 \times T} \quad (12)$$

Equation 12 gives an approximate value of the voltage to mass conversion factor which can be in error by 5% or more depending on the temperature and pressure conditions during an analysis. A more accurate value is obtained by multiplying the denominator by the compressibility factor⁹ (z) for the gas used in the calibration, and by correcting for temperature effects. Nitrogen gas in the pressure range of ultrahigh vacuum up to one atmosphere, at room temperature requires temperature correction only, because it behaves nearly ideally (from Van der Waal's equation of state for real gases).¹⁰ If the equation is multiplied by a factor of 10^3 and E_c is expressed in millivolts, the mass conversion factor will be in micrograms per millivolt. Assuming that both samples are run at the same temperature, if we include the compressibility factor (z) and correct for temperature, the final equation becomes:

$$S = \frac{(V_{b2} - V_{b1}) \times (MW) \times 10^3}{(S_{b2} - S_{b1}) \times 62.364 \times z \times T} \quad (13)^9$$

Calibration of the balance under control by the digital circuit described above was performed using nitrogen gas at low pressure. The calibration was performed using a gas density bulb for the larger

volume and an equal mass of gold for the smaller volume. All samples were cleaned, to remove organic and inorganic contaminants, prior to loading into the balance. After loading the sample, the balance was evacuated to less than 5×10^{-5} torr to remove residual solvents and check for leaks. When all leaks were found and sealed the balance was backfilled with dry nitrogen to 10 to 50 torr and allowed to stand until sample and tare weights stopped swinging. The system was then pumped to low pressure and calibration begun. Nitrogen gas was introduced into the balance in pressure increments of 10 to 30 torr at 15 minute intervals. Pressure and voltage readings were recorded by computer throughout the calibration. Representative values of the pressure/ voltage data can be found in Table II.

Figures 28a and 28b illustrate graphically the data plotted along with the "linear least squares fit". Figure 29 illustrates a sample calculation by substitution of the indicated values into equation 13.

Table II

Calibration data.

Gold		Gas Density Bulb	
Pressure (torr)	Output Voltage (volts)	Pressure (torr)	Output Voltage (volts)
1.07	.0299	1.00	4.6871
2.03	.0588	2.41	4.4332
3.06	.0866	5.08	3.9556
4.00	.1125	7.04	3.6109
5.02	.1413	9.66	3.1468
6.01	.1671	11.09	2.8990
7.01	.1935	13.12	2.5389
8.01	.2236	16.48	1.9429
9.01	.2515	17.97	1.6782
10.27	.2878	19.64	1.3821
11.20	.3166		
12.11	.3420		
13.05	.3662		
13.99	.3906		
15.11	.4256		
16.05	.4496		
17.01	.4775		
18.02	.5065		
19.00	.5318		
20.00	.5609		

Calibration Data for Gold/Nitrogen

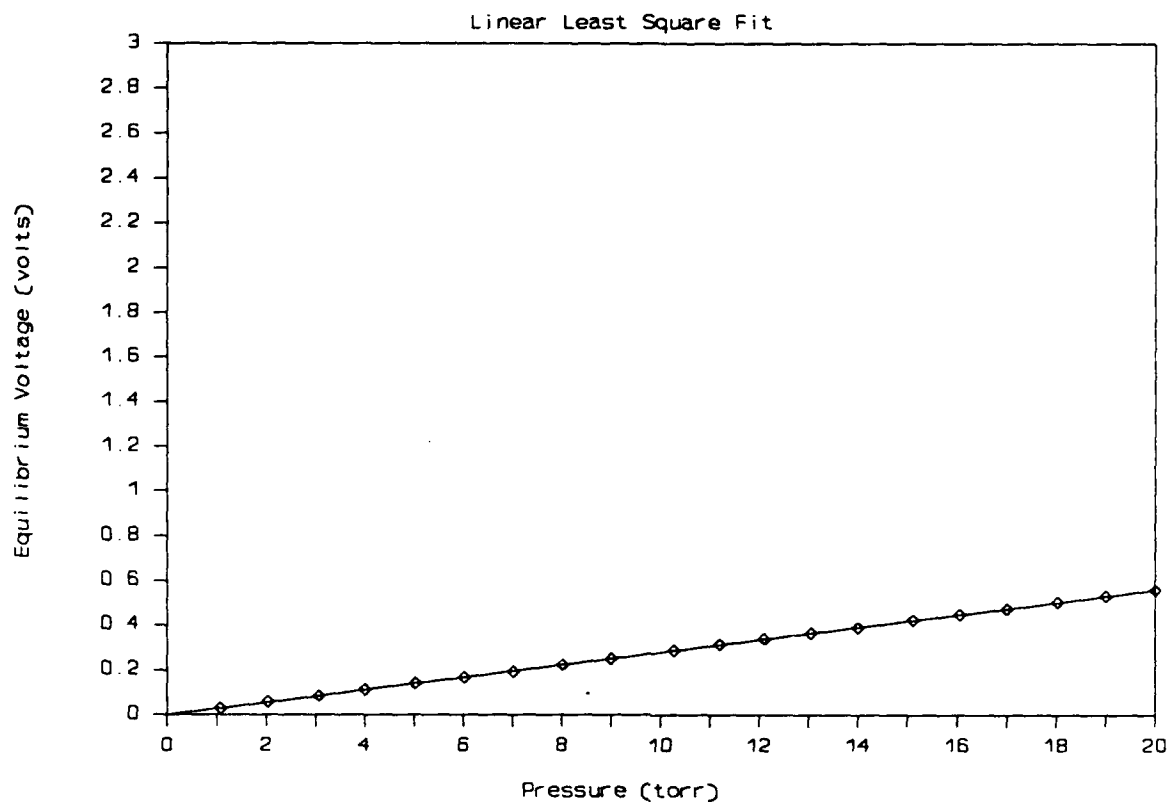


Figure 28a Sample buoyancy plot for gold metal in dry nitrogen.

Std Err of Y Est	1.5	mV
Slope	28.05	mV/torr
Std Err of Slope	0.06	mV/torr
Correlation Coefficient	0.99996	
Average Temperature	22.5	°C

Calibration Data for Gas Density Bulb

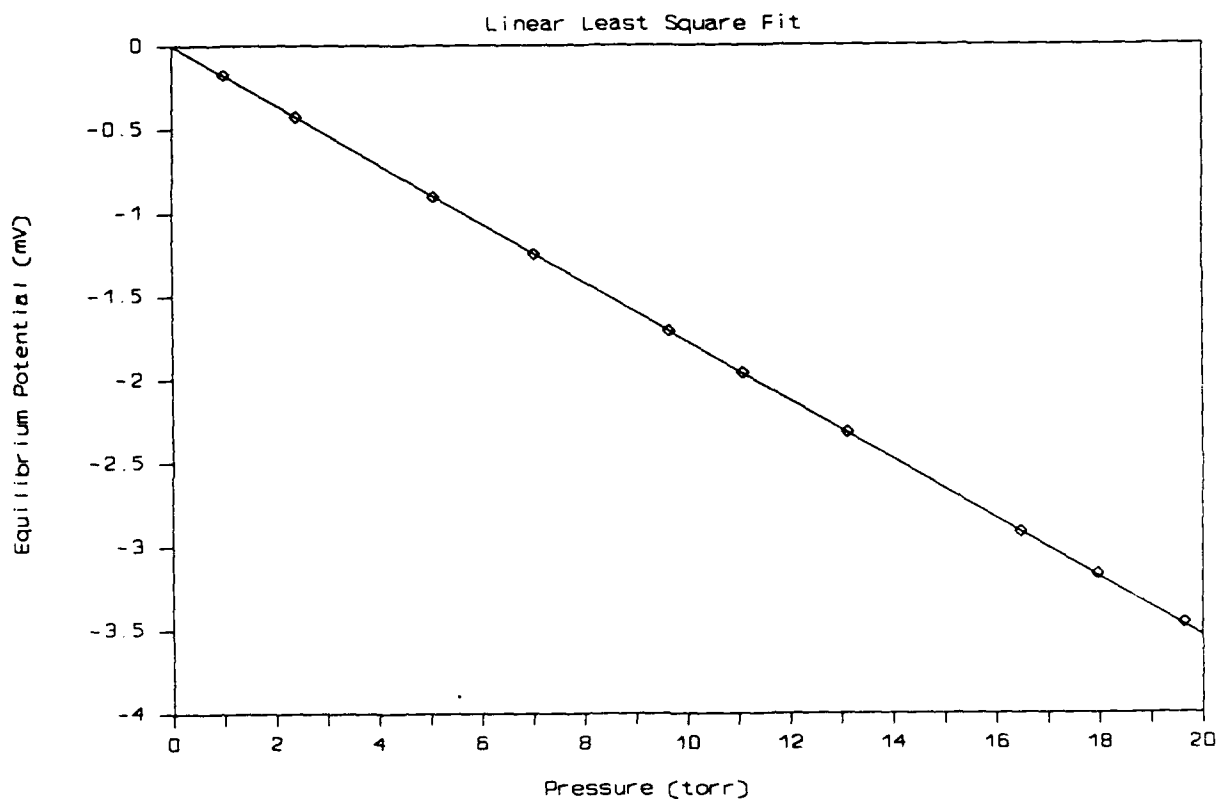


Figure 28b. Sample buoyancy plot for gas density bulb in dry nitrogen.

Std Err of Y Est	3.08	mV
Slope	- 176.97	mV/torr
Std Err of Slope	0.22	mV/torr
Correlation Coefficient	0.999995	
Average Temperature	22.2	°C

Volume of Gold	V_{b1}	0.02384	cm ³
Slope (GD Bulb cal curve)	S_{b2}	-176.97	mV/torr
Slope (Gold cal curve)	S_{b1}	28.05	mV/torr
Molecular Weight of Nitrogen	MW	28.02	gr/mole
Volume of Gas Density Bulb	V_{b2}	3.375	cm ³

$$S = \frac{(V_{b2} - V_{b1})}{(S_{b2} - S_{b1})} \times \frac{MW}{62.364} \times \frac{10^3}{zT}$$

$$S = \frac{(3.375 - .02384)}{(-176.97 - 28.05)} \times \frac{28.02}{62.364} \times \frac{1000}{273.16}$$

$$S = -.016346 \times 0.44929 \times 3.6608$$

$$S = .02688 \text{ } \mu\text{gr/mV}$$

FIGURE 29. Sample calculation.

VII. EXPERIMENTAL

The following experimental results are from data collected using the control hardware described above under "Digital Circuit Description." At the time the computer was not capable of performing the control function, however, the data was recorded by computer.

The sample under investigation was a devitrifying sealing glass (type 75-83) used for obtaining a hermetic seal in microcircuit packages. Under normal sealing conditions it was found that water vapor was being released into the package cavity during processing creating an excessively wet internal environment (15000 ppmv water vapor). However, over an extended period of time this water content slowly decreases even at temperatures in excess of 125°C, ultimately creating extremely dry conditions (2000 ppmv or less of water vapor) within the package after which the package cavity was found to remain dry even at temperatures greater than 200°C. To evaluate the possibility of moisture introduction into the package by the sealing glass at high temperatures during processing, and the affinity of the glass for water after processing, samples of the glass before and after processing were analyzed.

Initially the system was calibrated using the "buoyancy" technique as described above. The resulting values were substituted into equation 13 and a calibration factor of 0.05608 microgram/millivolt (0.1369 $\mu\text{gr}/\text{LSB}$ for a 12 bit DAC) was obtained. Glass from recently sealed packages (which had seen processing temperatures greater than

450°C) was removed from the sample package and pressed into a small pellet which had a mass of 0.5048 gram. This sample was designated as "glass sample B", "glass sample A" being the unprocessed glass. It was loaded into the microbalance in a quartz cup along with enough gold wire (approximately 14 gauge) to give a total mass of about 5 grams. The system was sealed and pumped down into the 10^{-4} torr region and held there for 1 to 2 hours. Nitrogen gas was then introduced into the system until a pressure of about 7 torr was reached. Buoyancy data was collected for several pressure increments for error correction and then the pressure was adjusted to about 5 torr. At that time approximately 5 torr of water vapor was introduced. (The system temperature was at room ambient -- approximately 23°C). The mass of the sample increased by more than 40 micrograms during the next 12 minutes (see figure 30). The system was then pumped to less than 10^{-4} torr and held there overnight.² Nitrogen gas was introduced into the system until a pressure of 10 torr was achieved. The sample was then heated to 200°C and held at that temperature for about 17 hours, during which there was a mass loss of 16.7 micrograms. The sample was still losing mass at the rate of 0.5 microgram per hour at the end of the 17 hour period.

² The mass change of the sample could not be tracked accurately during pumpdown. Once the pressure enters the laminar flow region the digital controller is not capable of tracking the rapidly changing force unless extremely slow pumping rates are used. During the uncontrolled state it is likely that changes in the moment arms will occur causing a change in the force required to maintain equilibrium in addition to the mass change that is occurring. This is one reason why development of the dynamic control software is important.

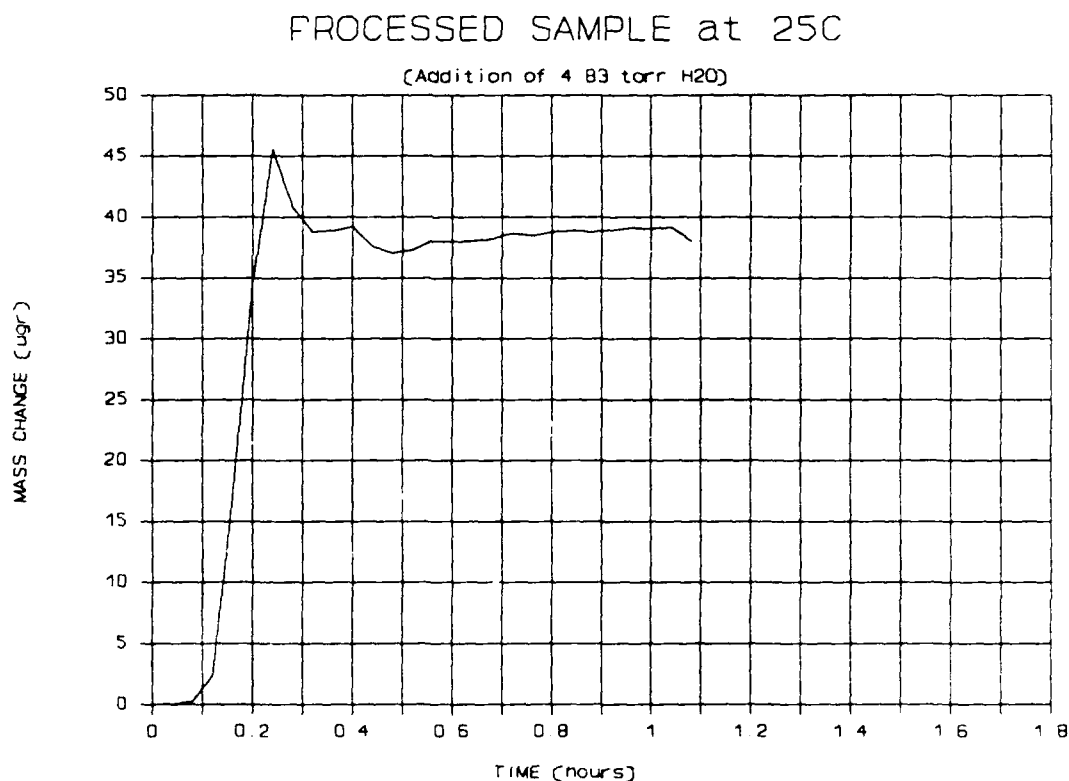


Figure 30. Adsorption of water vapor on sample of processed sealing glass.

With the sample temperature still at 200°C, water vapor was introduced into the system in several increments (see figure 31). The first increment corresponded to an increase in pressure of 2 torr. The sample mass increased about 20 micrograms during the following 2 hour period. At that time an additional 2 torr of water vapor was introduced for a total water vapor pressure content of 4 torr. There was an additional increase of 25 micrograms during the next 2 hour period and another 15 micrograms overnight. The total increase in mass at 200°C at 4 torr pressure was 77 micrograms (0.02%) in 24

hours. A final increment of 2 torr was introduced into the system giving a mass increase of another 15 to 16 micrograms in 4 hours. Note in figure 31 that each time the water vapor pressure was increased, there was an immediate uptake of approximately 10 micrograms, followed by a period of equilibration during which the glass continued to gain weight at a decreasing rate.

Release of moisture by the glass, into the package cavity at elevated temperature, would have a negative impact on device

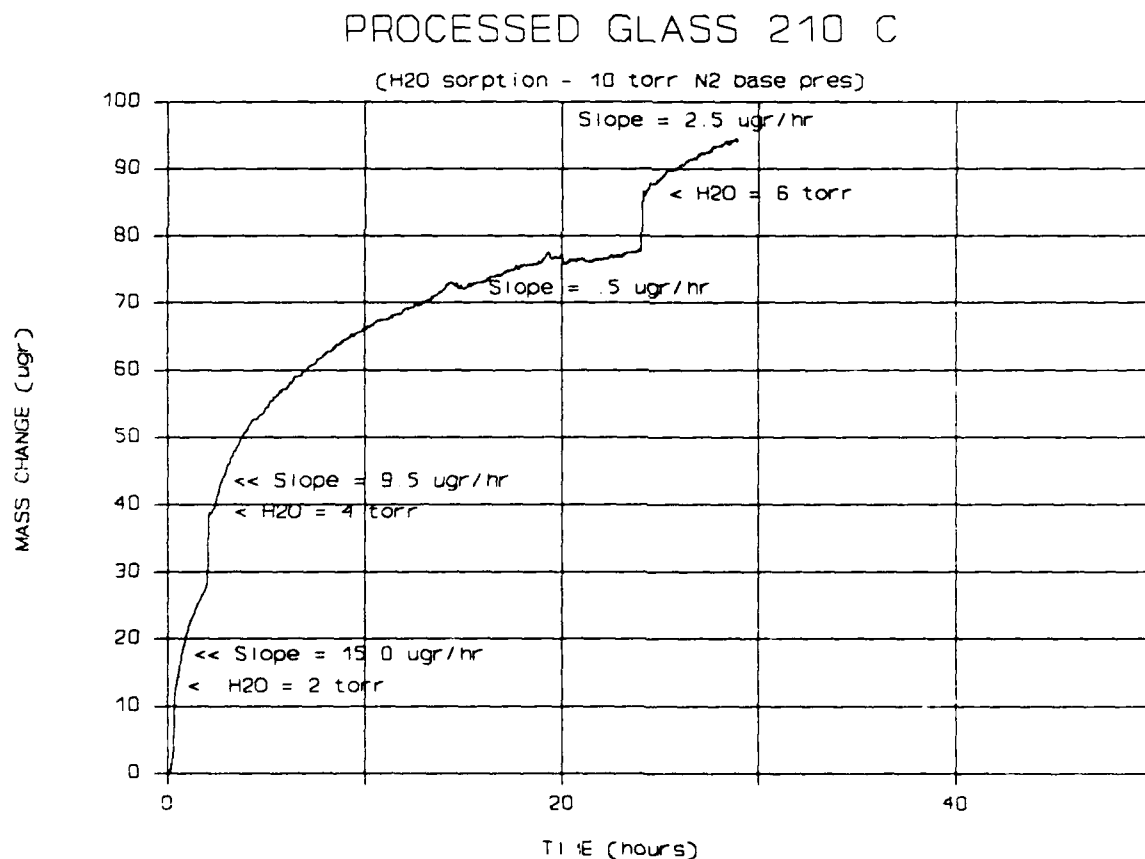


Figure 31. Adsorption of water vapor on unprocessed sealing glass powder at 210 °C.

reliability. The data, however, shows that exposure of the processed glass to temperatures of up to 250°C for up to an hour did not cause water to be released from the glass. In fact, it was found that water was adsorbed by the glass at temperatures in excess of 200°C.

Desorption of water from the glass was found to occur very slowly at temperatures below 300°C in dry ambients. At temperatures of 350°C and above, in a dry ambient, desorption is relatively fast and complete after a few hours. However, the glass undergoes a state or phase change (see figure 32) at temperatures in the range of 300°C to 350°C and above, and thus the glass cannot be effectively dried prior to sealing.

It was concluded that there is little or no degradation in device reliability when type 75-83 sealing glass is used because of the desiccant property of the glass. Within a few weeks the water vapor content of the package is reduced well below acceptable limits. This drying process is irreversible at temperatures likely to be experienced by any silicon based IC.

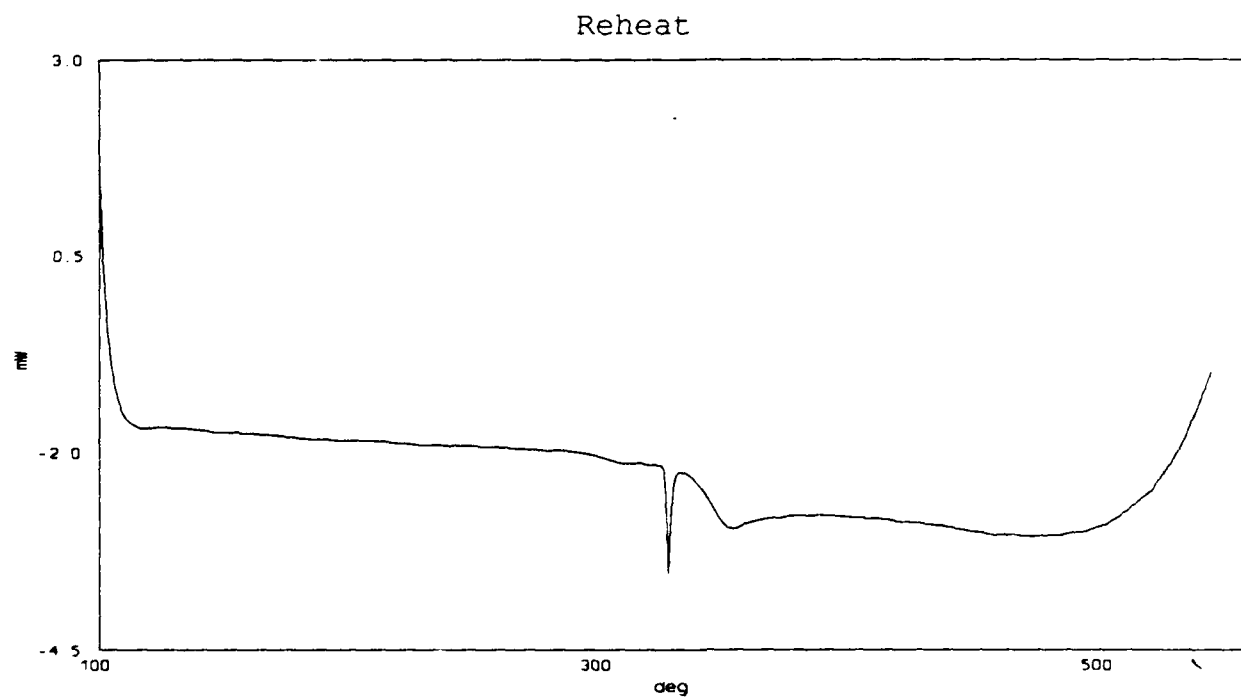
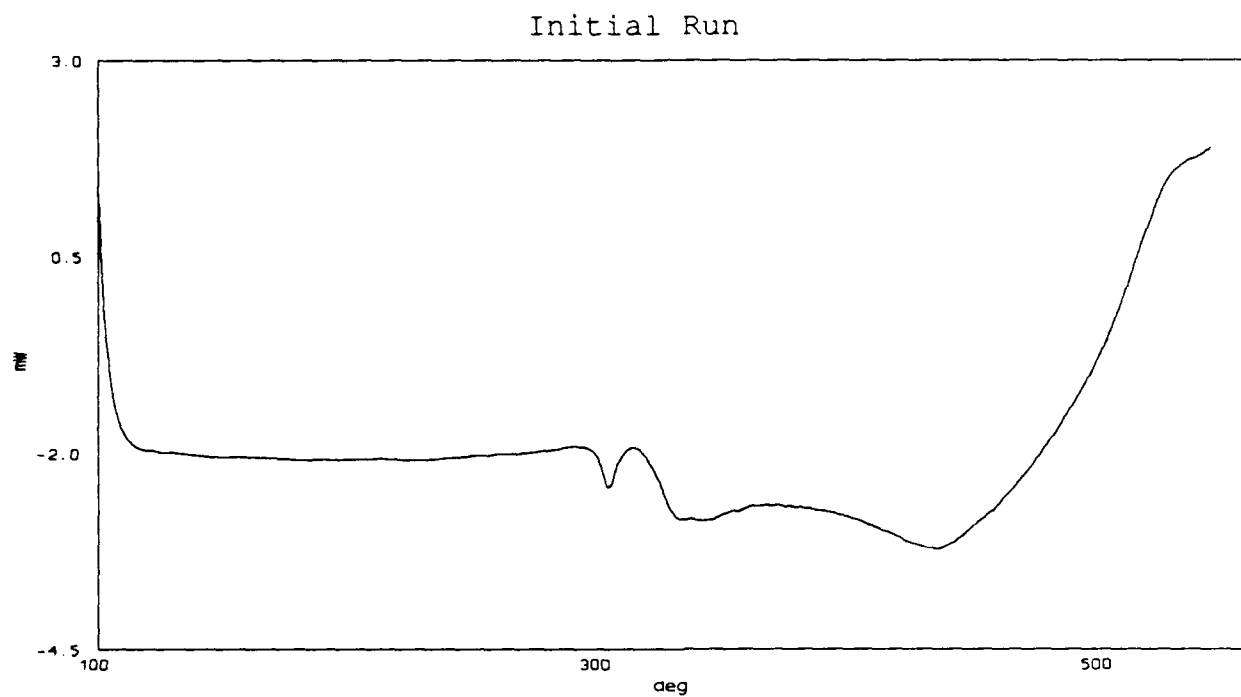


Figure 32. Differential scanning calorimeter (DSC) spectra showing irreversible change in sealing glass at processing temperatures.

VIII. SUMMARY

The objective of replacing the "Rodder" electronic microbalance control system with a more stable controller which is totally automatic has been satisfied. Faster response time and temperature compensation are still desirable features, and a number of alternatives have been presented which show promise in solving the problems that are preventing the completion of this task.

The digital circuit of figure 11 was the first successful working control system that met the majority of the requirements for a stable automatic system. It was capable of submicrogram resolution, operated reliably on a continuous basis and demonstrated acceptable response times for most operations. However, it does require occasional attention by the operator, has a very restrictive range to sensitivity ratio, and is not capable of total automation. Additional equipment including a computer is required for data collection, reduction and analysis. All the desired features of a completely automated system could be incorporated into the hardware but not as easily, efficiently, economically or with the same degree of flexibility as software implementation via computer.

Several variations of computer control have been discussed which have been defined as: static, dynamic, and modified dynamic. It was found that for the static case, the conditions for true static operation were not met. There is always some degree of oscillation of the beam as well as a significant amount of vibration. The response of

the system is relatively slow and this method lacks some useful features that are available with dynamic control methods. The use of the combined DAC and ADC codes to track mass change increased the range to sensitivity ratio by a factor of 40 over that of the "digital" controller. This is a significant improvement for 12 bit converters, but it does not represent optimum performance.

Much of the software development to date has been directed at bringing the balance to equilibrium quickly and reliably, and maintaining equilibrium once achieved. Software to maintain control during adverse conditions such as gas introduction or pump down into the low pressure region has not been implemented. Excessive noise on the detector signal has been an annoying and persistent problem that degrades and limits the capability of the microbalance dynamic control software. Limited sampling rate capability and aliasing problems have resulted in the use of passive filtering and buffering of the signal to minimize the noise problem, but at the expense of poorer response time. Data analysis and reduction techniques are still being developed and evaluated. As yet there is no indication of the ultimate sensitivity obtainable with the system, but a sensitivity of 0.2 microgram should be routinely obtainable.

In addition to electrical/electronic problems there are also mechanical effects that can affect the performance of the balance. These effects include but are not limited to the following.

1. Effects generated by other modes of oscillation of the

balance which may be induced by vibration, changes in pressure, magnetic disturbances, mechanical shock, etc.

2. The long suspension fibers and their associated masses at each end of the beam, act as pendulums. As such they have normal modes of oscillation as well as precession. It is this precession that complicates the harmonic spectrum and makes filtering of the resulting detector noise spectrum difficult. However, much of this oscillation will damp out relatively quickly at pressures above a few torr. It is usually at very low pressure that these become a problem because the oscillation can continue for an indeterminate length of time.
3. The hooks that attach the fibers to the balance beam and the sample and tare masses can also be a source of difficulty. If these are made too large they will act as springs giving harmonic oscillation induced by vibration that is difficult or impossible to damp. The only correction for this problem is replacement or rework of the fiber.

Temperature drift has been a major problem with all designs of the control system, and it limits the useful sensitivity of the balance for most analysis. The biggest contributor to temperature drift is

the infrared emitter/detector pair. The Rodder electronics used matched IRED's (infrared emitting diodes) and detectors in a bridge circuit to minimize temperature and aging effects. This has some advantages particularly when the infrared absorption properties of the path are changing during an experiment, but it was ineffective unless closely matched detector/emitter pairs were used. The use of a single high efficiency IR emitter in conjunction with a low leakage photodetector and proper temperature compensation of the IR emitter will reduce the temperature related drift to a few tenths of a microgram. Other probable sources of temperature drift include the coil resistance, the magnetic field generated by the permanent magnet and the quartz beam itself.

The temperature dependence of the coil resistance has been eliminated as a serious source of error by using a high compliance current source to supply the control current. Test results show no noticeable difference in the magnitude of drift when the equilibrium coil current is near zero as opposed to when it is carrying a significant current. This result indicates that the magnetic fields of both the coil and the magnet are not significantly affected by temperature.

At the present time there is no evidence to support a significant amount of temperature drift due to the quartz beam itself. All testing performed, thus far, singles out the detector circuitry as the major source of temperature drift, and there is strong evidence that this can be corrected through IRED biasing and/or calibration of one or more temperature sensitive parameters.

A routine analysis, on a devitrifying sealing glass (type 75-83) sample, was presented for demonstration purposes. The magnitude of the mass change during water adsorption and desorption during this analysis was large enough to mask the effects of temperature and buoyancy. Surface adsorption on bulk samples such as metal foils, semiconductor wafers, ceramic lids, passivation layers, and, also, determination of porosity and pore size of surface layers on bulk materials are more representative of the analytical capability of the instrument.

A number of other samples have been analyzed during the course of this work and are briefly mentioned for information. They include the following:

1. High voltage capacitors, from an aircraft related application, were causing system failures because of degradation of the capacitor dielectric properties. Analysis of the moisture absorption characteristics of a small volume removed from the interior of one of the supplied samples supported the theory that the capacitor seal was not hermetic and that water was diffusing into the dielectric causing high electrical leakage and, thus, degradation of in circuit performance.
2. A silicon wafer with a thick, thermally grown, oxide layer was analyzed to determine the effective surface

area, and the pore size and density. The wafer was a sample of material under investigation for use as an in-package moisture monitor. The analysis was not conclusive due to temperature drift, problems with the seal of the quartz tube encapsulating the magnet, and cracks in the quartz balance beam.

3. A sample of a porous ceramic material was analyzed for possible application as calibration standards for the moisture analysis of IC packages. Several water vapor adsorption and desorption test runs were made. The samples showed water vapor adsorption to be much less than 1 microgram, which was too little to be useful as a calibration standard.
4. Considerable experimental data for water adsorption on nickel metal foil has been collected. However, interfering reactions including temperature, and buoyancy effects have complicated the analysis. It is apparent that water vapor adsorption is occurring, but the exact shape of the adsorption curve is obscure.
5. A sample of gold metal foil with a surface area greater than 100 cm² was analyzed for water vapor adsorption. No detectable mass change was observed which supports

the findings of other researchers.

6. Vapor deposited aluminum on a silicon substrate was analyzed to determine the density of the aluminum film. The film thickness was found to be much less than expected making the volume immeasurable with the available support instrumentation.

Additional studies which have been performed with RADC's ultragravimetric microbalance are included in Appendix F.

BIBLIOGRAPHY

1. D S Peck and C H Zierdt, Jr, "Temperature-Humidity Acceleration of Metal-Electrolysis Failure in Semiconductor Devices," Proc. of the 1973 Reliability Physics Sym., pp. 146-152.
2. H Koelmans, "Metallization Corrosion in Silicon Devices by Moisture-Induced Electrolysis," Proc of the 1974 Rel Phys Sym, pp 168-171.
3. R W Thomas, "Moisture, Myths, and Microcircuits." IEEE Trans Parts, Hybrids, pkg, Vol PHP-12, pp 167-171, Sept 1976.
4. R.Vasofsky and A W Czanderna and R W Thomas, "UHV system for the ultramicrogravimetric study of samples loaded in a controlled environment." J Vac Sci Tech, 16(2), Mar/Apr 1979.
5. A W Czanderna, in Vacuum Microbalance Techniques, Vol 4, edited by P M Waters (Plenum, New York, 1965), p 175.
6. J Rodder, in Vacuum Microbalance Techniques, Vol. 8, edited by A W Czanderna (Plenum, New York, 1971), p.43.

7. R W Vasofsky, "Water Vapor Sorption of Package Sealants."
8. A W Czanderna and J M Honig, "Sensitive Quartz Beam Microbalance." Anal Chem, Vol 29, p1208, Aug 1957.
9. GW Castellan, PHYSICAL CHEMISTRY. Reading Massachusetts Addison - Wesley Publishing Co., p. 28-31, 1964.
10. Handbook of Chemistry and Physics, 47TH edition, edited by Robert C. Wheast, Ph. D. (The Chemical Rubber Co., 1978-1979), p. D-230.
11. METHODS AND PHENOMENA, THEIR APPLICATIONS IN SCIENCE AND TECHNOLOGY, Vol 4., Microweighing in Vacuum and Controlled Environments, edited by A.W. Czanderna and S.P. Wolshy. (Elsevier Scientific Publishing Co., Amsterdam, New York. 1980.

APPENDIX A

IBM DATA ACQUISITION AND CONTROL ADAPTER

The IBM data acquisition and control adapter has four (4) analog input channels (12-bit resolution), two (2) analog output channels (12-bit resolution), 16-channel digital input port, 16-channel digital output port, 32-bit timer (programmable sample rates), and 16-bit timer/counter (event counter, programmable rate generator, or programmable time delay).

ANALOG INPUTS

The analog input functions of the adapter operate in either programmed or interrupting mode. The analog input functions provide 12-bit relative accuracy.

Resolution	12 bits
Input channels	four, differential
Input modes	unipolar or bipolar, user selectable

Input ranges	
unipolar	0 to +/- 10 volts, user selectable
bipolar	+/- 5 and +/- 10 volts, user selectable
Output mode	
unipolar	straight binary
bipolar	offset binary
Input impedance	> 100 megohms with 100 pico-farads
Input Current	limited to < +/- 4 mA
Input voltage	
Normal mode	+/- 30 volts maximum, without damage, power on or power off
Common mode	+/- 11 volts maximum
Common mode	
Rejection ratio	72 db
Integral linearity	+/- 1 LSB maximum error

Differential Linearity

Error	+/- 1/2 LSB maximum
Stability	+/- 5 ppm/degree C of FSR (max)

Gain

Error	+/- 0.1% between ranges (max) any range adjustable to 0
Stability	+/- 32 ppm/degree C of FSR (max)

Offset

Error	adjustable to 0
Unipolar stability	+/- 24 ppm/degree C of FSR (max)
Bipolar stability	+/- 24 ppm/degree C of FSR (max)

Monotonicity	0 to 50 degrees C
--------------	-------------------

Throughput to memory	15000 conversions/sec (min)
----------------------	-----------------------------

ANALOG OUTPUTS

The analog output functions of the adapter operate in programmed I/O mode. The analog output functions provide 12-bit relative accuracy.

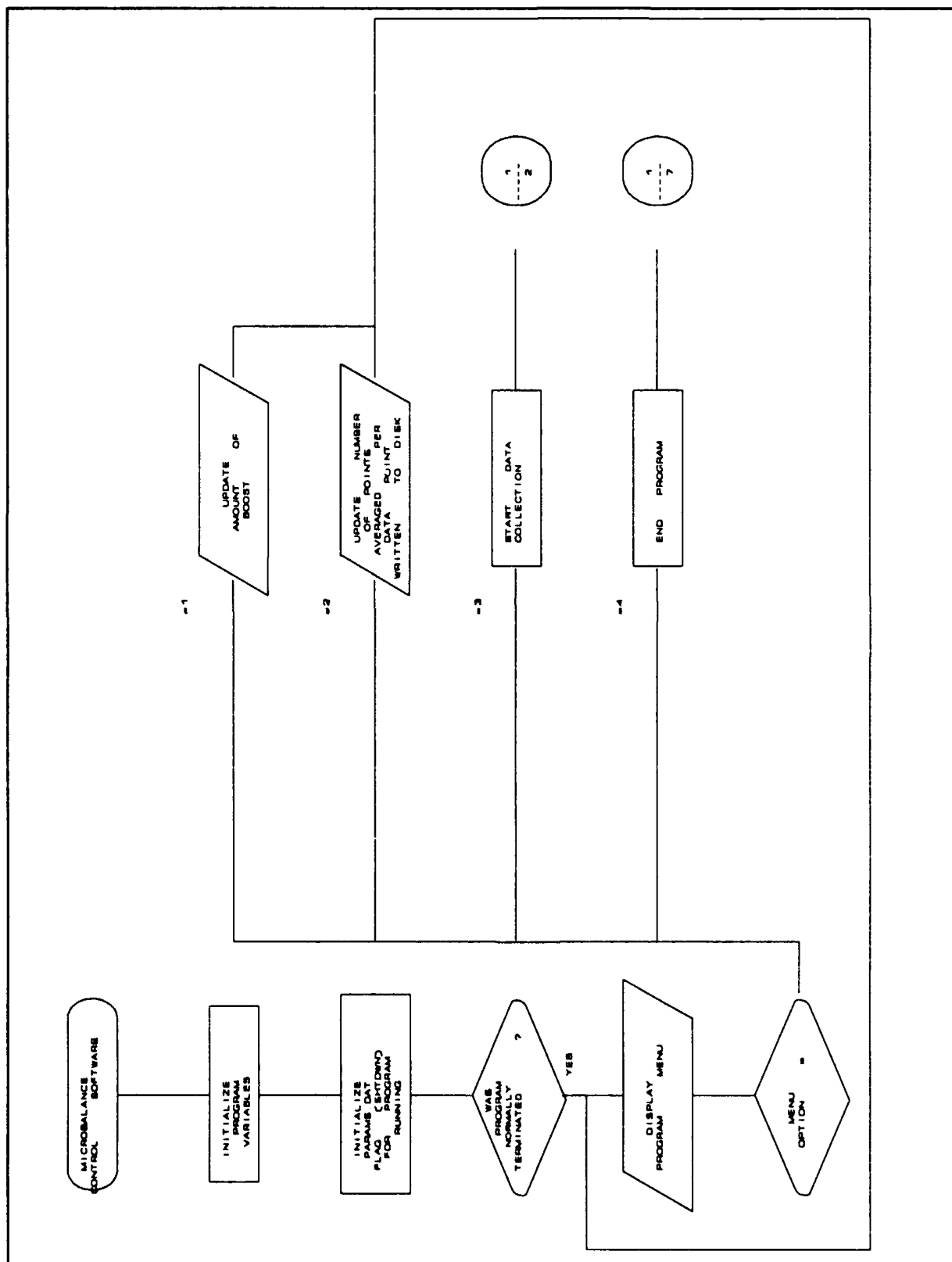
Resolution	12 bits
No. of output channels	2
Output modes	unipolar or bipolar, user selectable
Output ranges	
Unipolar	0 to +/- 10 volts, user selectable
Bipolar	+/- 5 and +/-10 volts, user selectable
Input code	
Unipolar	straight binary
Bipolar	offset binary
Output current	+5 milliamps min. with normal loading and protection from damage with the output shorted to common.
Output impedance	2 ohm max.
Capacitive loading	0.5 microfarads max

Gain	
Error	0.1 between ranges (max), any range adjustable to 0.
Stability	+/- ppm/degree C of FSR (max)
Offset	
Error unipolar	+/- 3.25 millivolt max
Error bipolar	adjustable to 0
Unipolar stability	+/-8 ppm/degree C of FSR(max)
Bipolar stability	+/- 24ppm/degree C of FSR(max)
MONOTONICITY	0 to 50 degrees C
SETTLING TIME	10 microvolts max to within 0.1% FSR for a 10 volt step with 1000 of load.
PROTECTION	Protected for short to common.
OVERSHOOT	+/- 1 % of FSR(max)
THROUGHPUT (from memory)	25,000 conversions/second

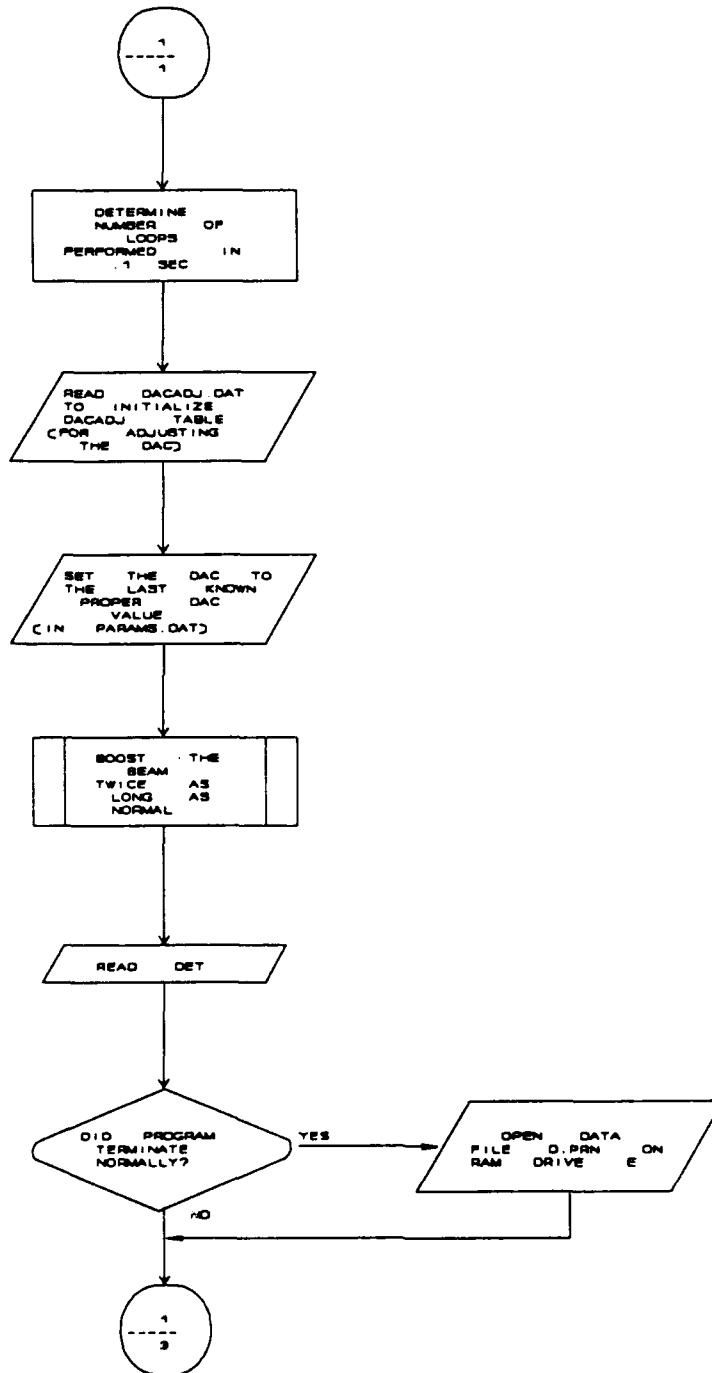
APPENDIX B

SYSTEM FLOW CHARTS

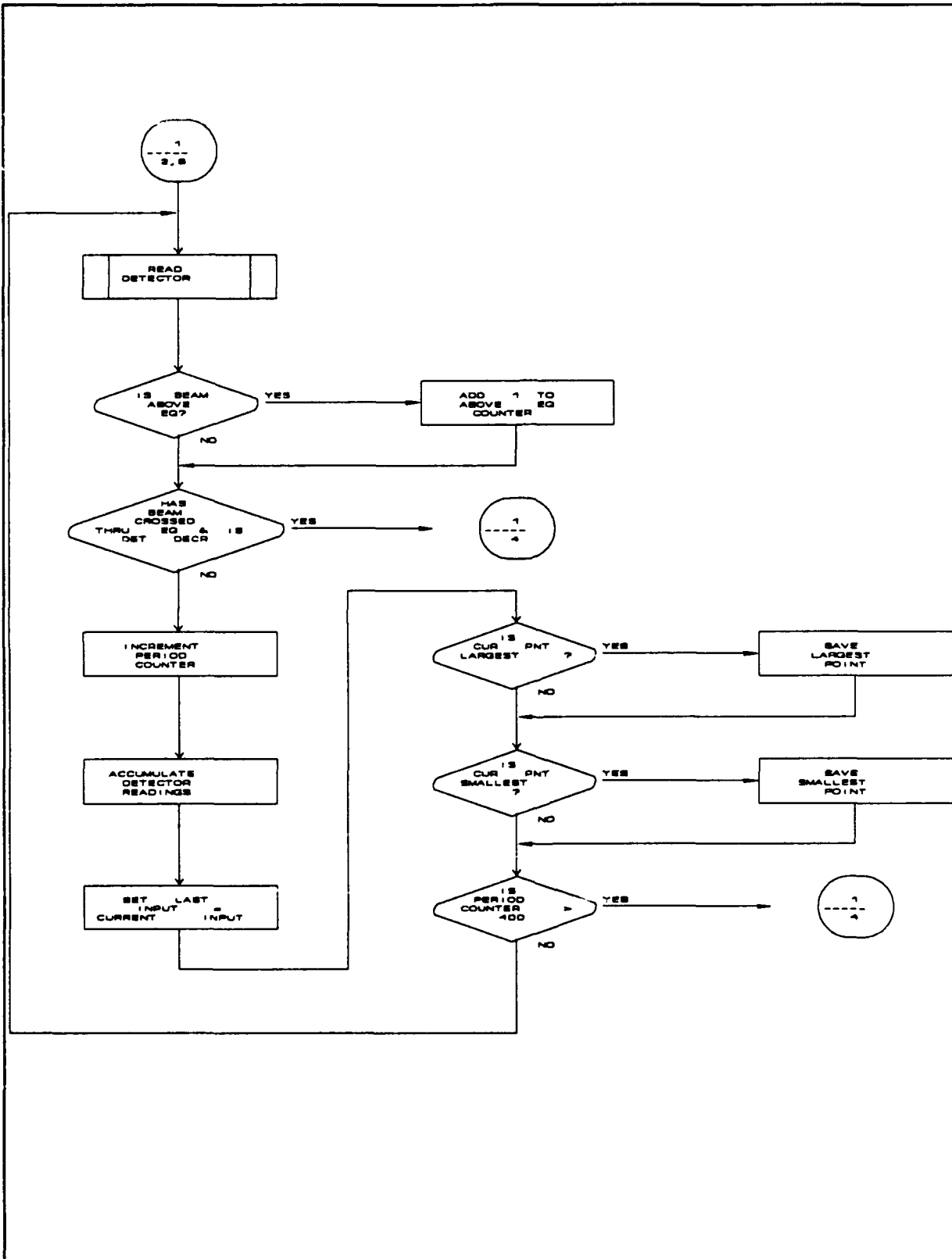
SYSTEM INITIALIZATION



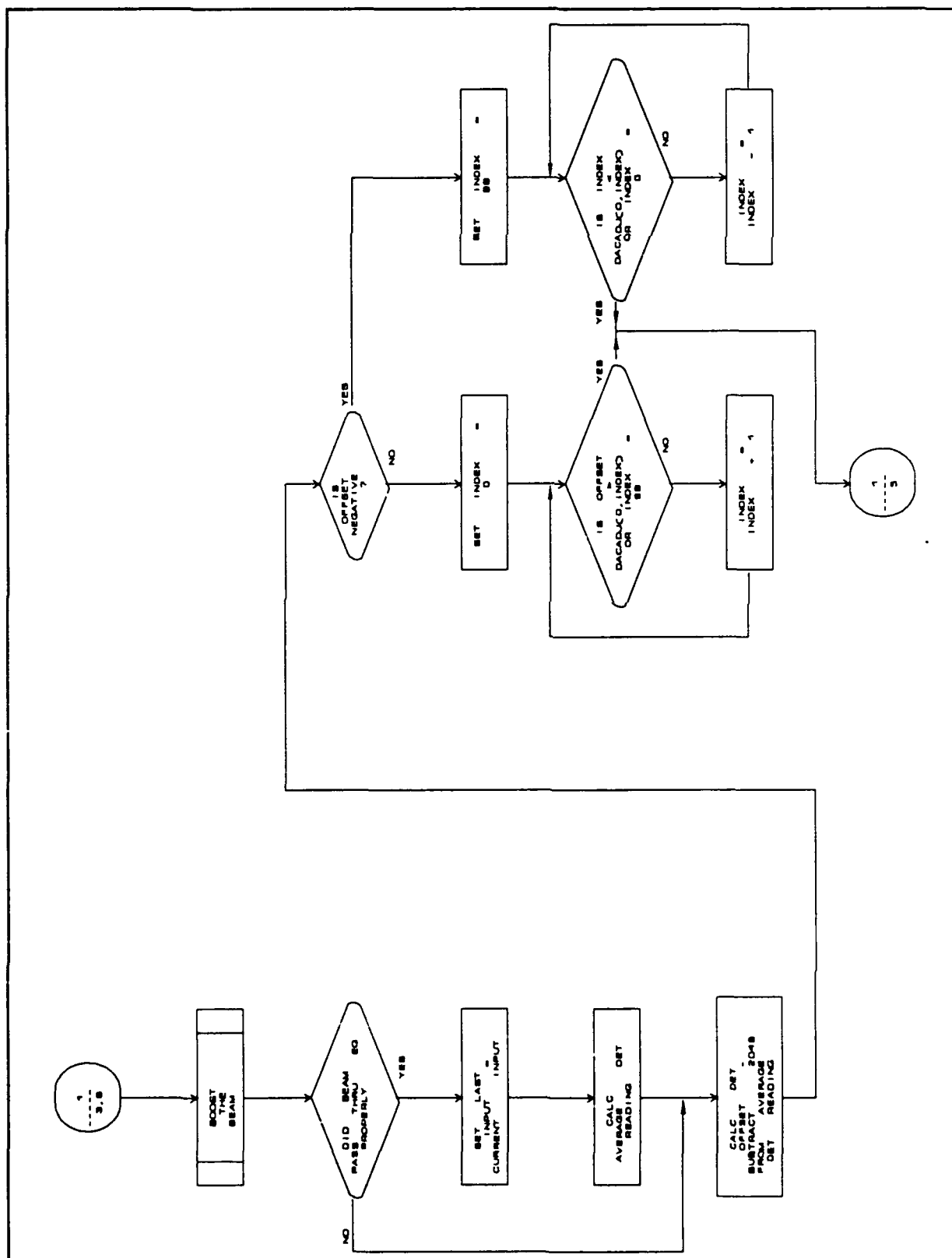
SYSTEM INITIALIZATION
(continued)



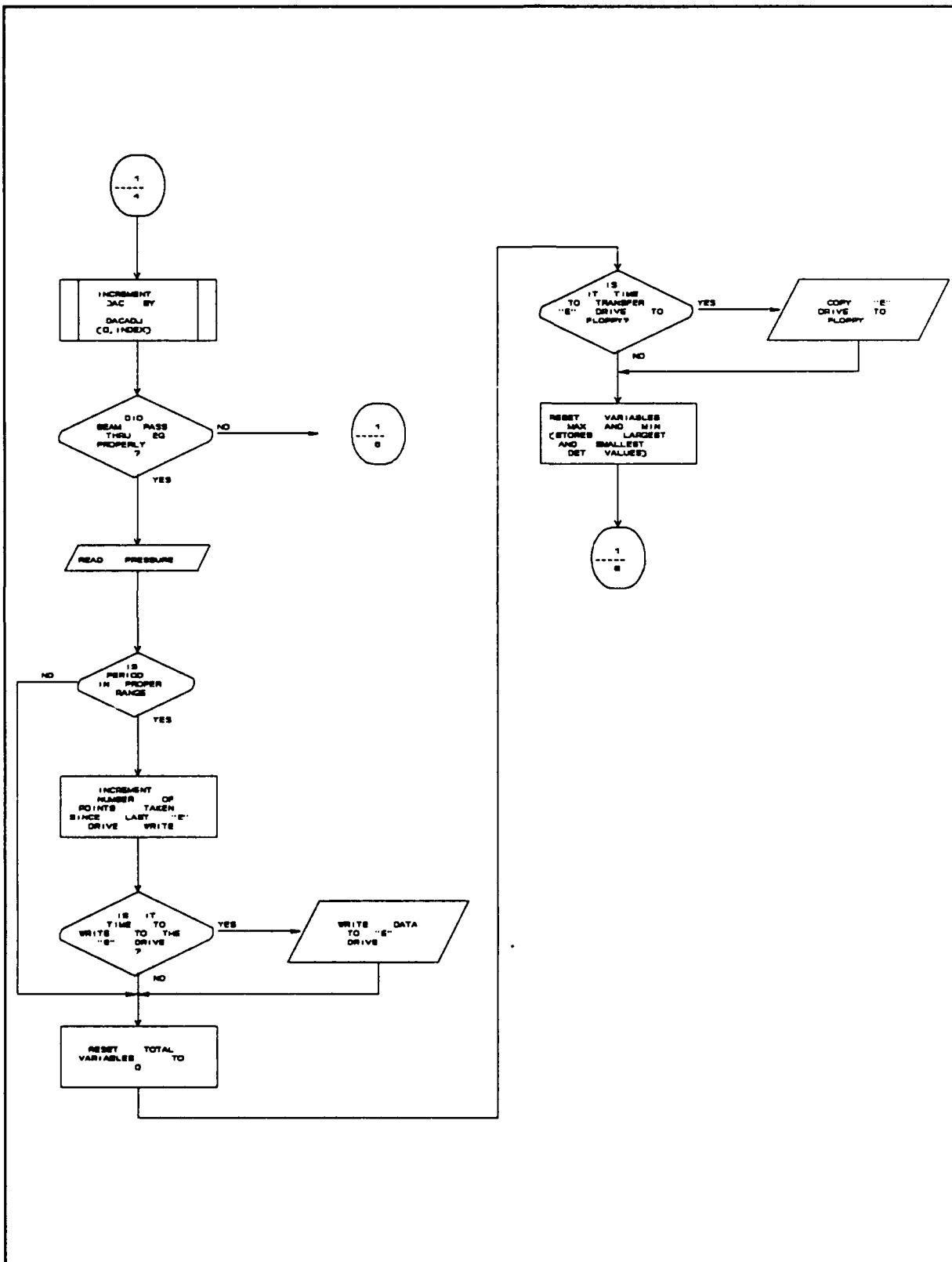
MASS DATA ACQUISITION



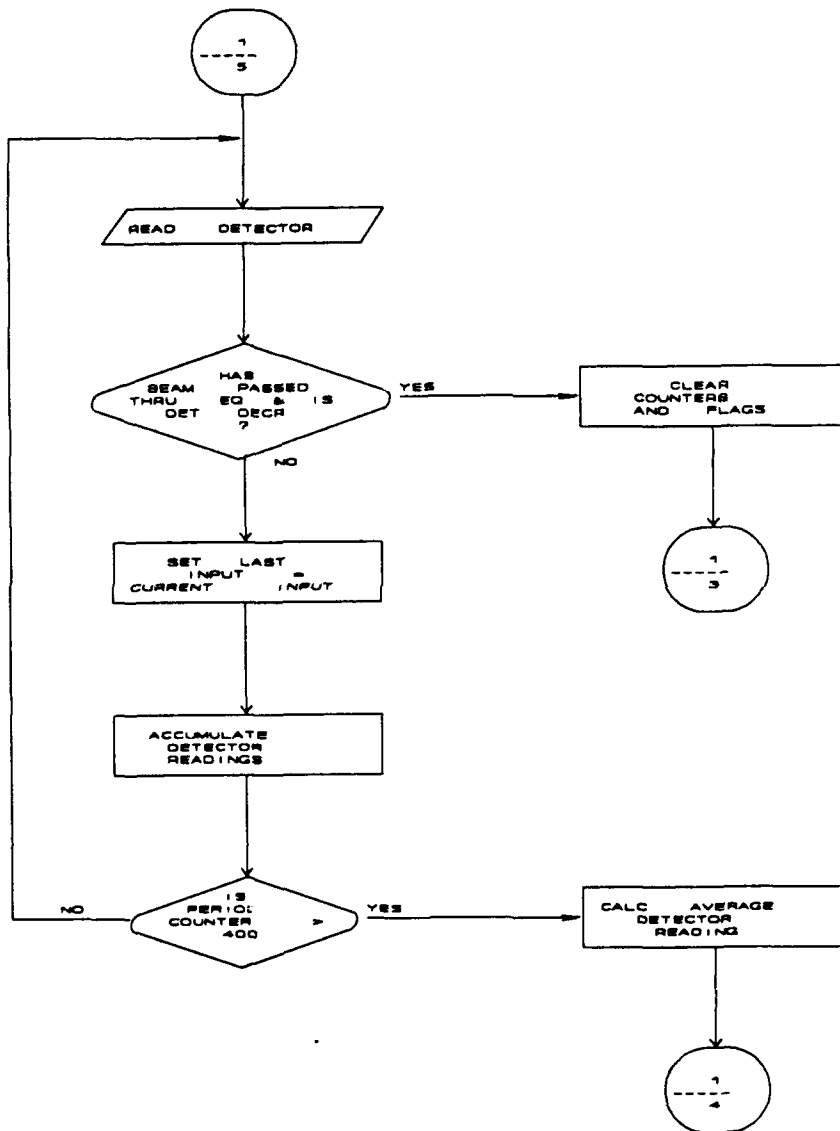
SYSTEM CONTROL & DATA ACQUISITION



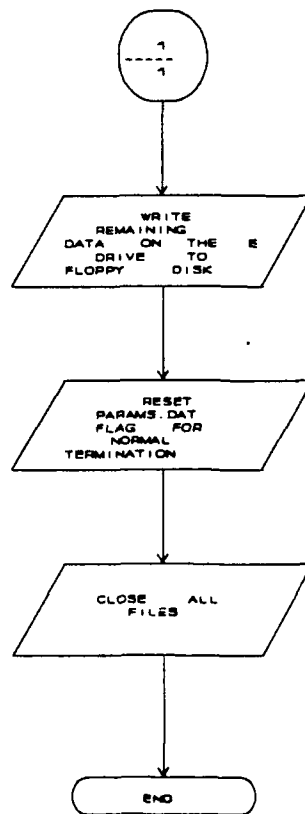
SYSTEM CONTROL & DATA ACQUISITION (continued)



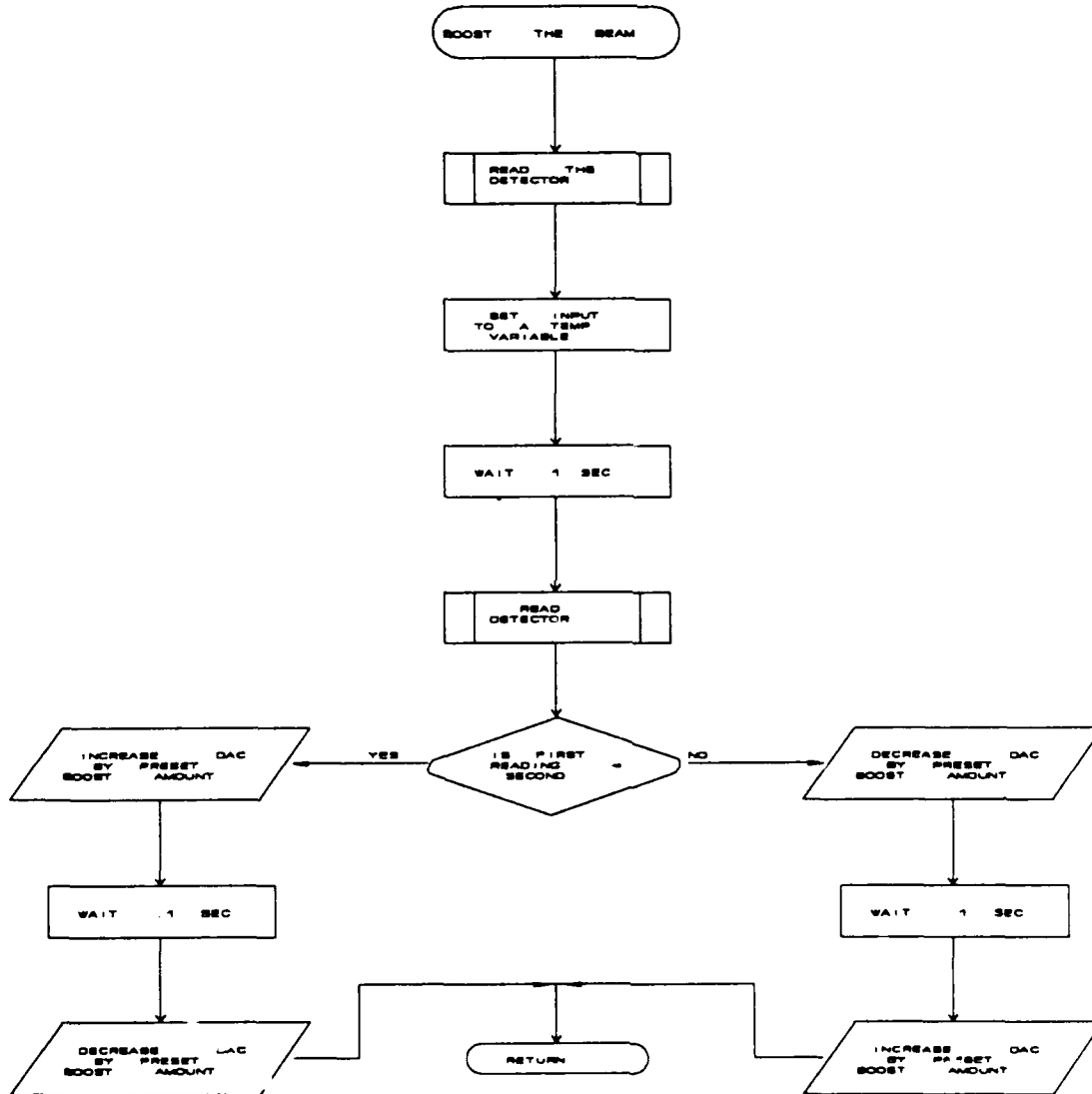
DETERMINE BEGINNING OF CYCLE



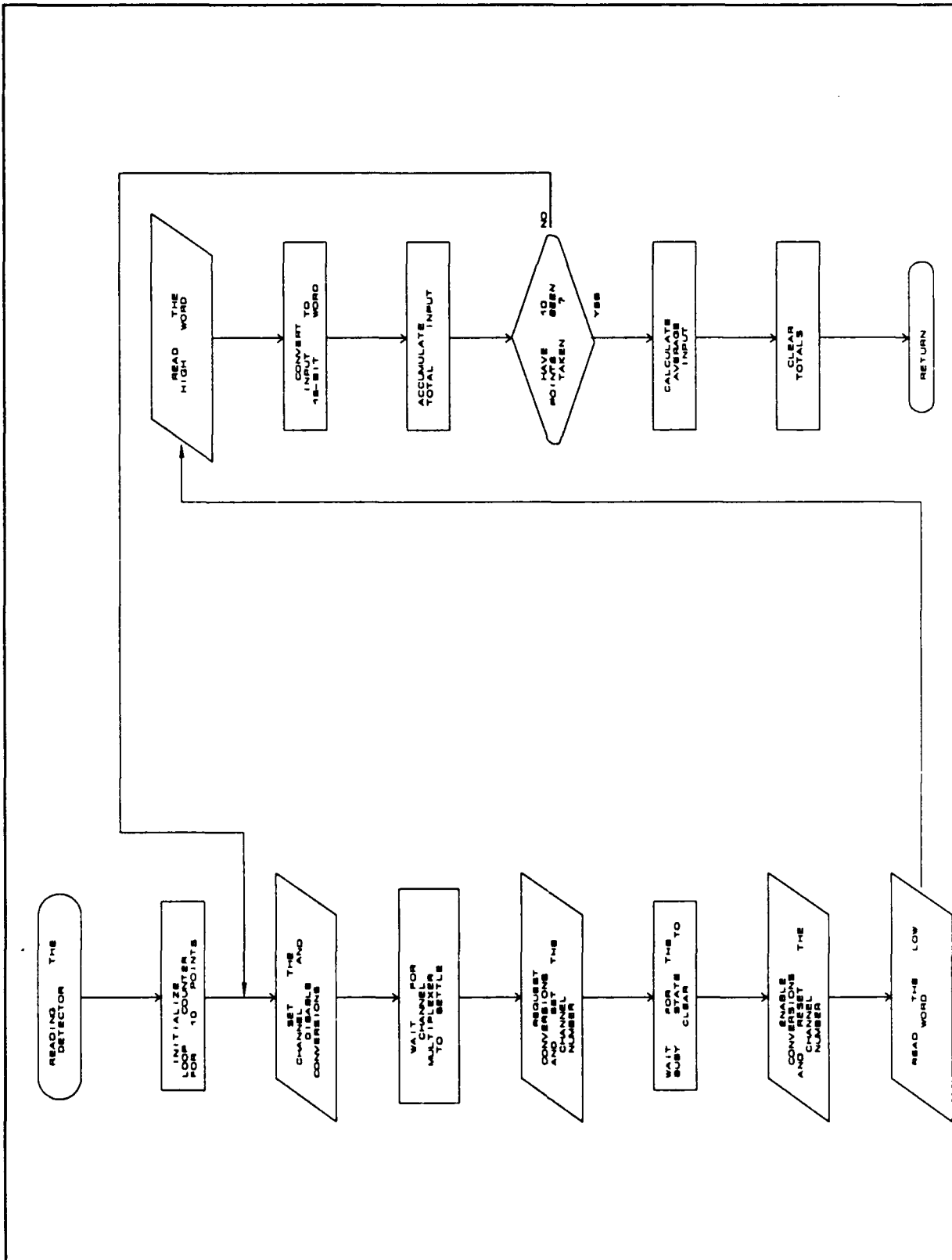
PROGRAM TERMINATION



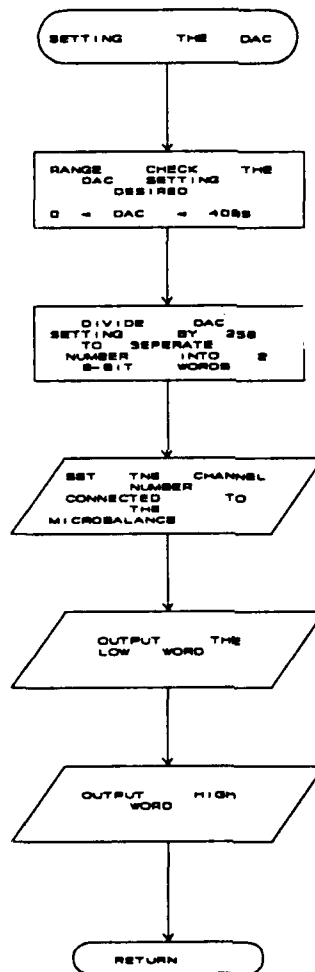
DATA TRANSFER TO FLOPPY DISK



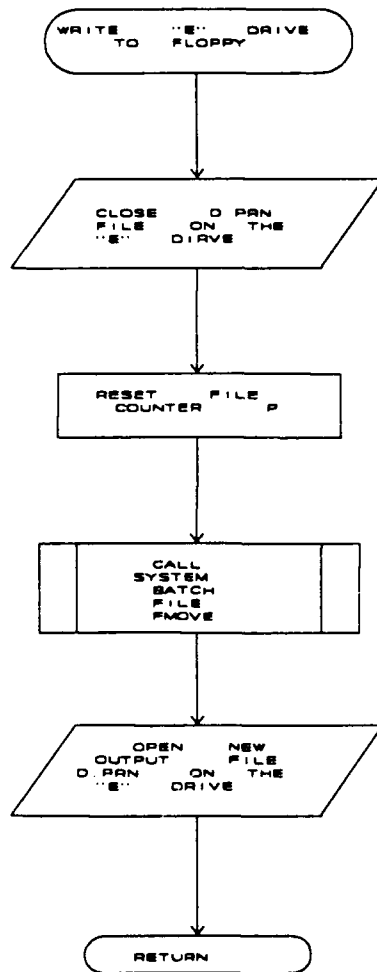
READ DETECTOR ADC CODE



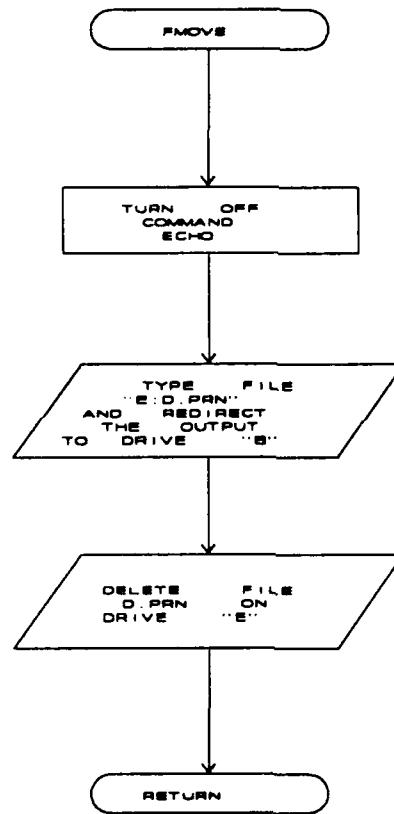
ADJUSTING DAC CODE



TRANSFER DATA FROM VIRTUAL DISK E TO FLOPPY DISK



SYSTEM BATCH FILE FOR DATA TRANSFER



APPENDIX C

SOURCE CODE FOR SOFTWARE CONTROL

```
9  OUT 49890!,9:REM INITIALIZE DAC FOR ANALOG I/O
10 REM                                MICROBALANCE DATA ACQUISITION
15 REM
20 REM          WRITTEN BY : JIM MCCARTHY
30 REM                                : ROME RESEARCH CORPORATION
31 REM
32 REM          CONTRACT # : F30602-88-C-0065
33 REM
34 REM          CONTRACT
35 REM          ENGINEER   : MR. JOSEPH BEASOCK
36 REM
40 REM          DATE      : 2-7-1990
50 REM
51 REM  Take data for 1 cycle, do calculations and store
52 REM  results, wait for next positive to negative cross, and
    continue
53 REM  Stores : DAC, DETECTOR, LENGTH OF PERIOD, DIFFERENCE
    IN  DET READINGS,
54 REM                                PRESSURE
56 REM  Number of points averaged controlled by user
57 REM  Boost is controlled by user
```

```

65 REM Using detector readings to control DAC via DACADJ
66 REM table writing to ram drive E then using the SHELL
67 REM command to execute batch file FMOVE, which appends
68 REM E:D.PRN to B:D.PRN and deletes file E:D.PRN.
80 LASTDET = 0
81 MAX = 0:MIN = 4095:MID = 2048
83 DIM DACADJ(1,101)
84 p = 0

90 OPEN "I",2,"A:PARAMS.DAT"
91 INPUT #2,SHTDWN,BSTDLY,PTAVG,TBTDPT
92 INPUT #2,COUNTS,OUTWORD,BSTAMT
93 CLOSE #2

97 TMP = SHTDWN:SHTDWN=1

98 OPEN "O",2,"A:PARAMS.DAT"
99 WRITE #2,SHTDWN,BSTDLY,PTAVG,TBTDPT
100 WRITE #2,COUNTS,OUTWORD,BSTAMT
102 CLOSE #2

104 SHTDWN = TMP
108 IF SHTDWN = 1 THEN CHANNEL = 2:GOSUB 9600:LASTCOMP = INWRD
120 IF SHTDWN = 1 THEN GOTO 2735
1000 CLS

```

```

1010 PRINT "      1)          BOOST AMT : ",BSTAMT
1020 PRINT "      2)          POINTS TO AVERAGE : ",PTAVG
1030 PRINT "      3)          START PROGRAM
1035 PRINT "      4)          END PROGRAM

1040 INPUT X

1060 IF X = 1 THEN GOTO 2000
1070 IF X = 2 THEN GOTO 2100
1080 IF X = 3 GOTO 2700
1085 IF X = 4 THEN GOTO 2500
1090 GOTO 1000


2000 CLS

2010 PRINT "OLD BOOST : ",BSTAMT
2020 INPUT "NEW BOOST : ",BSTAMT
2030 GOTO 1000


2100 CLS

2110 LOCATE 15,10
2120 PRINT "OLD POINTS TO AVERAGE : ",PTAVG
2130 LOCATE 16,10
2140 INPUT "NEW POINTS TO AVERAGE : ",PTAVG
2141 IF PTAVG < 1 THEN PTAVG = 1
2145 NDAT = 0
2150 GOTO 1000

2500 REM          END PROGRAM CHOICE #7

```

2505 IF P > 0 THEN GOSUB 10510

2510 CONFLG = 0

2515 SHTDWN = 0

2518 REM

2520 OPEN "O",2,"A:PARAMS.DAT"

2530 WRITE #2,SHTDWN,BSTDLY,PTAVG,TBTDPT

2535 WRITE #2,COUNTS,OUTWORD,BSTAMT

2540 CLOSE #2

2545 CLOSE #3

2546 CLOSE #1

2560 END

2700 REM START EXPERIMENT CHOICE #6

2710 REM DETERMINE NO LOOPS PERFORMED IN .1 SEC TO CONTROL

2711 REM THE AMOUNT OF TIME THE BOOSTING IS PERFORMED

2720 T1=TIMER:FOR I=1 TO 20000:NEXT:T2=TIMER

2730 COUNTS=INT(20000/(T2-T1)/10+.5)

2735 CLS

2736 IF ANS\$="P" OR ANS\$="p" THEN GOTO 6295

2741 OPEN "I",2,"A:DACADJ.DAT"

2743 FOR I = 0 TO 99

2745 INPUT#2,OFFS,ADJDAC

```

2846 DACADJ(0,I)=OFFS:DACADJ(1,I)=ADJDAC
2850 NEXT I
2855 CLOSE #2

5020 GOSUB 9800:FOR I = 1 TO 15000:NEXT I
5040 CHANNEL = 2
5050 TMP=BSTDLY:BSTDLY=2:GOSUB 7500:BSTDLY=TMP
5060 gosub 9600:last = inwrđ
5065 IF ANS$ = "P" OR ANS$ = "p" THEN GOTO 6010
5070 OPEN "O",1,"E:D.PRN"
5080 GOTO 6295

6010 B$ = INKEY$ : IF LEN(B$) = 0 THEN GOTO 6100 ELSE GOSUB 10510
6020 PRINT "CONTINUE, QUIT, OR CHANGE PARAMETERS ?"
6030 PRINT "          < C OR Q OR P >  "
6040 INPUT ANS$
6050 IF ANS$ = "C" OR ANS$ = "c" THEN CLS:GOTO 6295
6060 IF ANS$ = "P" OR ANS$ = "p" THEN CLS:GOTO 1000
6062 IF ANS$ = "Q" OR ANS$ = "q" THEN CLS:GOTO 2500
6063 GOTO 6020

6064 REM MAIN LOOP
6100      GOSUB 9600
6113      IF INWRD > 2048 THEN TABV = TABV + 1
6115      IF LAST >= MID AND INWRD <= MID AND CNT > 1 THEN GOTO

```

```

        6200
6116      CNT = CNT + 1
6117      TOTDET = TOTDET + INWRD
6122      LAST = INWRD
6124      IF INWRD > MAX THEN MAX = INWRD
6125      IF INWRD < MIN THEN MIN = INWRD
6130      IF CNT > 400 THEN GOTO 6200
6140 GOTO 6100

6200 GOSUB 7500
6201 IF WFLG = 1 THEN GOTO 6206
6203 LAST = INWRD
6205 MBOUT = TOTDET/CNT
6206 OFFSET = MBOUT - 2048
6207 IF OFFSET < 0 THEN GOTO 6215

6208 DONE = 1 : INDEX = 0
6209 WHILE DONE
6210      IF OFFSET > DACADJ(0,INDEX) OR INDEX = 100 THEN DONE
          = 0:GOTO 6214
6211      INDEX = INDEX + 1
6213 WEND
6214 GOTO 6240
6215 DONE = 1:INDEX = 100
6216 WHILE DONE

```

```

6217      IF OFFSET < DACADJ(0,INDEX) OR INDEX = 0 THEN DONE =
          0:GOTO 6240
6218      INDEX = INDEX - 1
6219 WEND

6240 OUTWORD = OUTWORD + DACADJ(1,INDEX)
6260 GOSUB 9800:IF WFLG=1 THEN GOTO 6300
6261 channel = 1:gosub 9600:pres = inwrđ:channel = 2
6263 IF CNT<130 OR CNT>999 THEN THOUT=THOUT+1:GOTO 6278
6264 OUTW=OUTW+OUTWORD:CNTTOT=CNTTOT+CNT:MBOUTTOT=MBOUTTOT+MBOUT
6269 NDAT=NDAT+1
6274 IF NDAT=PTAVG THEN PRINT#1,OUTWORD,CNT,OFFSET,PRES, TABV/CNT,
      MAX-MIN
6275 IF NDAT=PTAVG THEN OUTW=0:CNTTOT=0:PRESTOT=0:P=P+1:NDAT=0
6278 TOTDET = 0:CNT = 0:TABV= 0
6280 IF P > 19 THEN GOSUB 10510
6284 MIN = 4095
6286 MAX = 0

6295 REM      WAITING
6300      GOSUB 9600
6305      WCNT = WCNT + 1
6310      IF LAST >= MID AND INWRD <= MID AND WCNT > 1 THEN GOTO
          6380
6340      LAST = INWRD

```



```

6345      TOTDET = TOTDET + INWRD
6370      IF WCNT>400 THEN WFLG=1:MBOUT=TOTDET/WCNT:WCNT=0:
          TOTDET=0:GOTO 6200
6375      GOTO 6300
6380 WCNT:CNT = 0:TOTDET=0:WFLG=0:WCNT=0
6390 GOTO 6010

7500 REM  BOOSTING THE BEAM
7510 GOSUB 9600
7520 FIRST = INWRD
7530 FOR W = 1 TO 100:NEXT W
7540 GOSUB 9600
7550 IF INWRD - FIRST > 0 THEN GOTO 7700

7600 REM BOOST BEAM WHEN TRAVELING DOWNWARD
7610 OUTWORD = OUTWORD - BSTAMT
7620 GOSUB 9800
7630 FOR W = 1 TO BSTDLY*COUNTS
7640 NEXT W
7650 OUTWORD = OUTWORD + BSTAMT
7660 GOSUB 9800
7670 RETURN
7700 REM BOOST BEAM WHEN TRAVELING UPWARD
7710 OUTWORD = OUTWORD + BSTAMT
7720 GOSUB 9800

```

7730 FOR W = 1 TO BSTDLY*COUNTS

7740 NEXT W

7750 OUTWORD = OUTWORD - BSTAMT

7760 GOSUB 9800

7770 RETURN

9599 REM READ CHANNEL 2 THE DETECTOR

9600 REM READ CHANNEL 1 THE PRESSURE GAUGE

9601 REM READ CHANNEL 0 THE COMPARATOR

9610 FOR JDM = 1 TO 10

9620 OUT 738,0

9630 OUT 739,0

9640 OUT 739,CHANNEL

9650 OUT 738,1

9660 OUT 739,CHANNEL

9670 X = INP (738)

9680 Y = X AND 1

9690 IF Y <> 0 THEN GOTO 9670

9700 OUT 738,0

9710 OUT 739,0

9729 L = INP (8930)

9730 H = INP (8931)

9735 TOTINWRD = TOTINWRD + H * 256 + L

9740 NEXT JDM

9742 INWRD = TOTINWRD/10

9745 TOTINWRD = 0

9750 RETURN

9800 IF OUTWORD > 4095 THEN OUTWORD = 4095

9805 IF OUTWORD < 0 THEN OUTWORD = 0

9810 DAC0HIBYTE = INT(OUTWORD/256)

9820 DAC0LOBYTE = INT(OUTWORD - DAC0HIBYTE*256)

9830 OUT 4835,0

9840 OUT 13026,DAC0LOBYTE

9850 OUT 13027,DAC0HIBYTE

9860 RETURN

10510 REM timer

10540 CLOSE #1

10550 LASTDET = 0

10580 p = 0

10581 SHELL "FMOVE"

10588 OPEN "O",1,"E:D.PRN"

10590 RETURN

11620 END

APPENDIX D

ULTRAGRAVIMETRIC MICROBALANCE

CONTROL AND DATA ACQUISITION

SOFTWARE DOCUMENTATION

BEAM INITIALIZATION

- Initialize variables.
- Initialize PARAMS.DAT flag (SHTDWN) for program running.
- Determine if last program termination was on purpose.
 - if yes
 - present menu

option	action
(1)	update boost amount
(2)	update # of points averaged
(3)	start program
(4)	end program
- (1) Display current boost amount.
 - Input new boost amount.
 - Redisplay menu.
- (2) Display current # of points averaged.
 - Input new # of points averaged.

- Redisplay menu.
- (3) Determine # of loops performed in .1 sec. Used to control length of time boost is applied.
- Read in DACADJ.DAT table.
 - information on when and how much to adjust the DAC when the beam is not at equilibrium.
 - Set the DAC to the last known proper DAC value.
 - Boost beam twice as long as normal (to begin oscillation).
 - Take initial det reading.
 - If it is initial pass through the program, open data file d.prn on drive E:.
 - Goto DATA ACQUISITION.
- (4) Write remaining data to disk.
- Reset PARAMS.DAT flag for normal program termination.
(SHTDWN)
 - Close all files.
 - End program.

MAIN DATA ACQUISITION

- Read detector.
- If beam is above EQ add 1 to above eq counter (TABV).
- If beam has passed through EQ and the DET readings are decreasing,
stop data acq and go to data analysis & beam control.
 - If the last reading is > 2048 and the current reading is < 2048 ,
the beam has passed through EQ.
- Increment period counter (CNT).
- Accumulate total DET readings (TOTDET).
- Set last input (LAST) = current input (INWRD).
- Check for is the current point $>$ the largest or $<$ the smallest point
so far in the current cycle.
- If the period counter is > 400 the beam is out of EQ cease data acq,
goto data analysis & beam control.
- repeat

DATA ANALYSIS & BEAM CONTROL

- Boost the beam.
 - If the beam did not get "stuck" waiting,
 - set last input to current input.
 - Calc average DET reading - total DET/period counter.

- Subtract 2048 from average det reading to determine beam's offset from EQ.
- Search through DACADJ table to determine the need & if so, how much to inc/dec the DAC.
- If the beam did not get "stuck" waiting:
 - Read pressure.
 - If period counter is within valid range (beam did not get "stuck" during data acquisition)
 - if it is time to write data, # points/avg since last data point.
 - Write DAC setting, period counter, DET reading, beam's offset from EQ, pressure, % of time beam was above EQ, and the amplitude of the oscillation to the E drive.
 - Reset DET total, period counter, above EQ counter.
 - If needed write contents of E drive to floppy disk.
 - Reinitialize MAX & MIN.
 - goto to WAIT.

WAIT

- Read detector.
- Increment wait loop counter.
- If beam has passed through EQ and the DET readings are decreasing

- clear counters and flags.
- goto DATA ACQUISITION.
- Set last input (LAST) = current input (INWRD).
- Accumulate total DET readings.
- If beam is "stuck"
 - Determine average detector reading.
 - Goto DATA ANALYSIS & BEAM CONTROL
- repeat

BOOSTING THE BEAM

- Determine the direction of the beam.
- Add/subtract from the DAC accordingly.
- Wait .1 sec.
- reset DAC to previous setting.

SETTING THE DAC

- Ensure the desired DAC setting is between 4095 and 0
- Divide DAC setting by 256 to separate number into 2 8-bit words
- Subtract high word from DAC setting to get low 8-bit word.
- Set the channel number connected to the microbalance.
- Output the low word.

- Output the high word.

READING THE DETECTOR

- Initialize the averaging loop for 10 points.
- Set the channel and disable conversions.
- Wait for channel multiplexer to settle.
- Request conversions and set the channel number.
- Wait for the busy state to clear
- Enable conversions and reset the channel number.
- Read the low word.
- Read the high word.
- Convert input to 16-bit word
- Accumulate total input
- repeat
- Calculate average input
- Clear totals

WRITE E DRIVE TO FLOPPY

- Close file on the E drive.

- Reset file counter P.
- Call batch procedure FMOVE
- Open new output file on the E drive.

BATCH PROCEDURE FMOVE

ECHO OFF

- Do not display the commands being performed.

TYPE E:D.PRN >> B:PRN

- Type file D.PRN on drive E:, but redirect the output to append to the end of file D.PRN on drive B:.

DEL E:D.PRN

- Delete file D.PRN on drive E.

APPENDIX E

VARIABLE LIST

ADJDAC	- Amount to adjust the DAC when beam is out of range. Read from file DACADJ.DAT, written to array DACADJ.
ANS	- Operator response to interrupt prompt : continue, change parameters, end program.
B\$	- Character received when keyboard is scanned for input.
BSTAMT	- Amount DAC is inc/dec when boosting the beam.
BSTDLY	- Amount of time boost is applied.
CHANNEL	- Channel number program is going to read.
CNT	- Counter denoting the length of the period.
COUNTS	- Number of loops performed in .1 seconds. Used to control the length of the boost.

DAC0HIBYTE - Upper 8-bit word resulting from splitting 16-bit word OUTWORD for output.

DAC0LOBYTE - Lower 8-bit word resulting from splitting 16-bit OUTWORD for output.

DACADJ(1,101) - Holds detector offsets and corresponding amounts to inc/dec the DAC when it is not at equilibrium.

DONE - While loop control variable. Set to 0 when loop is terminated.

FIRST - The first detector value read when determining the direction of the beam.

H - Upper 8-bit word read from the A/D converter, multiplied by 256 to convert to its 16-bit equivalent.

I - For/next loop control variable.

INDEX - Array index for DAC control array DACADJ.

INWRD - 16-bit word converted from 2 8-bit words that were read from the A/D converter.

JDM - For/next loop control variable.

L - Lower 8-bit word read from the A/D converter.

LAST - Last detector value read from A/D converter.

MAX - Largest detector reading taken in current cycle.

MBOUT - Averaged detector reading.

MID - Midpoint of the detector readings. (= 2048)

MIN - Smallest detector reading taken in current cycle.

NDAT - Number of data points taken since last write to
the "E" drive.

OFFS - Detector offset read from file DACADJ.DAT and
written to DAC control array DACADJ.

OFFSET - Number of A/D bits the detector readings are from
the midpoint.(2048)

OUTWORD - Current DAC setting.

P - Number of data points written to the "E" drive.

PRES - Pressure reading taken from channel 1.

PTAVG - Number of points to take before writing to the "E" drive.

SHTDWN - Flag indicating an abnormal termination of program. If it is set, program resets all variables to the values set before program execution was interrupted.

TABV - Counter for the amount of time the beam spent above equilibrium.

THOUT - Counter for number of data points thrown out.

TMP - Holds the value of the SHTDWN flag while it is reset to program running.

TOTDET - Accumulator for detector readings.

TOTINWRD - Accumulator for A/D readings.

- W - For/next loop control variable.

- WCNT - Counter for amount of time spent waiting for the
 next positive to negative beam crossing.

- WFLG - Flag indicating next positive to negative did not
 occur in reasonable time, and to adjust the DAC
 accordingly.

- X - Operator response to program main control menu.

APPENDIX F

PUBLICATIONS

The following is a list of published articles and in house reports which were the result of research work related to the development and/or application of the ultragravimetric micro-balance.

Lt. C.J. Bolan, "Design of a Digital Controller for an Ultragravimetric Microbalance." Masters Thesis, AFIT/GE/ENG/85D-4.

Lt. M.W. Prairie, "The Effects of Water and Hydrogen on Materials Used in Integrated Circuit Packages." Masters Thesis, AFIT/GE/ENG/84D-51.

Lt A. Potts, "Characterization of Polyimide Film Used in VHSIC Package Decal." (Presented at Minnowbrook.)

A. W. Czanderna and R. Vasofsky, "Surface Studies with The Vacuum Microbalance", Progress in Surface Science, 1979. Vol. 9, pp.45-82.

R. Vasofshy, A. W. Czanderna and R. W. Thomas, "UHV System for the Ultramicrogravimetric Study of Samples Loaded in a Controlled Environment", J. Vac. Sci. Technol., 16(2), Mar./Apr 1979.

R. Vasofsky, A.W. Czanderna, and Karel K. Czanderna, "Mass Changes of

Adhesives During Curing, Exposure to Water Vapor, Evacuation and Outgassing," Part I: Aklefilms 529, 535 and 550.

A.W. Czanderna and R. Vasofsky, "Mass Changes of Microcircuit Adhesive Materials During Curing, Exposure to Water Vapor, Evacuation and Outgassing."

B. van Pul, "Automation of an Ultramicrobalance."